3 1176 00156 3726

NASA CR-159, 181

NASA Contractor Report 159181

NASA-CR-159181
1980 000 9767

CONCEPTS FOR GENERATING OPTIMUM VERTICAL FLIGHT PROFILES

John A. Sorensen

Contract NAS1-15497
September 1979

NASA

NASA Contractor Report 159181

CONCEPTS FOR GENERATING OPTIMUM VERTICAL FLIGHT PROFILES

John A. Sorensen

Analytical Mechanics Associates, Inc.
Mountain View, California

Prepared for
Langley Research Center
under Contract NAS1-15497

National Aeronautics and
Space Administration

Langley Research Center
Hampton, Virginia 23665
AC 804 827-3966

September 1979

FOREWORD

This effort for development of concepts for generating optimum vertical flight profiles that minimize fuel and direct operating costs was supported under NASA Contract No. NAS1-15497, by Langley Research Center, Hampton, Virginia. The project Technical Monitors at Langley Research Center were Samuel A. Morello and Robert E. Shanks. Technical discussion and suggestions from Messrs. Morello and Shanks, Robert T. Taylor of Langley Research Center, Jack Wiggs of Bennett College, and John S. Bull, Heinz Erzberger, and Homer Q. Lee of NASA Ames Research Center are gratefully acknowledged. The mathematical model of the aircraft used for study in this report was provided by NASA Ames Research Center.

At AMA, Inc., the project manager was John A. Sorensen, with technical support provided by Antony W. Merz and Anil V. Phatak. The project programmer was Marianne N. Kidder.

CONCEPTS FOR GENERATING OPTIMUM VERTICAL FLIGHT PROFILES

John A. Sorensen

Analytical Mechanics Associates, Inc.
Mountain View, California 94043

SUMMARY

The objective of this project is to develop and evaluate one or more algorithms and flight management concepts for the on-board minimization of fuel and/or direct operating costs. These concepts are to be used for steering a CTOL aircraft in the vertical plane between fixed origin and destination airports along a given horizontal path.

In this report, a summary is first made of work that has been conducted to date concerning the generation of optimum vertical profiles. Then, algorithms for generating optimum vertical profiles are derived and examined. These algorithms form the basis for the design of on-board flight management concepts. The variations in the optimum vertical profiles (resulting from these concepts) due to variations in wind, takeoff weight, and range-to-destination are next presented. Further considerations for mechanizing two different on-board methods of computing near-optimum flight profiles are then outlined. Finally, the results are summarized, and recommendations are made for further work.

Two appendices are included which give technical details of optimum trajectory design, steering requirements for following these trajectories, and off-line computer programs for testing the concepts. The two computer programs developed are called OPTIM and TRAGEN, and they are available from the Computer Software Management Information Center, Barrow Hall, University of Georgia, Athens, Georgia 30601.

TABLE OF CONTENTS

		Page
I	INTRODUCTION	1
II	BACKGROUND	5
III	COMPUTATION OF THE NOMINAL OPTIMUM VERTICAL PROFILE	15
	Derivation of the Optimization Algorithm	15
	Generation of Nominal Optimum Trajectories	19
	Example Optimum Trajectories	23
IV	PROGRAM VERIFICATION AND SENSITIVITY RESULTS	31
	Optimization Verification	32
	Sensitivity Analysis	37
V	MECHANIZATION OPTIONS	49
	Off-line Optimum Profile Generation	49
	On-board Optimum Profile Generation	51
	Method Comparison	53
VI	SUMMARY, CONCLUSIONS, AND RECOMMENDATIONS	55
	Summary and Conclusions	55
	Recommendations	57
APPENDIX A.	TRAJECTORY OPTIMIZATION USING THE ENERGY STATE METHOD	63
APPENDIX B.	AIRCRAFT EQUATIONS OF MOTION AND AUTOPILOT MODELS	87
REFERENCES		97

LIST OF FIGURES

Figure		Page
1.	Projected Free World Petroleum Production Capacity vs Consumption.	2
2.	Free World Air Carrier Jet Fuel Consumption Projection	2
3.	Contours of Constant Energy Increase per lb. of Fuel Burned and Minimum-Fuel Energy-Climb Path	8
4.	One Solution to the Minimum Fuel-Fixed Range Problem	10
5.	Time-Fuel Tradeoff for Fixed Ranges	11
6.	Minimum Cruise Fuel Consumption per Unit Range for the DC-10 . . .	12
7.	State Variables for an Optimum Climb Profile of a 200 n.mi. Range Flight	24
8.	State Variables for an Optimum Descent Profile of a 200 n.mi. Range Flight	26
9.	Comparison of Minimum Direct-Operating-Cost Flight Profiles. . . .	29
10.	Effect of Range Variation on Optimum Climb Flight Path Angle and Mach Number	39
11.	Effect of Initial Weight Variation on Optimum Climb Flight Path Angle and Mach Number	40
12.	Wind Profiles Used to Study Sensitivity Effects on Optimum Profiles	42
13.	Effect of Wind Variations on Optimum Climb Flight Path Angle and Mach number.	43
14.	Effect of Wind Variations on Optimum Descent Altitude and Mach Number as Functions of Range-to-go.	44
15.	Block Diagram Depicting On-Board Climb Steering Based on Computing the Nominal Optimum Profile Off-line	50
16.	Block Diagram Depicting On-Board Climb Steering Based on Computing the Nominal Optimum Profile in the Background.	52
A.1	Assumed Structure of Optimum Trajectories	67
A.2	Measurement of Range from the Origin or to the Destination	69
A.3	Optimum Cruise Cost as a Function of Cruise Energy	73
A.4	Optimum Profile Energy vs Range for $H_c > 0$ at Cruise	75
A.5	Optimum Profile Energy vs Range for $H_c = 0$ at Cruise	75
A.6	Plot of Thrust and Drag vs Airspeed at a Particular Altitude . . .	79
A.7	Optimum Cruise Cost as a Function of Altitude for Cruise Weight of 54,431 kg (120,000 lb)	79
A.8	Optimum Cruise Cost and Cruise Altitude as Functions of Cruise Weight for the 727 Flying into a Particular Head Wind	80

List of Figures, Continued

Figure		Page
A.9	Relationship Between the Cruise Cost Parameter ψ and the Associated Range of Flight	86
B.1	Vector Diagram of Longitudinal Forces	88
B.2	Elements of the Longitudinal Aircraft Model	91
B.3	Control Loops for Perturbation Control of Airspeed and Flight Path Angle	93

LIST OF TABLES

Table		Page
1.	Comparison of Flight Costs for 200 n.mi. Range with Varying Wind Conditions	30
2.	Comparison of Optimization and Trajectory Generation Program Climb Results for Different Range Flights	35
3.	Comparison of Optimization and Trajectory Generation Program Climb Results in the Presence of Winds.	35
4.	Comparison of Optimization and Trajectory Generation Program Results Descending from 10668 m (35000 ft) to 3048 m (10000 ft).	36
5.	Comparison of Optimization and Trajectory Generation Program Results Descending from 10668 m (35000 ft) to 1.8 m (6 ft)	37
6.	Initial Weight Error Cases Considered - Climb Profile	46
7.	Wind Profile Error Cases Considered - Climb Profile	47

SYMBOLS

Roman Symbols

C, C_d - unit direct operating cost

C_D - drag coefficient

C_f - cost of fuel ($/lb)

C_L - lift coefficient

C_t - cost of time ($/hr)

D, D_c - drag

DOC - direct operating cost combining fuel and time costs

d_c - cruise distance

d_f - total distance traveled

d_{up}, d_n - climb and descent range

E - specific energy

E_{copt} - optimum value of specific energy during cruise at the optimum altitude

F - fuel burned

F_{up}, F_c, F_{dn} - fuel burned during climb, cruise and descent

G_B, G_C - constants in the transfer functions relating perturbations in γ and V_a to perturbations in α

g - acceleration due to gravity

H, H_c - the Hamiltonian used for optimization

H_{up}, H_{dn} - value of Hamiltonian during climb and descent

h - altitude

J - cost function to be minimized

K_1, K_2, K_3, K_4 - control law gains

L - lift

L(x,u,t) - cost per unit time along a trajectory

m - aircraft mass

P - ratio of cruise cost ψ to optimum cruise cost $\psi_{c_{opt}}$

p_1, p_2 - origin and destination values of range

q - pitch rate

R_{min}, R_{max} - values of range where P = 1.5 and 1.01 on optimum trajectories

r - ratio of fuel to time costs $(C_f/C_t)/(1+C_R/C_t)$

r_d - range-to-go

s - Laplace transform operator

T - thrust

t - time

t_{ci}, t_{cf} - time at beginning and ending of cruise

t_o, t_f - initial and final times of trajectory

V, V_a, V_c - airspeed

V_{up}, V_{dn} - airspeed during climb and descent

V_w - longitudinal component of wind

V_{wup}, V_{wdn} - wind speed during climb and descent

W, W_i, W_f - weight of the aircraft; initial and final weight

W_c - weight during cruise

$\dot{w}$ - fuel flow rate

x - range traveled during climb and descent

x_{up}, x_{dn} - components of range traveled during climb and descent.

Greek Symbols

α - angle-of-attack

γ, γ_c - flight path angle (with respect to air mass)

γ_I, γ_{Ic} - inertial flight path angle

δ_T - throttle setting

λ - adjoint variable or costate used for optimization

π - throttle position or thrust control

π_{up}, π_{dn} - throttle setting during climb and descent

ζ - damping term in transfer function

τ - time-to-go

τ_B, τ_C - constants in the transfer functions relating perturbations in γ and V_a to perturbations in α

ϕ - terminal cost function

ψ, ψ_c - cost per unit distance of cruise

ω - natural frequency in transfer function

σ - specific fuel consumption (lb/lb thrust)

I

INTRODUCTION

Virtually every segment of civilization is being affected by the energy crisis, and we are awakening to the fact that we live in a system with finite resources. Our natural supplies of hydrocarbon fuels are being rapidly consumed, so that it has become mandatory that we seek to develop every feasible means to conserve fuel. The energy crisis and its effect on developing technology is especially impacting the air transportation industry which accounts for about 4 percent of our national petroleum consumption [1].

The current motivating factor for our air transportation industry to conserve fuel is the escalating cost of jet fuel. To the commercial air carrier, reduction in fuel usage means reduction in operating costs and an increased profit margin [2]. For military air operations, fuel reduction also implies increased aircraft range, greater payloads, more missions, and an enhanced defense reserve [3,4]. The U.S. Air Force has an annual fuel usage of over 4 billion gallons [3], while our domestic commercial fleet used about 10 billion gallons in 1978 [1,2].

Figures 1 and 2, taken from Ref. 2, illustrate the dilemma that exists for commercial aviation - increasing air transportation demand versus decreasing production capacity. Figure 2 also illustrates that accelerated technological advancements can potentially reduce future usage of fuel for air transportation by more than 30%. One of these advancements is developing the ability to fly each aircraft along profiles which minimize total fuel consumption.

Commercial airline flight profiles are presently generated using a pseudo-optimization procedure. Given a reasonable knowledge of the jet stream, computer programs based on dynamic programming techniques test a series of horizontal paths between the departure and destination points to find the one providing minimum time or fuel usage. The horizontal paths tested are predetermined, and they typically consist of a series of interconnected segments between VOR/DME and TACAN stations. The vertical

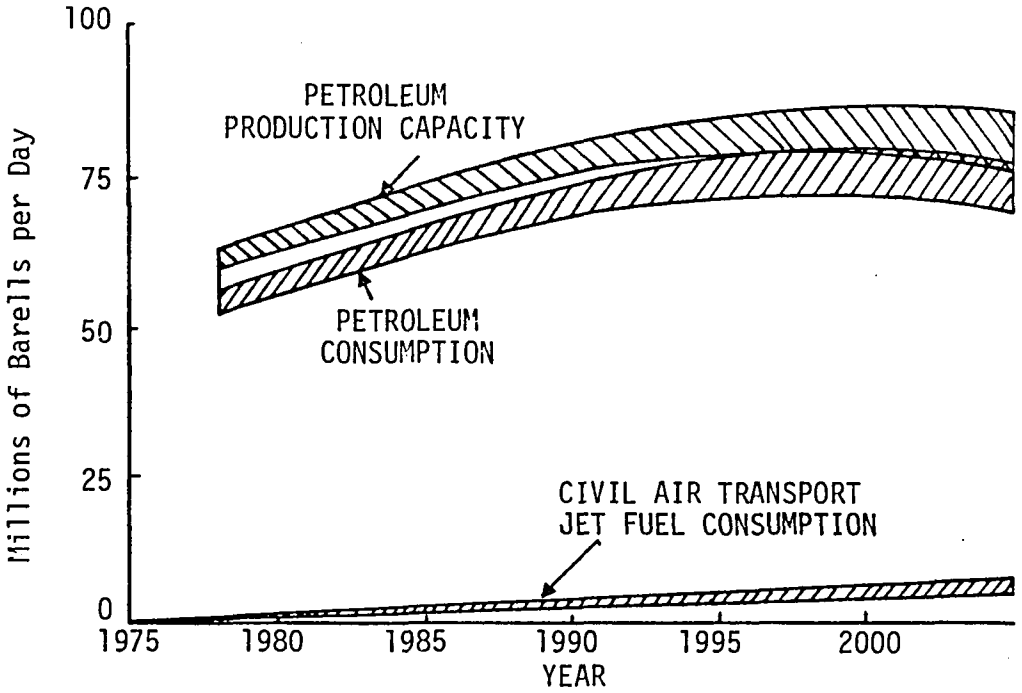

Figure 1. Project Free World Petroleum Production Capacity vs Consumption [2].

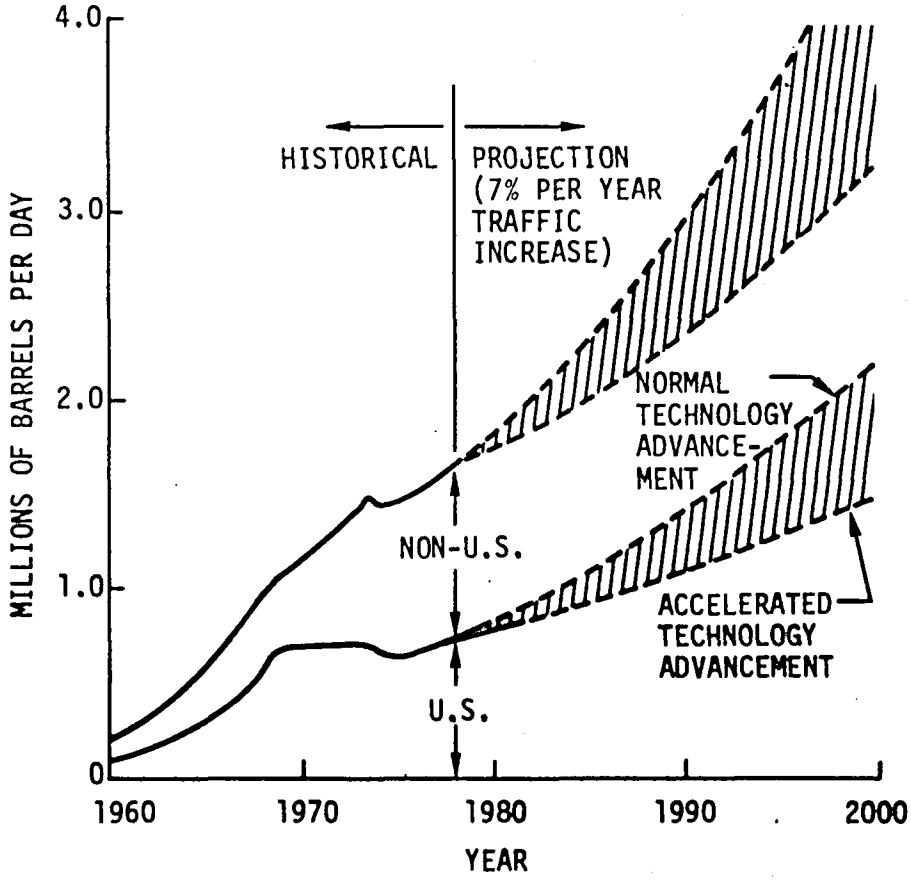

Figure 2. Free World Air Carrier Jet Fuel Consumption Projection [2].

path then consists of a fixed Mach number/indicated airspeed profile for climb and descent combined with a series of step changes in altitude during cruise. The altitude changes are governed by predetermined fuel burnoff rates and ATC considerations. This report is focused on various aspects of computing improved vertical profiles.

There is a pressing need to reduce fuel usage and costs for all types of flights. In addition, increasing labor costs and penalties on air travel time make it desirable to minimize the flight time. These factors motivate the search for a flexible procedure for generating a vertical reference profile which can minimize the total cost of an operation between two airports.

This procedure should be capable of minimizing fuel usage, flight time, or a combination of these variables (direct operating cost - DOC). Furthermore, it should be computationally efficient and implemented so that it can be used by the pilot while airborne to change the flight profile in case of change in weather conditions or final destination. Finally, this procedure should serve as a means of automatically driving the aircraft control surfaces and engine throttle settings. The work summarized in this report has been directed at developing such a procedure that can be mechanized on-board to achieve the optimum path.

This report is organized as follows:

a) A summary is made of publicly available work that has been conducted to date concerning the generation of optimum vertical profiles.

b) Algorithms of methods for generating optimum vertical profiles are derived. These procedures form the basis for specifying on-board mechanization requirements.

c) Sensitivity results are presented of the variation in the optimum vertical profile as a function of variations in wind, takeoff weight, and range-to-destination. These sensitivity results also impact the mechanization requirements.

d) Considerations are outlined concerning the on-board computation of the near-optimum profiles and the interface with the autopilot/autothrottle. This is the first step in the design of an experimental prototype system.

e) Recommendations are made regarding further work that is required so that the algorithms for minimizing DOC are available to all potential aircraft users and avionics designers.

These items are covered in turn in the next five chapters of this report. Also, Appendices A and B are presented to give technical details of trajectory optimization, steering requirements for implementing these trajectories, and off-line computer programs for testing the concepts.

II

BACKGROUND

The basic principles of trajectory optimization are an outgrowth of applying the calculus of variations. These principles are outlined in the first part of Appendix A, and they are referred to throughout this chapter. The purpose of this chapter is to outline the known work that has been accomplished to this time using trajectory optimization methods for minimizing various cost functions including aircraft direct operating costs. This background serves to put into perspective the methods for generating near optimum trajectories described in Chapters III and IV.

As mentioned in the Introduction, the first problem solved by the flight planner is to determine what horizontal path to fly between origin and destination to take best advantage of the winds aloft (jet stream). Here, they may be wishing to minimize fuel, time, or a combination of fuel and time (i.e., DOC). This problem is usually solved by assuming that a single flight level will be used and a particular wind vector field exists over this horizontal plane. This type of problem is typically solved using a computational technique called dynamic programming [7]. Computerized flight planning based on dynamic programming is available on a commercial basis to airlines and other users [8]. Some large airlines currently have their own facilities for weather forecasting, prediction of wind fields, and planning of horizontal route structures.

However, the primary subject addressed here is how to fly the aircraft in the vertical plane once the horizontal path has been specified. That is, the origin, destination, horizontal route, starting and ending altitudes and airspeeds, and takeoff weight are fixed. The problem then is to choose the vertical flight profile (altitude, airspeed, thrust, and flight path angle time histories) to minimize cost.

A set of non-linear differential equations describing a point mass model of the aircraft longitudinal motion is adequate to describe the vertical motion of the aircraft for optimization purposes [9]. This model is, for no wind,

$$\begin{aligned} \dot{mV} &= T\cos\alpha - D - mg\sin\gamma, \\ \dot{mV\gamma} &= T\sin\alpha + L - mg\cos\gamma, \\ \dot{h} &= V\sin\gamma, \\ \dot{x} &= V\cos\gamma, \\ \dot{m} &= -\dot{w}/g\ . \end{aligned} \tag{1}$$

Here, the state variables are the airspeed V, flight path angle γ, altitude h, horizontal range x, and mass m. The control variables are the thrust T and angle-of-attack α which are both amplitude limited. The variables lift L and drag D are functions of h,V, and α. The fuel flow rate $\dot{w}$ is a function of h, V, and T. These equations are analogous to Eqs. (A.1) in Appendix A. The cost function to be minimized is of the form,

$$J = \int_{t_o}^{t_f} \left(C_f \dot{w} + C_t\right) dt\ , \tag{2}$$

where C_f and C_t are the unit costs of fuel ($/lb) and time ($/hr). The final time t_f is free. The problem is to choose the sequence of controls (T and α) that drive Eqs. (1), satisfy the initial and final constraints, and minimize the cost of the flight, as governed by Eq. (2).

In addition to dynamic programming, other iterative procedures such as steepest descent, first and second order gradient, quasi-linearization, and neighboring extremal methods [5] have been developed and applied to solve aircraft trajectory optimization problems. All of these are computationally time consuming [3,9,10] and require a certain amount of art (gained by experience) in solving for the sequence of optimal controls. These problems led researchers to seek simplifications and assumptions to allow solving for an approximate optimum solution more quickly.

An early attempt at obtaining simplified solutions to the minimum time-to-climb and minimum fuel-to-climb problems was made by Rutowski [11] using graphical methods. He also suggested that the aircraft could adequately be represented in such a problem by its specific energy state,

$$E = h + V^2/2g \quad . \tag{3}$$

The use of this state assumes that kinetic and potential energy can be instantaneously interchanged.

Bryson, Desai, and Hoffman [12] used the energy state approximation and differentiated Eq. (3) to obtain

$$\dot{E} = V(T - D)/mg \tag{4}$$

as the single equation of motion. This assumed that lift L balanced weight mg, and airspeed V was treated as a control variable. With these assumptions, simple solutions to the minimum time-to-climb problem were found by maximizing energy rate E, or

$$\max_V \{V(T(E,V) - D(E,V))\} \tag{5}$$

for all values of E. Minimum fuel-to-climb solutions were found by maximizing

$$\max_V \{V(T(E,V) - D(E,V))/(-\dot{m})\} \tag{6}$$

at each energy level. A typical solution to Eq. (6) is shown in Fig. 3. Solutions to maximum range for a given amount of fuel and maximum range for a given amount of time were also found.

The work was extended to treat the minimum-fuel fixed-range problem by Schultz and Zagalsky [13-15]. In Ref. 13, they used range as the independent variable and the state equations

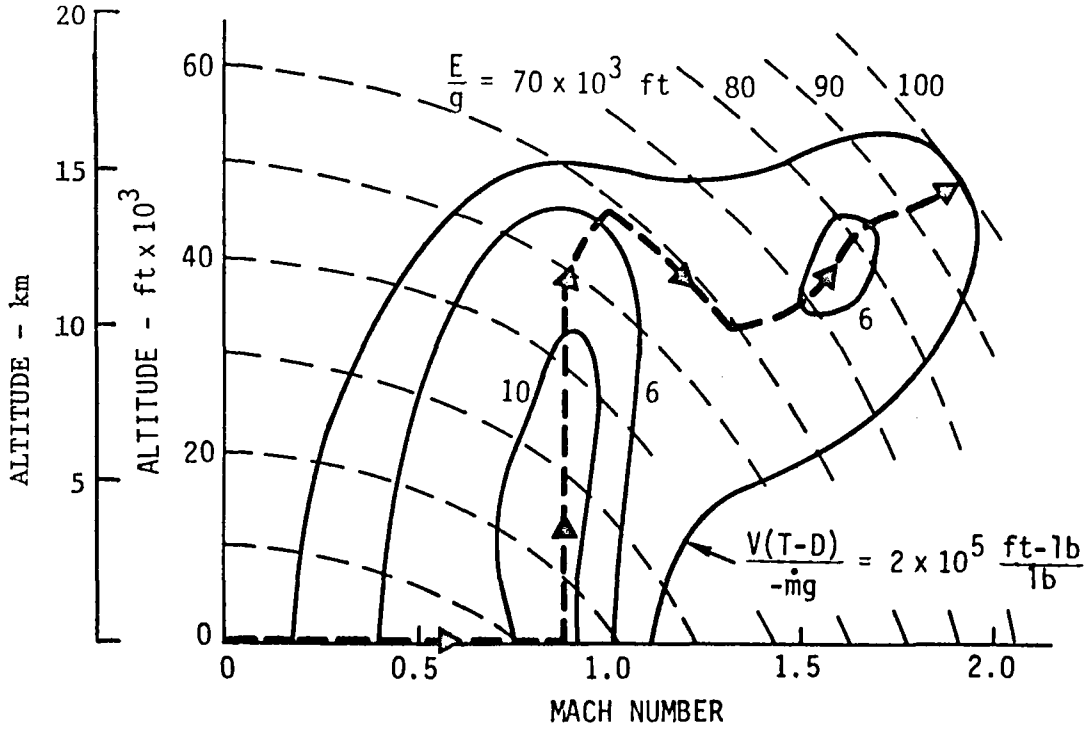

Figure 3. Contours of Constant Energy Increase per lb. of Fuel Burned and Minimum-Fuel Energy-Climb Path [12].

$$dE/dx = (T(E,V,\pi) - D(E,V))/mg, \qquad (7)$$
$$dm/dx = -\sigma(E,V,\pi)T(E,V,\pi)/V,$$

where π is the throttle position and σ is the specific fuel consumption. With π and V as control variables, they formed the Hamiltonian (See Appendix A),

$$H = -\sigma T/V + \lambda(T-D)/mg. \qquad (8)$$

Here, λ is the adjoint (or costate) variable. This Hamiltonian is independent of x (and therefore constant) which eliminates the need to solve for λ. H is maximized with respect to V and π and is used to show that for sufficient range, suboptimal trajectories consist of minimum fuel energy climbs, classical steady state minimum fuel cruises, and maximum range descending glides.

In Ref. 14, Schultz and Zagalsky critiqued the energy state approximation solutions by posing second, third, fourth, fifth, and seventh order models of the longitudinal aircraft equations of motion and then found and compared solutions to the associated fixed endpoint flight-path optimization problems. These included (a) minimum fuel-fixed range, (b) minimum time-fixed range, and, (c) minimum fuel-fixed range-fixed time trajectories. For the climb-cruise-descent trajectory, the steady cruise conditions were found to minimize.

$$\min\ (\sigma\ D/V) \triangleq \sigma_c\ D_c/V_c\ . \tag{9}$$

Then, the climb solution was found by maximizing

$$\max_h \left[\frac{(T - D)V/m}{\sigma T - \sigma_c\ D_c\ V/V_c}\right] \tag{10}$$

for π_{max} and constant values of E. The descent solution minimized

$$\min_h\ (D/m) \tag{11}$$

to maximize range by assuming thrust and fuel flow are zero. A typical solution is shown in Fig. 4. In Ref. 15, range was again used as the independent variable, and the function

$$\frac{1}{\lambda} = \max_{\pi,V} \left[\frac{(T - D)/mg}{H_o + \dot{w}}\right] , \tag{12}$$

derived from Eq. (8), was suggested as a means to formulate on-board algorithms for minimum time and fuel trajectories.

Of corollary interest to the above work is the technical argument between Schultz [16] and Speyer [17] concerning whether steady-state cruise can ever be part of the optimum trajectory solution. However, from a practical point-of-view, cruise should be defined in a simple way (such as the steady state condition) so that on-board mechanization of the reference trajectory is facilitiated.

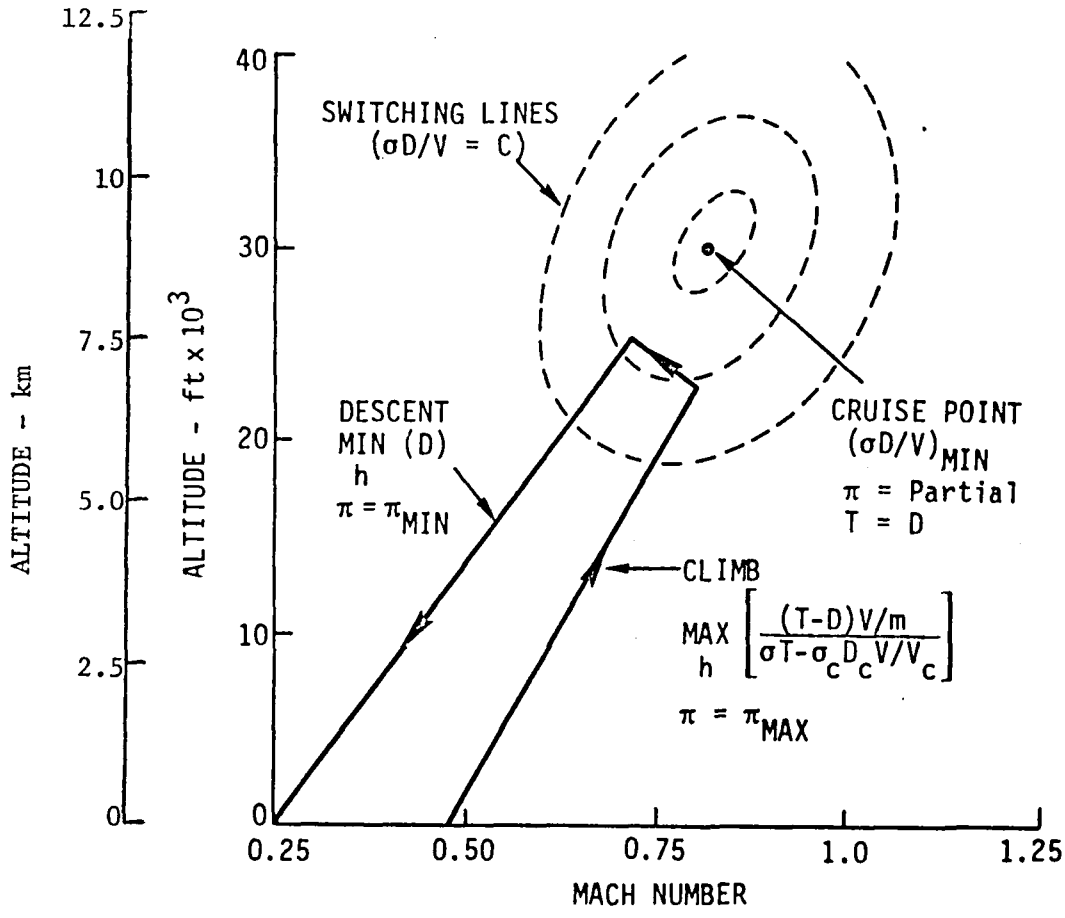

Figure 4. One Solution to the Minimum Fuel-Fixed Range Problem [14].

Also of related interest are the efforts of Kelley [18], Calise [4,19], and Ardema [20] in applying singular perturbation theory to find rapid solutions to the "exact" trajectory optimization problems and to improve the results of energy state methods. In Ref. [20], Ardema compares energy state, zeroth order and first order singular perturbation, and steepest descent solutions to the minimum time-to-climb problem. The first-order singular perturbation solution produced essentially the same trajectory but required about 1/40th the computation cost of the steepest descent solution. Aggarwal and Calise [4] found zeroth order reference solutions for the minimum cost climb-cruise-descent problem for five different Air Force bombers and tankers flying over fixed ranges.

Recent contributions to the practical solution of minimum cost vertical profiles have been obtained by Erzberger and his collegues at NASA Ames Research Center [21,22,24,27]. Erzberger uses the assumption that aircraft

energy is monotonically increasing during climb and monotonically decreasing during descent. Thus, E is chosen to serve as the independent variable. This result produces a constant value for the adjoint variable λ on an optimum trajectory - that being the steady-state cruise cost. The result is minimization of the Hamiltonian at increasing energy values during climb, or

$$\min_{\pi,V} \left[\frac{C_f \dot{w} + C_t - \lambda(V + V_w)}{(T-D)V/mg} \right], \tag{13}$$

where the controls are airspeed and throttle setting. Here, V_w is the longitudinal component of the wind. (More details are given about the derivation of Eq. (13) in Chapter III.) The descent portion of the trajectory is generated backwards in time with energy rate constrained to be negative. As can be seen, Eq. (13) is the inverse of Eq. (10) when allowance is made for the cost of time, the longitudinal effect of wind, and the difference in controls. The algorithm developed from Eq. (13) was used to determine the tradeoff between fuel and time for fixed range flights as shown in Fig. 5. Equation (13) also can be incorporated as an on-board algorithm, as discussed in Chapter V.

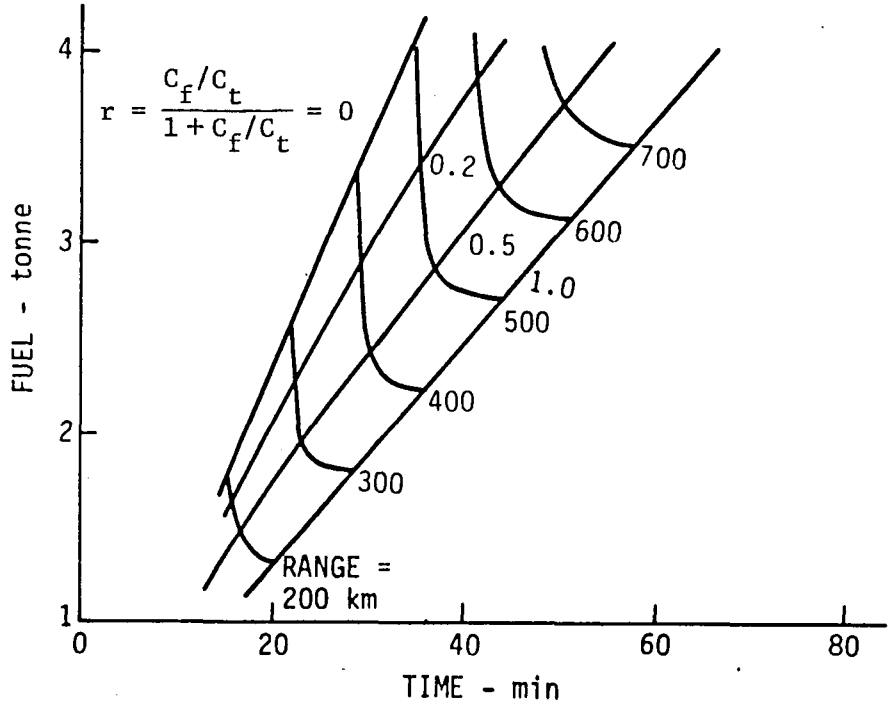

Figure 5. Time-Fuel Tradeoff for Fixed Ranges [21].

It was further recognized by Erzberger (24) that optimum trajectories with thrust constrained to the maximum value for climb and to the idle value for descent have different characteristic shapes than those where climb and descent thrust are free. These characteristic shapes were derived by analysis of the transversality conditions, and they are sketched in Figs. A.4 and A.5 of Appendix A. Using variable thrust can reduce fuel consumption by about 1% for certain engines (where fuel flow rate is not linearly proportional to thrust). It was also revealed by Erzberger and others [22,23] that with a shear headwind, there could be more than one optimum cruise altitude for the same range. This is illustrated in Fig. 6.

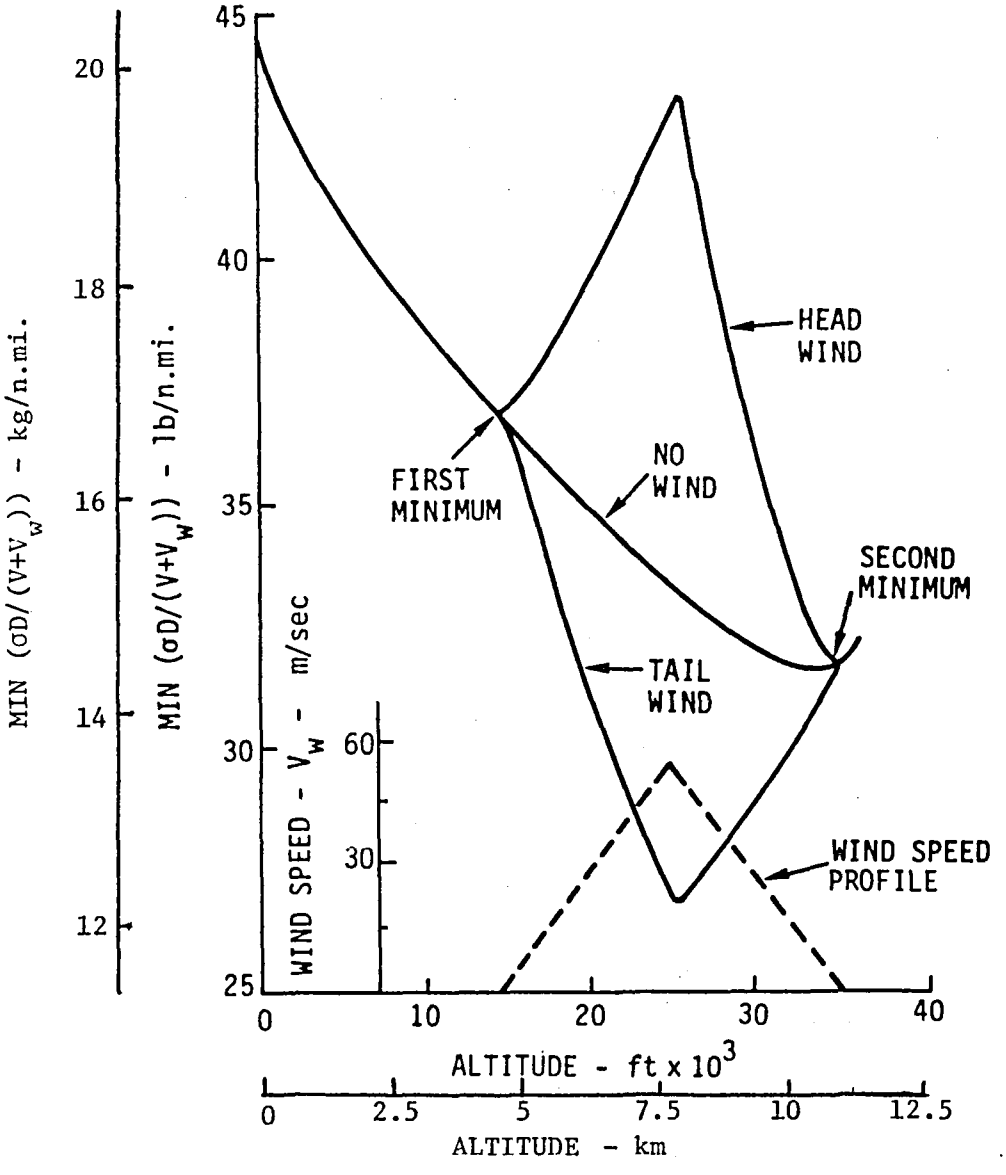

Figure 6. Minimum Cruise Fuel Consumption per Unit Range for the DC-10 [23].

Bochem and Mossman [25] have investigated the implementation of flight path and thrust management strategies outlined in Ref. 24. This effort involved real-time simulation of the flight path guidance algorithms on a DC-10 simulator, and evaluation of the system performance in a simulated environment.

The Boeing Company [26] is also studying the application of the above methods to generate near-optimum vertical profiles. One Boeing algorithm used to find reference trajectories which reduces fuel usage finds

$$\max_{V} \left[\frac{(T-D)/mg}{(\sigma T/V) - \sigma_c D_c/V_c} \right]; \qquad \pi = \pi_{max} \tag{14}$$

for climb and

$$\min_{V} \left[\frac{(D-T)/mg}{(\sigma_c D_c/V_c) - \sigma T/V} \right]; \qquad \pi = \pi_{min} \tag{15}$$

for descent. These can be seen as variations of Eq. (10) and a special case of Eq. (13).

Current work being conducted by NASA Langley Research Center includes developing the on-board capability for making idle thrust fuel efficient descents to a metering fix at a desired time previously specified by the ATC system [27]. They have also studied advanced air transportation concepts using flying wings which may reduce fuel usage up to 90% [28]. NASA Ames Research Center is currently flight testing minimum noise/fuel descents for powered lift STOL aircraft [29].

In summary, there has been considerable research work that has been directed at the problem of reducing in-flight direct operating costs. Several companies today advertise that they sell such systems (black boxes) which can be used to reduce flight fuel consumption. However, the following details are normally missing in discriptions of these systems: what specific algorithm is implemented, how is it interfaced to sensors and other avionics equipment, what computer capacity is required, and what amount of fuel (and time) is actually saved by the system compared to a true optimum. It is the intent of this work to begin to provide such details for a near-optimum system.

III

COMPUTATION OF THE NOMINAL OPTIMUM VERTICAL PROFILE

In this chapter, an algorithm is derived which serves as the basis for generating an optimum vertical profile. This profile can either be generated before flight or as a background computation while in flight. Considerations of the mechanization are discussed in Chapter V.

Derivation of the Optimization Algorithm

Begin with the cost function given as Eq. (2) and repeated here.

$$J = \int_0^{t_f} (C_f \dot{w} + C_t) dt. \tag{16}$$

That is, over the length of flight, it is desired to minimize a combination of both fuel and time. These quantities cost C_f (\$/lb) and C_t (\$/hr). This cost function is general in the sense that if C_f is zero, the trajectory will be in minimum time. If C_t is zero, the trajectory will be minimum fuel.

For general trajectory shaping, the flight path angle dynamics of Eqs. (1) can be neglected, and it can be assumed that the angle-of-attack α is small. Then, the equations of motion of the aircraft in the longitudinal plane are

$$\begin{aligned} \dot{V} &= (T-D)/m - g \sin \gamma \ , \\ \dot{h} &= V \sin \gamma \ , \\ \dot{x} &= V \cos \gamma + V_w , \end{aligned} \tag{17}$$

where the longitudinal component of the wind velocity is included.

Now, based on previous researchers' experience, the specific energy and its derivative are defined according to Eqs. (3) and (4). The first and second of Eqs. (17) are replaced with

$$\dot{E} = V(T-D)/mg \ . \tag{18}$$

Consider again the cost function of Eq. (16). What is actually desired is to minimize the cost in flying from origin P_1 to destination P_2, where the time of flight t_f is considered to be free. The cost function can be changed to have range as the independent variable by dividing Eq. (16) by the expression for range rate, or

$$J = \int_{P_1}^{P_2} \frac{(C_f \dot{w} + C_t)}{V \cos \gamma + V_w} dx \triangleq \int_{P_1}^{P_2} \frac{dc}{dx} dx \ . \tag{19}$$

The remaining state equation (Eq. (18)) also is changed as

$$\frac{dE}{dx} = \frac{dE}{dt} / \frac{dx}{dt} \ ,$$

$$= \frac{(T-D)}{mg} \left(\frac{V}{V \cos \gamma + V_w} \right) \ . \tag{20}$$

This neglects the rate of fuel flow as a function of distance. Practical experience [24] has shown that as long as the current value of aircraft weight (mg) is used in Eq. (20), this simplification is appropriate.

Equations (19) and (20) are combined, using the procedures outlined in Appendix A to form the Hamiltonian,

$$H = \frac{dc}{dx} + \lambda \frac{dE}{dx} \ , \tag{21}$$

$$= \frac{C_f \dot{w} + C_t + \lambda V(T-D)/mg}{V \cos \gamma + V_w} \ .$$

As can be seen, this is a more elaborate Hamiltonian than assumed by Schultz and Zagalsky in Eq. (8). It allows for penalizing of time, it assumes no particular form for the fuel flow rate $\dot{w}$, and it takes into account the horizontal component of the wind V_w.

Note, again however, that none of the terms in Eq. (21) are explicit functions of the independent variable x. Then, according to the arguments associated with Eq. (A.12) in Appendix A, this Hamiltonian is a constant. This greatly facilitates obtaining the optimum profile solution.

Again, assume that the thrust T is a function of the engine pressure ratio (EPR) setting π. The two control variables can then be considered to be π and airspeed V for this simplified dynamic model. (Later, these arguments will be extended so that the conventional controls - throttle and elevator deflection - are used). Both π and V have upper and lower bounds. By following Eq. (A.11), the Hamiltonian H is minimized according to

$$\frac{\partial H}{\partial \pi} \delta\pi \geq 0 , \tag{22a}$$

$$\frac{\partial H}{\partial V} \delta V \geq 0 , \tag{22b}$$

for all admissible values of π and V. For an assumed constant value for H, Eqs. (21) and (22) constitute three equations with three unknowns - π, V, and λ at every point along the optimum trajectory.

Using the arguments of Ref. (21) - (24), assume that the vertical flight profile consists of three phases:

(a) a climb portion where both altitude and energy are monotonically increasing with range;

(b) an essentially equilibrium cruise portion where thrust equals drag and lift equals weight; and

(c) a descent portion where both altitude and energy are monotonically decreasing as range-to-go decreases.

For the cruise portion, the Hamiltonian can then be written as,

$$H_c = \frac{C_f \dot{w} + C_t}{V + V_w} . \tag{23}$$

For a given cruise altitude and weight, the EPR setting and airspeed are found by numerical search techniques such that the value of this expression is minimized. This value of the Hamiltonian is then the constant value used to climb to and descend from this altitude. It also represents the minimum cost per unit distance traveled along the cruise path. (This implies that the cruise altitude and weight are known. These issues are also discussed later.)

The constant value of H_c can be substituted into Eq. (21), and Eq. (21) can be solved for the negative value of the unknown costate:

$$-\lambda = \frac{C_f \dot{w} + C_t - H_c (V\cos\gamma + V_w)}{V(T-D)/mg} . \tag{24}$$

Thus, to minimize the cost function expressed by Eq. (21) requires that values of π and V be chosen such that Eq. (24) is minimized at every point along the climb and descent path. Equation (24) is the key algorithm to both offline and on-board computation of the optimum trajectory that minimizes direct operating cost. It can be seen again that this is a more elaborate version of the algorithm suggested by Zagalsky in Eq. (12).

The work of Erzberger [21,22,24,26,30] has been based on an alternate approach to this problem. He used specific energy E as the independent variable with the assumption it always increases monotonically during climb and that it decreases monotonically during descent. Thus, the remaining state variable is the last of Eqs. (17), and Eq. (21) is replaced by

$$H = \frac{dc}{dE} + \lambda \frac{dx}{dE} ,$$

$$= \frac{C_f \dot{w} + C_t + \lambda (V\cos\gamma + V_w)}{V(T-D)/mg} . \tag{25}$$

This is a repeat of Eq. (13) with a sign change on λ.

Equation (25) can be compared to Eq. (24), and it can be seen that the Hamiltonian H and the costate variable λ have reversed roles. Thus, these two solutions are duals of one another. For energy as the state variable, Erzberger shows, using transversality conditions, that λ is constant and is equal to the negative value of the cruise cost. In this case, the Hamiltonian varies in magnitude because variables within Eq. (25) vary with the magnitude of the specific energy (the independent variable).

Generation of Nominal Optimum Trajectories

Because Eq. (24) and (25) are essentially identical in character and concept, it was convenient to make use of the computer program previously developed by Erzberger and Lee [30] to procede with generating optimum profiles. This program is based on the use of Eq. (25). To avoid confusion, the following description refers to minimizing the Hamiltonian of Eq. (25) with the costate variable λ treated as the constant. The computer program uses principles described in Ref. 30 and is summarized in the second part of Appendix A. This program (referred to as OPTIM) which generates an optimum profile between origin and destination points was extended to have additional desired features, and its specific characteristics (from a programming point of view) have been documented in a companion users' guide [31] to this report. It is instructive here, to present in general terms, the elements and steps required to generate an optimum trajectory.

The following quantities must be input to the program for generating points on the optimum profile:

a) The aircraft initial takeoff altitude, airspeed, and weight,

b) The final desired aircraft altitude and airspeed,

c) The range between and heading to be followed by the aircraft from the origin to the destination points,

d) The wind velocity and temperature profiles (if other than normal) as functions of altitude, and

e) The values of the constants C_f and C_t in the cost function.

The program must have access to numerical data (either tables or polynomials) which produce values of lift and drag coefficients C_L and C_D, thrust T, and fuel flow rate $\dot{w}$ as functions of altitude, airspeed, temperature, and EPR setting. Also, for the particular aircraft being used, the program must have the following two sets of empirical equations:

a). A method of guessing the approximate initial cruise weight based on initial takeoff weight and the values of fuel and time cost; and

b). A method of guessing the approximate landing weight based on the final cruise weight.

Finally, the program must have an efficient procedure which can be used to find the minimum value of the Hamiltonian (Eq. (25)) at each energy level by varying one or more variables (here, π and V) over their admissible regions. For the OPTIM program, the Fibonacci search technique is used.

It must be mentioned that for some cases, there is no cruise section of flight, as is explained in Appendix A. In this case, the constant value of the costate variable refers to what would be the cruise cost at the highest point on the trajectory where the profile transitions from climb to descent.

The basic steps that the optimum profile generation program follows are:

1). The minimum value of cruise cost (Eq. (23) and Eq. (36)) is evaluated for various cruise weights and with altitude varying from sea level to ceiling height. The results are tabulated in a "cruise table". A typical example of cruise cost as a function of altitude is shown in Fig. A.7.

2). Based on initial weight and values of C_f and C_t, the amount of fuel required for the climb is approximated (See Eq. (A.38)). This produces cruise weight which is used to determine the optimum cruise cost and altitude from the cruise table. The cruise cost (λ in Eq. (25); $-\psi(E_c)$ in Appendix A) is required for minimization of Eq. (25). Also, choosing the cruise cost from the cruise table also produces the associated maximum values of energy E_c where the climb portion of flight ends.

3). The next step is to minimize the Hamiltonian (Eq. (25)) at each point along the climb trajectory. This begins at the computed initial energy and stops with the precomputed final climb energy. The numerical procedure procedes as follows:

a). A step is made in specific energy ($E_n = E_{n-1} + \Delta E$), where the step size is held constant.

b). The range of acceptable values of V and π are computed for this energy value.

c). Over these ranges, the Hamiltonian (Eq. (25)) is minimized with γ assumed to be small ($\cos\gamma \cong 1$). This, then specifies the values of airspeed, lift, drag, thrust, altitude, fuel flow rate, and energy rate (Eq. (18)).

d). The time required to make this step is computed as

$$\Delta t = \Delta E/\dot{E} \quad . \tag{26}$$

e). The flight path angle is then computed as

$$\gamma = \sin^{-1} (\Delta h/\Delta t)/V. \tag{27}$$

f). The value of range is increased by Δx, where

$$\Delta x = (V \cos\gamma + V_w(h))\Delta t. \tag{28}$$

g). The aircraft weight is decreased by Δw, where

$$\Delta w = \dot{w} \Delta t. \tag{29}$$

This procedure is repeated until the initial cruise energy level is reached. This produces an accurate measure of the fuel burned during climb and the range traveled during climb.

4). A final approach (or landing) weight is approximated by estimating the cruise range, cruise fuel, and other related quantities (See Eqs. (A.42) - (A.46)). This procedure also produces an estimate of the final cruise altitude, energy, and cruise cost.

5). The procedures for generating the descent profile are now followed using the same sequence as for Step (3) but by going backwards in time and constraining the energy rate to be negative. This is continued until the estimated final cruise energy level is reached. This produces an accurate estimate of the fuel burned during descent and the range traveled during descent.

6). The cruise distance is now recomputed by subtracting the climb and descent ranges from the total required. This cruise distance is used to compute the final cruise weight and the final approach (landing) weight,

7). With the revised final approach weight, the descent trajectory is recomputed using Step (5). This also provides refinement of the cruise distance, the total fuel burned, and time required to travel from origin to destination airports.

The above description is somewhat simplified in that profiles of short range flights (e.g., less than 250 n.mi.) require special computations. Figures A.4 and A.5 in Appendix A depict the shapes of the trajectories for short range for two types of control strategies. If both V and π are used as controls, the trajectories have the shapes depicted in Fig. A.5. For this case, with short range there is no cruise segment, and an iterative process is required to obtain the constant value of λ and the maximum energy state used to compute the climb and descent profiles.

If only airspeed is used as the control variable, then thrust is set at maximum climb value for climb and idle value for descent. For the 727 aircraft model used in this study, this increased the cost of the typical short-range profile about 1%. However, it simplifies mechanization and it reduces the time required to compute the profile. Trajectories for this case have the characteristics depicted in Fig. A.4. That is, they have cruise segments, but these segments occur at altitude and energy levels lower than the optimal value E_{copt}. Again, the program must iterate on the correct value of λ, and Eq (A.48) in Appendix A is used to compute the corresponding length of the cruise segment.

The OPTIM program has been constructed so that various options can be exercised:

1). No wind or arbitrary wind

2). Optimize with V and π or V only

3). Arbitrary cost terms C_f and C_t

4). With or without a speed constraint of 250 kt below 3048 m (10,000 ft.)

5). Start in cruise or after takeoff. For starting in cruise, the cruise altitude can be set to a fixed value, or the program will compute the best value associated with the given cruise weight.

In addition to generating optimum nominal profiles for the 727 aircraft, OPTIM can be used to examine the sensitivities in trip cost due to variations in wind, range, takeoff weight, and the cost terms C_f and C_t. Examples of these variations will be given in the next chapter.

The computations that take place in OPTIM for off-line generation of optimum vertical profiles are also the same as would be used by an on-board flight management system. For the on-board mechanization, the flight engineer would enter initial and final altitude and airspeed, initial weight, range, and heading. Wind and temperature profiles and aircraft weight estimates would be updated during flight. The seven basic steps listed earlier would be recomputed every few minutes to provide a current reference trajectory to be followed.

Example Optimum Trajectories

Figures 7 and 8 show plots of various state variables as functions of time (or time-to-go) for optimum climb and descent of a 727 aircraft traveling 200 n.mi. in range. For this example, the indicated airspeed was constrained below 250 kt below 3048 m (10,000 ft). Also, Optimization was done by varying V only, with π set to the maximum value for climb and idle value for descent. The cost constants were \$0.265/kg (\$0.12/lb) fuel and \$600.00/hr. As can be seen, when 3048 m (10,000 ft) is reached, the aircraft levels off and accelerates before continuing to climb. The opposite is true for the descent profile. For these profiles, the reference flight path angle is rough because of the inherent assumption that either altitude, airspeed, or both can be abruptly changed to obtain a change in energy. Flight path angle can be smoothed after it is generated to provide a more flyable path. Note also that no where on either the climb or descent is Mach number constant (contrary to profiles that are specified in aircraft handbooks and normally flown).

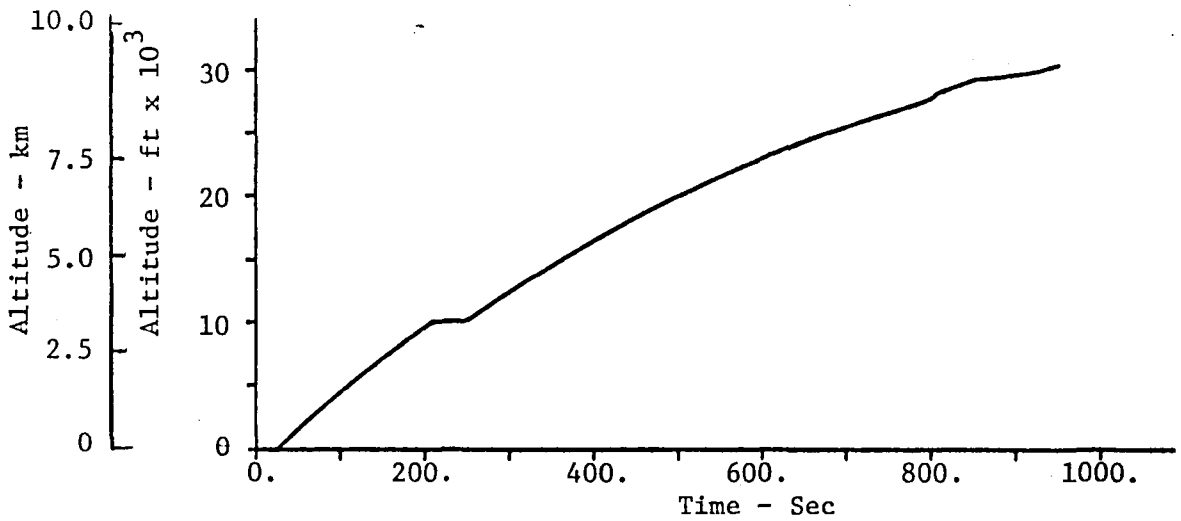

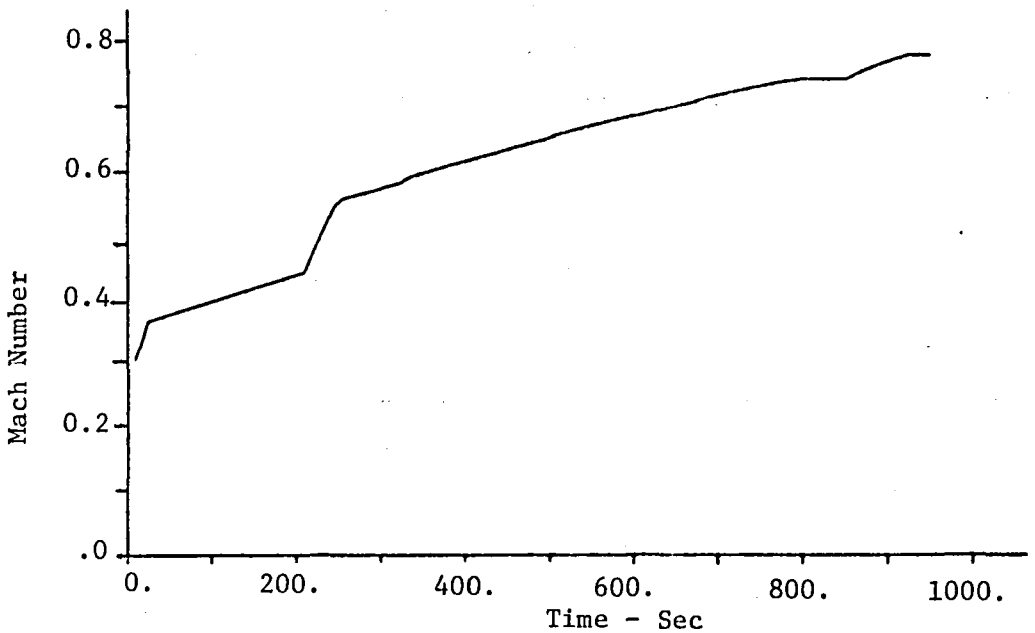

Figure 7. State Variables for an Optimum Climb Profile of a 200 n.mi. Range Flight

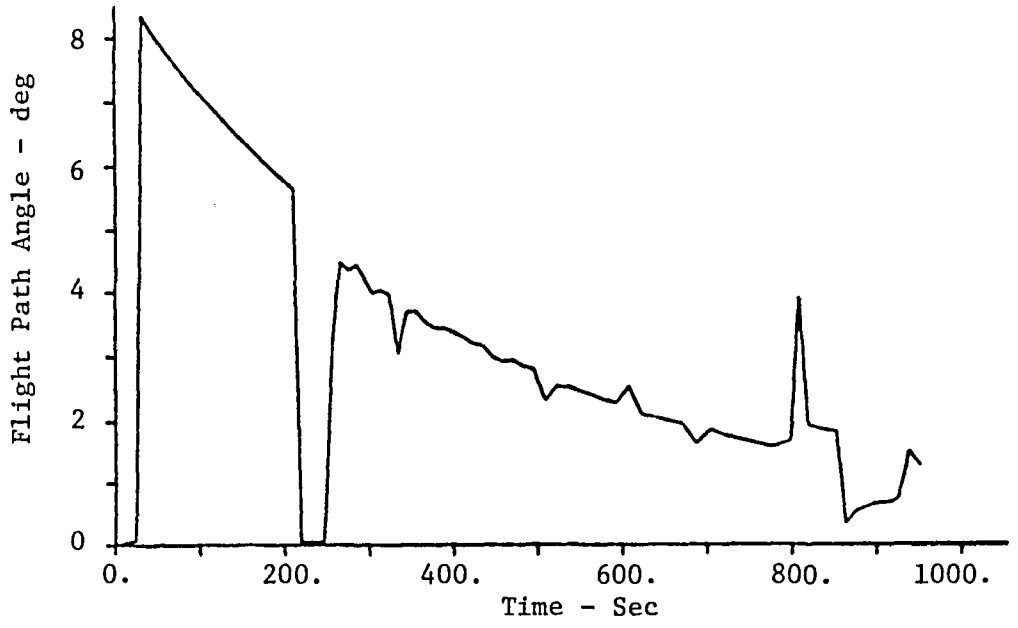

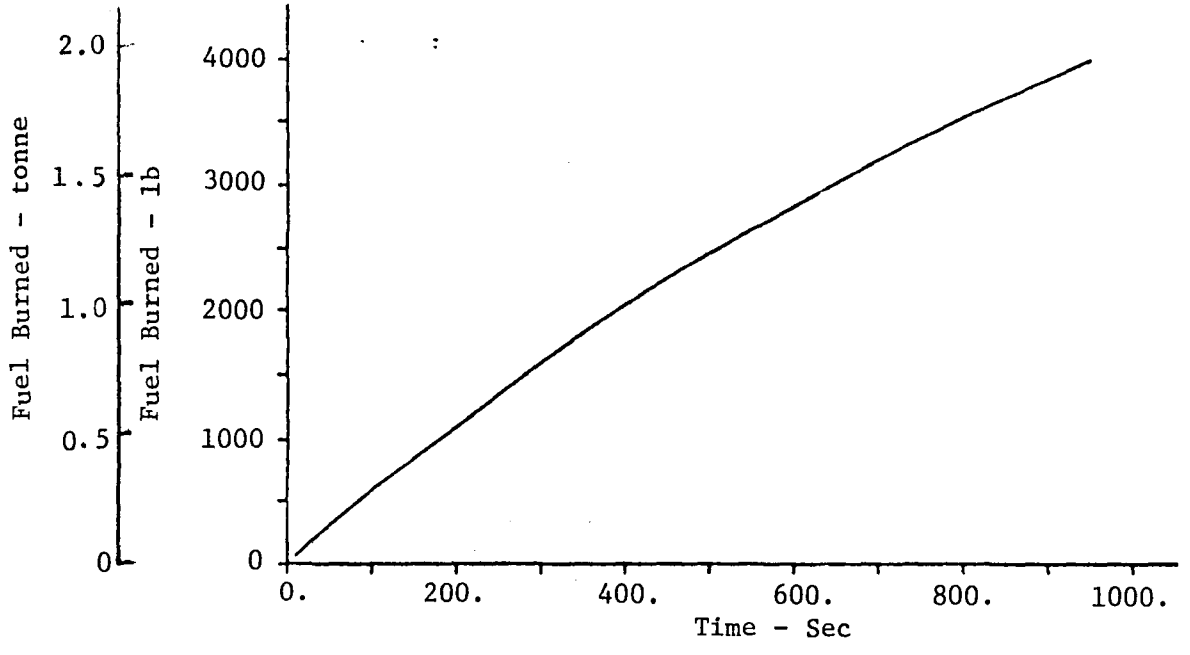

Figure 7. Concluded

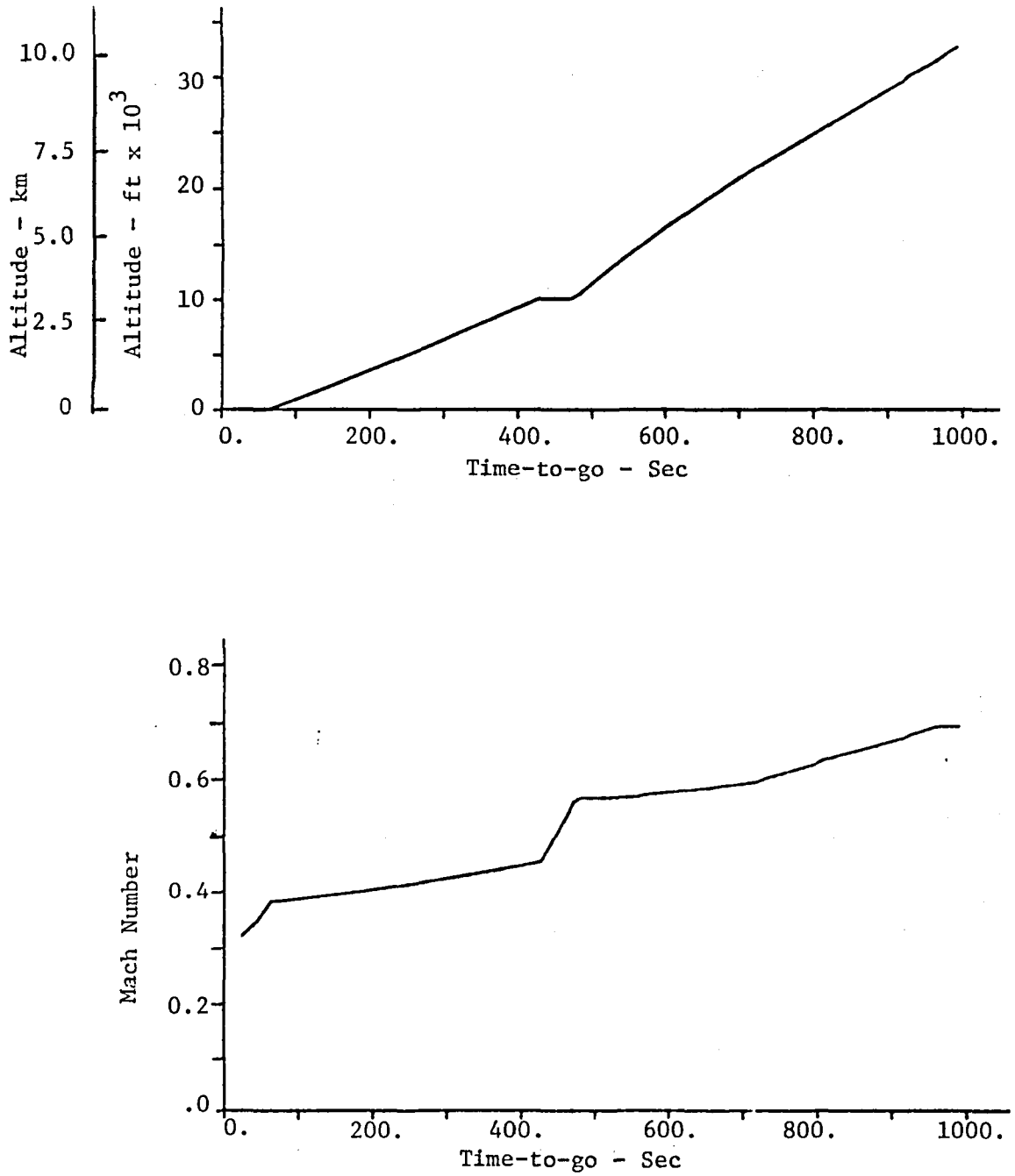

Figure 8. State Variables for an Optimum Descent Profile of a 200 n.mi. Range Flight.

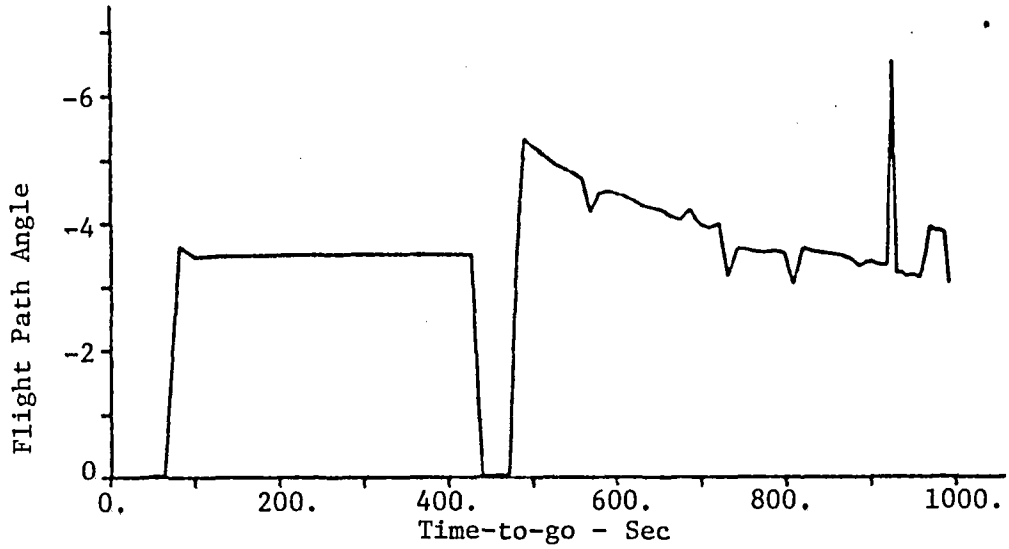

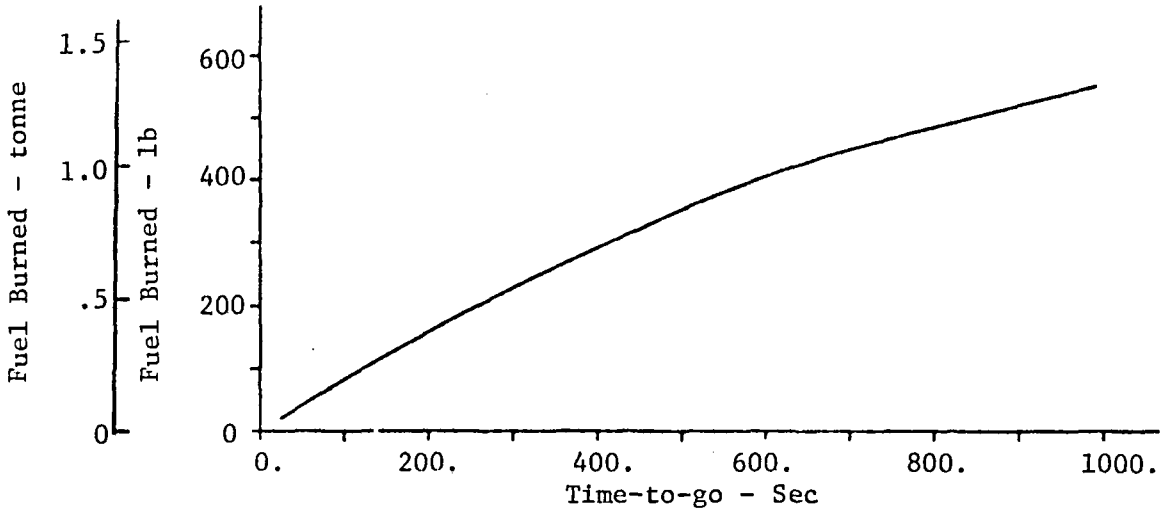

Figure 8. Concluded

Figure 9 compares the altitude vs. range profiles for three cases of a 727 aircraft covering 200 n.mi. For these, both V and π were varied. However, a head wind and tail wind were added in two of the cases to produce the differences. The wind magnitude profile is also shown in Fig. 9, and it is representative of the Denver wind measured in August, 1977.

Table 1 makes various range and cost comparisons of the three profiles shown in Fig. 9, based on values of C_f of \$0.138/kg (\$0.0628/lb) and C_t of \$500.00/hr. It is seen that the head wind caused a total cost increase of \$24.95 (or 4.3%) while the tail wind decreased the cost \$23.59 (or 4.1%) compared to the no wind optimum case. No procedures were available for predicting the cost of these flights if the 727 aircraft were to follow the profile specified in the aircraft handbook. Data, such as presented in Table 1, are printed for each run of OPTIM so that the trajectory costs and other characteristics can be readily evaluated (Again, see Ref. 31).

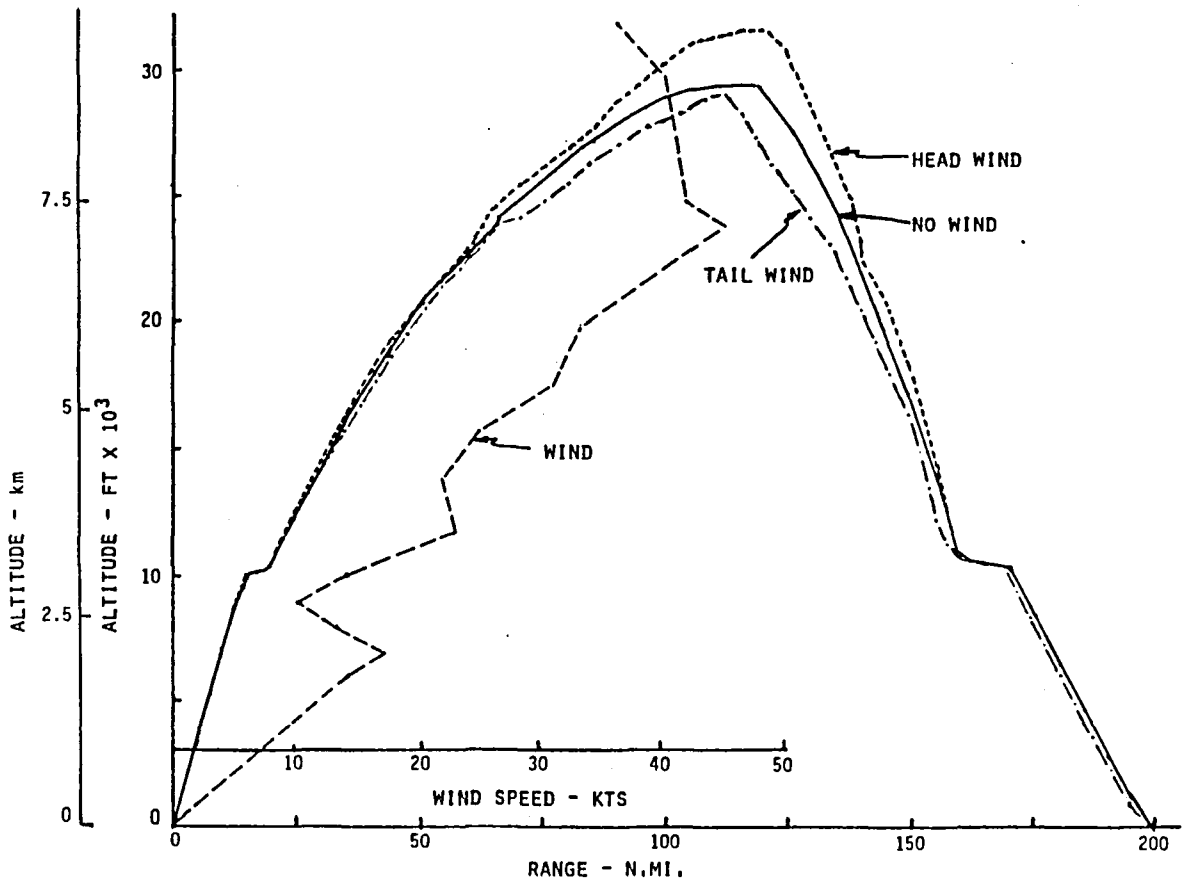

Figure 9. Comparison of Minimum Direct-Operating-Cost Flight Profiles

Table 1. Comparison of Flight Costs for 200 n.mi. Range with Varying Wind Conditions

	Case		
	No Wind	Head Wind	Tail Wind
Fuel Used (kg (lb))			
Climb	1945.8 (4289.60)	2013.0 (4437.82)	1805.2 (3979.66)
Descent	272.2 (600.19)	295.1 (650.57)	284.9 (628.13)
Total	2218.0 (4889.79)	2308.1 (5088.39)	2090.1 (4607.80)
Range (n.mi.)			
Climb	115.51	115.90	107.36
Descent	85.24	85.78	94.60
Total	200.75	201.68	201.96
Time (min:sec)			
Climb	17:31	18:33	15:41
Descent	15:05	15:33	16:11
Total	32:36	34:06	31:53
Cost ($)			
Climb	414.51	432.40	379.91
Descent	163.29	170.35	174.30
Total	577.80	602.75	554.21
Cost/Distance ($/n.mi.)			
Climb	3.59	3.73	3.54
Descent	1.92	1.99	1.84
Total	2.88	2.99	2.74

IV

PROGRAM VERIFICATION AND SENSITIVITY RESULTS

The previous chapter and Appendix A describe an efficient way in which near-optimum flight profiles can be generated without using time-consuming numerical techniques such as described in Refs. 9 and 10. Instead of iteratively solving the two-point boundary value problem, assumptions were made so that the dynamics are simplified to two state variables. One state variable (either range or energy) becomes the independent variable, and the other was included as the single state in the Hamiltonian. Thus, the problem of solving for minimum cost profiles reduced to algebraic minimization of the Hamiltonian at each point along the profile.

Now, although this method is a convenient way of generating a trajectory, the resulting trajectory must be verified by using a more accurate model of the aircraft dynamics. Verification implies that:

1) The reference trajectory that is generated must be flyable when the full aircraft equations of motion and constraints are taken into account.

2) The trajectory cost (Eq. (2)) as predicted by OPTIM must be essentially identical to that experienced by simulating more complete aircraft equations of motion.

Thus, the first objective of this chapter is to describe a companion program to OPTIM which was developed for verification of the optimization results. This program is referred to as TRAGEN (for trajectory generation).

With OPTIM and TRAGEN as computer tools, the user has the capability to study the characteristics of optimum profiles in great detail and to examine alternate ways these profiles can be implemented on-board. Trajectory characteristics are obtained by making sensitivity studies which is the subject of the second part of this chapter.

Optimization Verification

To achieve optimization verification required the development of a companion computer program to OPTIM which can be used to simulate the longitudinal trajectory of an aircraft commanded to follow the reference path output from OPTIM. Some details of this program (TRAGEN) are presented in Appendix B, and a separate user's guide for this program has also been written [32].

In addition to verification of the optimization program's results, the TRAGEN program has the following utility:

1). It provides a means for testing guidance laws for steering the aircraft to follow the input reference trajectory.

2). It enables study of the effect of following an incorrect reference trajectory. For example, if the OPTIM results were based on one particular wind profile and initial aircraft weight, and a different weight and wind profile actually existed, the TRAGEN simulation would allow assessment of the effect of these errors on trajectory cost.

3). It can be used to determine the flight cost that would result from the aircraft being commanded to follow a reference trajectory suggested in the manufacturer's aircraft handbook. For example, for climb, handbook reference trajectories usually consist of following a constant indicated airspeed until a given Mach number is reached. Then, the reference trajectory follows this fixed Mach number until the reference cruise altitude is reached.

4). It can be used to test perturbation control schemes for removing the effect of wind gusts and other non-nominal performance sources (navigation errors, transient temperature profiles, non-standard engine performance).

5). It is expandable to test candidate on-board mechanizations of a system of equations for generating the near-optimum vertical profile.

A five state-variable model of the aircraft is currently used in TRAGEN to simulate longitudinal motion. State variables are altitude, altitude rate, longitudinal range, airspeed, and aircraft mass. Currently neglected are the rapid transient dynamics of throttle response, angle-of-attack, and pitch rate (δ_T, α, q). The throttle is assumed to be set so

that maximum thrust is achieved during climb and idle thrust is used during descent. The cruise phase is not simulated. The altitude control variable is taken to be the angle-of-attack which has maximum and minimum limits. This degree of sophistication is adequate for testing the OPTIM results.

The TRAGEN program can readily be expanded to include throttle dynamics and short period dynamics. This would be required for further study of autothrottle and autopilot design to steer the aircraft to follow input reference trajectories. The control variables would be throttle position and elevator deflection for this expanded capability. A requirement for implementing this expanded simulation would be to obtain the necessary stability and control derivatives to complete the dynamic model.

The specification of reference profiles used in TRAGEN is based on using altitude as the independent variable for climb and range-to-go to the destination as the independent variable for descent. For climb, the reference trajectory consists of specifying airspeed and flight path angle (with respect to the air mass) as piecewise linear functions of altitude. At the 3048 m (10000 ft) point, the aircraft is commanded to level off and accelerate until the airspeed is reached where the climb should again continue.

To generate the control law to follow the commanded climb profile, a linear perturbation model was made of the dynamic equations,

$$T \cos \alpha - D(\alpha,h,v) - W \sin \gamma = m\dot{V} \,, \tag{30}$$

$$T \sin \alpha + L(\alpha,h,v) - W \cos \gamma = mV\dot{\gamma} \,.$$

The perturbation equations and transfer functions from Eqs. (30) are given in Eqs. (B.10) and (B.11) in Appendix B. Here, it is assumed that a perturbation $\delta\alpha$ to the nominal angle-of-attack can be used to obtain the desired perturbations in flight path angle ($\delta\gamma$) and airspeed (δV) to maintain the aircraft on the desired reference climb profile.

Because both commanded values of airspeed and flight path angle are assumed to vary linearly with altitude, they are ramp functions, and a Type 1 control system is suggested. The original climb control law was thus set to be

$$\delta\alpha = \left(K_1 + \frac{K_2}{s}\right)(V_c - V) + \left(K_3 + \frac{K_4}{s}\right)(\gamma_c - \gamma) \qquad (31)$$

where V_c and γ_c are the commanded reference values of V and γ. K_1, K_2, K_3, and K_4 are control gains. The commanded values were derived according to Eqs. (B.12) and (B.13).

Experience with this control law revealed two points:

1) The integral control gain K_2 on airspeed error was not needed and did not particularly improve performance. Thus, it was nominally set to zero.

2) Constant values of the gains K_1, K_3, and K_4 could be selected to provide good, stable performance throughout the climb phase. Thus, there was no need to have altitude dependent gains programmed.

No attempt was made to select the control gains so that the perturbation response was optimized. The main objective was to obtain a set of gains which caused the aircraft simulation to track the input reference trajectory adequately (which was accomplished). Gain selection for control response optimization should remain as a task to be conducted when an actual autopilot/autothrottle is being implemented where the complete aircraft dynamics are considered.

Several optimum trajectories were computed by using OPTIM and then subsequently used as inputs to drive the TRAGEN simulation. For example, Table 2 presents a comparison of OPTIM and TRAGEN results for the climb portion of a 727 initially weighing 61236 kg (135000 lb), and traveling a total range of 150, 225, and 275 n.mi. with no wind. As can be seen the match is exceptional. The same degree of comparison was found using the two programs for different range and different initial weight flights.

Table 2. Comparison of Optimization and Trajectory Generation Program Climb Results for Different Range Flights. No Wind. 61236 kg (135000 lb) Takeoff Weight.

Range n. mi.	Fuel Burn - kg (lb)		Time - Sec		Altitude - m (ft)		Airspeed - m/s (ft/s)		Range - m (ft)	
	OPTIM	TRAGEN	OPTIM	TRAGEN	OPTIM	TRAGEN	OPTIM	TRAGEN	OPTIM	TRAGEN
150	1405 (3097)	1405 (3097)	682	680	7597 (24924)	7597 (24926)	230 (756)	229 (752)	125127 (410522)	125054 (410281)
225	1931 (4258)	1931 (4258)	1060	1060	9760 (32021)	9760 (32021)	244 (801)	244 (800)	211441 (693704)	212936 (698609)
275	2075 (4574)	2073 (4570)	1185	1178	10319 (33855)	10321 (33861)	244 (802)	244 (800)	242116 (794345)	241033 (790790)

The results with head and tail winds were not as close. Table 3 presents a comparison of OPTIM and TRAGEN results when the wind profile of Fig. 9 was used as both a head and tail wind for the 225 n.mi. range flight. In both cases, the more detailed simulation from TRAGEN shows that it takes a longer time period (14-22 sec) and greater range (4000 - 5000 m (14000 - 15000 ft)) than predicted by OPTIM (However, range traveled is not significant for climb.) The biggest discrepancy is the 2.6% extra fuel required for the tail wind case. In the future, the modeling simplifications of OPTIM and the steering accuracy of the TRAGEN control law should be investigated to resolve this point.

Table 3. Comparison of Optimization and Trajectory Generation Program Climb Results in the Presence of Winds. 225 n.mi. range. 61236 kg (135000 lb)

Type Wind	Fuel Burn - kg (lb)		Time - Sec		Altitude - m (ft)		Airspeed - m/s (ft/s)		Range - m (ft)	
	OPTIM	TRAGEN	OPTIM	TRAGEN	OPTIM	TRAGEN	OPTIM	TRAGEN	OPTIM	TRAGEN
Head	2084 (4594)	2082 (4591)	1180	1202	10294 (33772)	10362 (33996)	244 (802)	244 (802)	225177 (738770)	229818 (753997)
Tail	1701 (3751)	1747 (3851)	897	911	9145 (30003)	9074 (29770)	233 (766)	235 (772)	183238 (601174)	187433 (614936)

For the descent portion of the flight, the more likely variable - range-to-go to the destination point - was used as the independent variable for specifying the reference path. In this case, the descent altitude was specified as a function of range. This defined the inertial flight path angle that the aircraft should be on which is defined by Eq. (B.16). In the current version of TRAGEN, no attempt was made to control airspeed during the descent. The control law to compute the perturbation to the angle-of-attack was of the form

$$\delta\alpha = (K_3 + \frac{K_4}{s})(\gamma_{Ic} - \gamma_I) , \tag{32}$$

where γ_{Ic} is the commanded inertial flight path angle.

Despite the lack of control of airspeed during descent, the descent steering provides the same degree of matching performance between OPTIM and TRAGEN results as was experienced during the climb simulation (where airspeed was controlled) down to 3048 m (10,000 ft). Table 4 compares OPTIM and TRAGEN results at about 3048 m (10,000 ft) for a 727 descending with idle thrust from 10668 m (35,000 ft). The three cases are with no wind and the Denver head and tail winds shown in Fig. 9. The biggest error is in airspeed where variations of +5.8 to -1.5 m/s (+19 to -5 ft/sec) are seen.

Table 4. Comparison of Optimization and Trajectory Generation Program Results Descending from 10668 m (35000 ft) to 3048 m (10000 ft).

Type Wind	Fuel Burn - kg (lb)		Time-to-go- s		Altitude - m (ft)		Airspeed- m/s (ft/s)		Range-to-go - m (ft)	
	OPTIM	TRAGEN	OPTIM	TRAGEN	OPTIM	TRAGEN	OPTIM	TRAGEN	OPTIM	TRAGEN
No Wind	117 (259)	117 (258)	444	447	3154 (10348)	3148 (10328)	149 (490)	151 (497)	56704 (186036)	56598 (185688)
Head	110 (242)	110 (242)	444	449	3154 (10348)	3148 (10328)	149 (490)	148 (485)	55465 (181973)	55494 (182066)
Tail	123 (271)	124 (273)	440	441	3154 (10348)	3148 (10329)	149 (490)	155 (509)	57911 (189998)	57856 (189816)

These same cases are compared again at the altitude of 1.8 m (6 ft) in Table 5. The head wind case has a -3.4 m/s (-11 ft/sec) difference in airspeed which causes 7 sec time and 4.5 kg (10 lb) fuel burn differences at this point. The tail wind case has a +5.8 m/s (+19 ft/sec) difference in airspeed which causes - 14 sec time and -1.8 kg (-4 lb) fuel burn differences. These differences could possibly be lessened with airspeed control added.

Table 5. Comparison of Optimization and Trajectory Generation Program Results. Descending from 10668 m (35000 ft) to 1.8 m (6 ft).

Type Wind	Fuel Burn - kg (lb)		Time-to-go - s		Altitude - m (ft)		Airspeed - m/s (ft/s)		Range-to-go - m (ft)	
	OPTIM	TRAGEN	OPTIM	TRAGEN	OPTIM	TRAGEN	OPTIM	TRAGEN	OPTIM	TRAGEN
No Wind	237 (523)	237 (523)	0	8	1.8 (6)	-3.1 (-10)	124 (407)	126 (413)	0	-49 (-157)
Head	230 (506)	234 (516)	0	7	1.8 (6)	-5.2 (-17)	124 (407)	121 (396)	0	-96 (-314)
Tail	243 (535)	241 (531)	0	-14	1.8 (6)	-4.3 (-14)	124 (407)	130 (426)	0	-85 (-280)

Despite the differences between OPTIM and TRAGEN results, it is believed that the match between them is very good. That is, the results provided by OPTIM (fuel burn, time expired, trajectory followed) can be concluded as being accurate, and sensitivity runs based on using both programs will also produce accurate conclusions. A better match between the two programs can be obtained by minor adjustments to both programs.

Sensitivity Analysis

In conducting the sensitivity analysis of the optimum profiles, there are two items that are of particular interest:

1). The establishment of how the characteristics of optimum profiles change with variations in initial weight, range-to-go, wind profiles, and other variables affecting the aircraft performance. Knowing these variations affects how an on-board algorithm should be constructed to account for measured changes in the flight conditions.

2). The analysis of the effect that errors in the assumed flight conditions (i.e., different initial weight, different wind profile) have on the cost of flying a particular profile. For example, if assuming the wrong initial weight of the aircraft has little effect on the overall cost, then the algorithm can be constructed so that initial weight is assumed to be a nominal value.

The purpose of this section is to begin to address these items for wind, initial weight, and range variations. Both OPTIM and TRAGEN are required for this purpose. Other variables that may have an effect are temperature, lift coefficient, drag coefficient, and thrust variations as well as measurement errors of altitude, flight path angle, airspeed (or Mach number), and range-to-go. These variations should be addressed at a future time.

It is assumed for climb that Mach number and flight path angle as functions of altitude specify the optimum profile to a given cruise altitude. Thus, by presenting plots of these variables as functions of altitude, the effect of the variations to the nominal conditions is directly seen.

Figure 10 shows the variations in the climb profile as the total range is varied, in steps of 25 n.mi. from 75 n.mi. to 275 n.mi. As can be seen, there is no variation below 3048 m (10000 ft). Above 3048 m (10000 ft), the flight path angle is initially higher and the climb Mach number is initially lower as the total range is increased. But it is seen that these curves are essentially parallel, and they merge into a common curve for range exceeding 175 n.mi. Thus, it would be relatively easy to model these curves as a polynominal function of altitude with parameter variation due to change in range.

Figure 11 shows the variation in the profile as initial weight is varied. Again, there appears to be a parallel offset with a greater effect on flight path angle. These is no effect on Mach number below 3048 m (10000 ft).) Also, again it can be seen that this variation would be easy to account for in specifying an on-board reference trajectory.

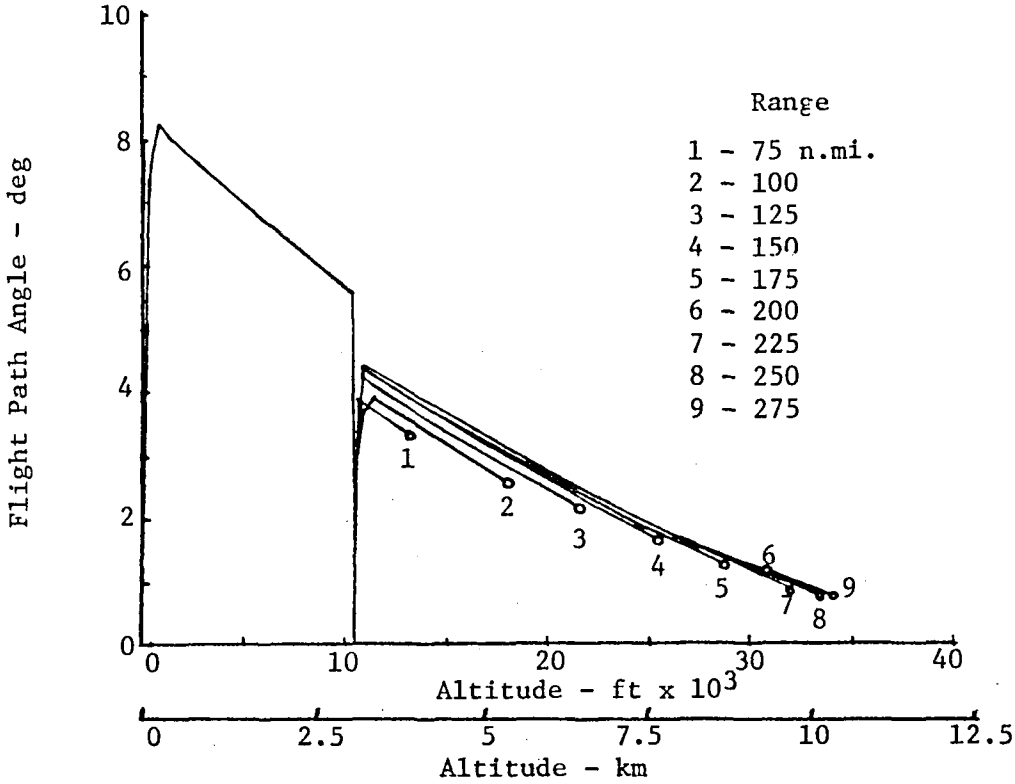

a) Flight Path Angle

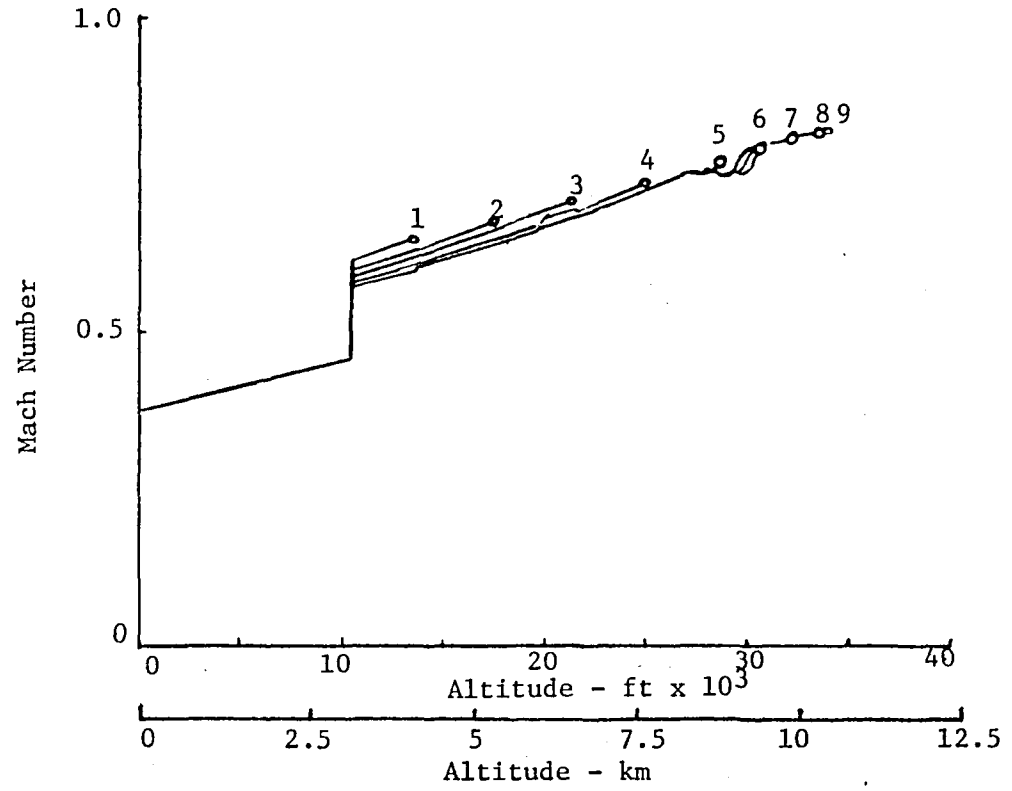

b) Mach Number

Figure 10. Effect of Range Variation on Optimum Climb Flight Path Angle and Mach Number

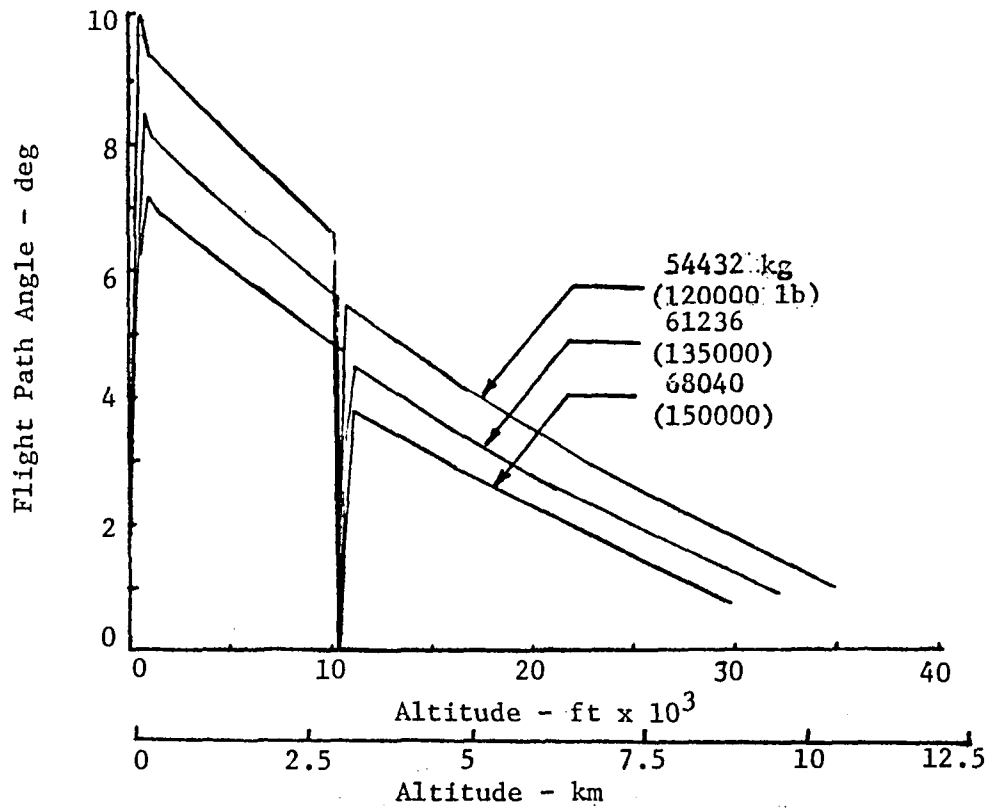

a) Flight Path Angle

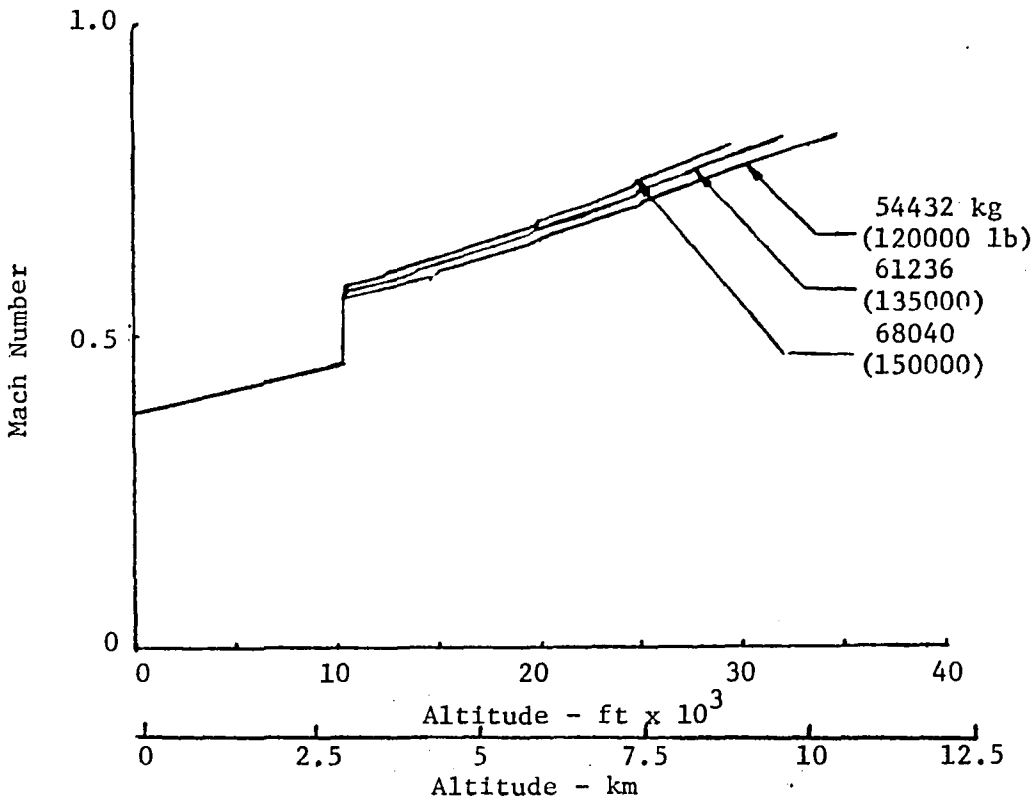

b) Mach Number

Figure 11. Effect of Initial Weight Variation on Optimum Climb Flight Path Angle and Mach Number

The biggest uncertainty that would be experienced during the climb and descent would be the variations in the longitudinal wind. To study this effect, the two wind profiles of Fig. 12 were used as program inputs. The Denver wind is the same as is shown in Fig. 9, but Fig. 12 also has the wind headings indicated at discrete points. The "triangle" wind is a constant 270^{o} heading wind varying linearly in magnitude with altitude at a rate of 1 knot per 305 m (1000 ft). These winds profiles were assumed to act as both tail and head winds by setting the aircraft heading to be 90^{o} or 270^{o}.

Figure 13 shows the effect of each of these wind profiles on the optimum climb trajectory compared to the nominal profile having no wind. As can be seen, the Mach number variation with altitude is essentially a parallel offset. The effect on flight path angle is mainly seen going from zero to 3048 m (10000 ft) where a fan out of $\pm$ 0.3^{o} is seen. Above 3048 m (10000 ft), the variation appears more as a steady offset. Thus, again it appears that accounting for various wind profiles can be done in the on-board system in a relatively simple way. This conclusion is discussed more in the next chapter.

Figure 14 shows the effect of each of the wind profiles on the optimum descent from 10058 m (3000 ft). There, the plots show altitude and Mach number as functions of range-to-go to the landing point. From the first plot, it is seen that wind causes a $\pm$ 10 n.mi. range variation in where the optimum descent should begin. This is predictable based on knowing how far the air mass moves due to the wind during the descent period. Also, there is up to a $\pm$ 0.05^{o} variation in the optimum Mach number as a function of range-to-go. From the earlier results presented, it was shown that if the altitude-range profile was followed closely down to 3048 m (10000 ft), the Mach number would also follow the nominal profile. Thus, from an implementation point-of-view, the Mach variations seen above 3048 m (10000 ft) in Fig. 14b are not of concern. Below 3048 m (10000 ft), only one profile needs to be stored.

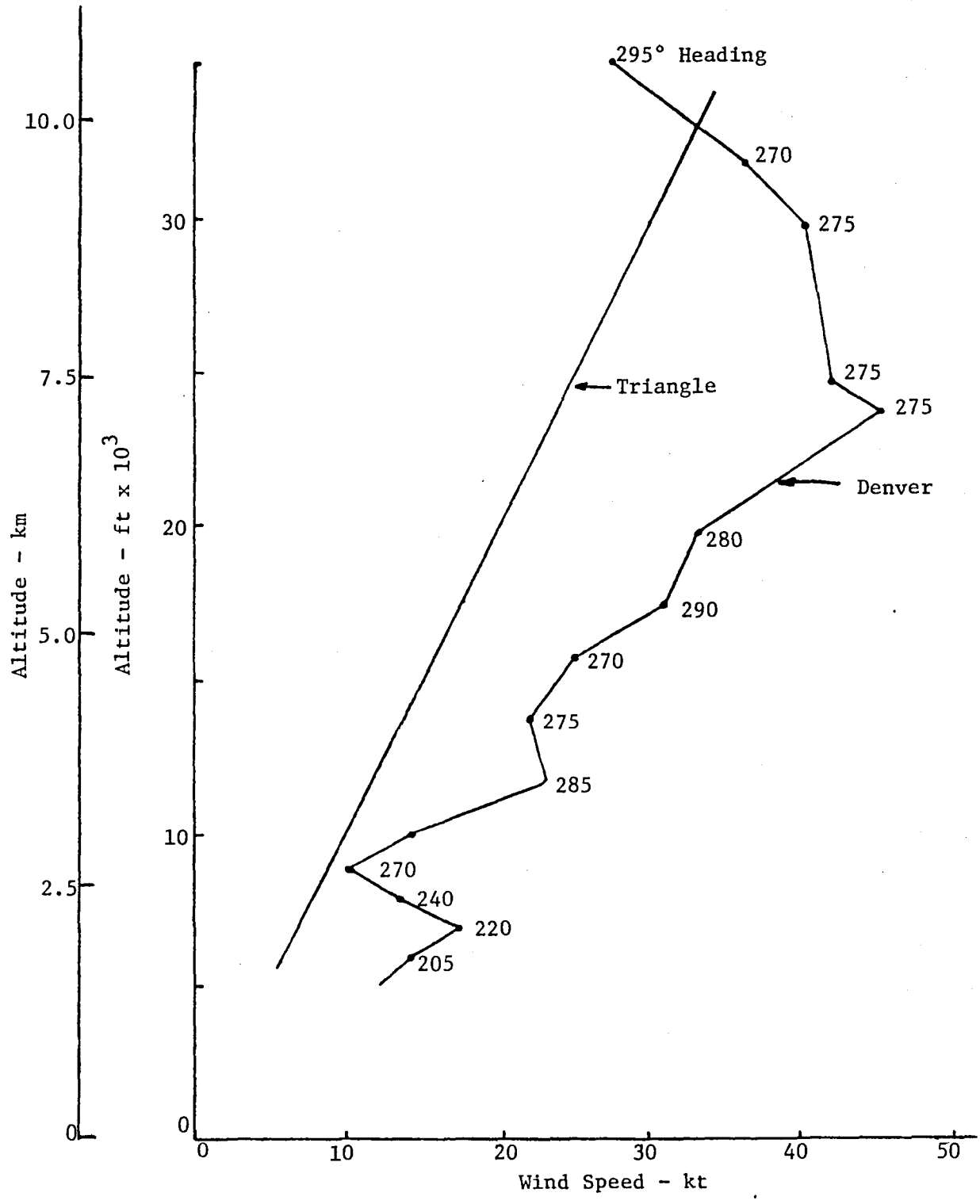

Figure 12. Wind Profiles Used to Study Sensitivity Effects on Optimum Profiles.

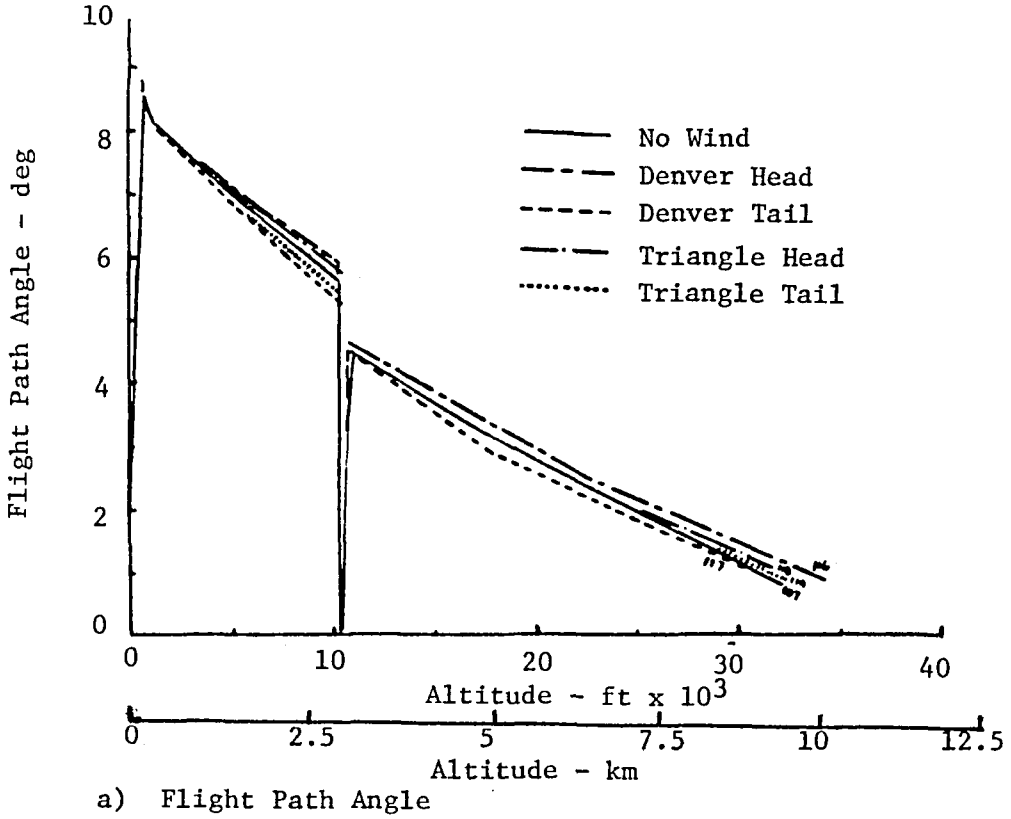

a) Flight Path Angle

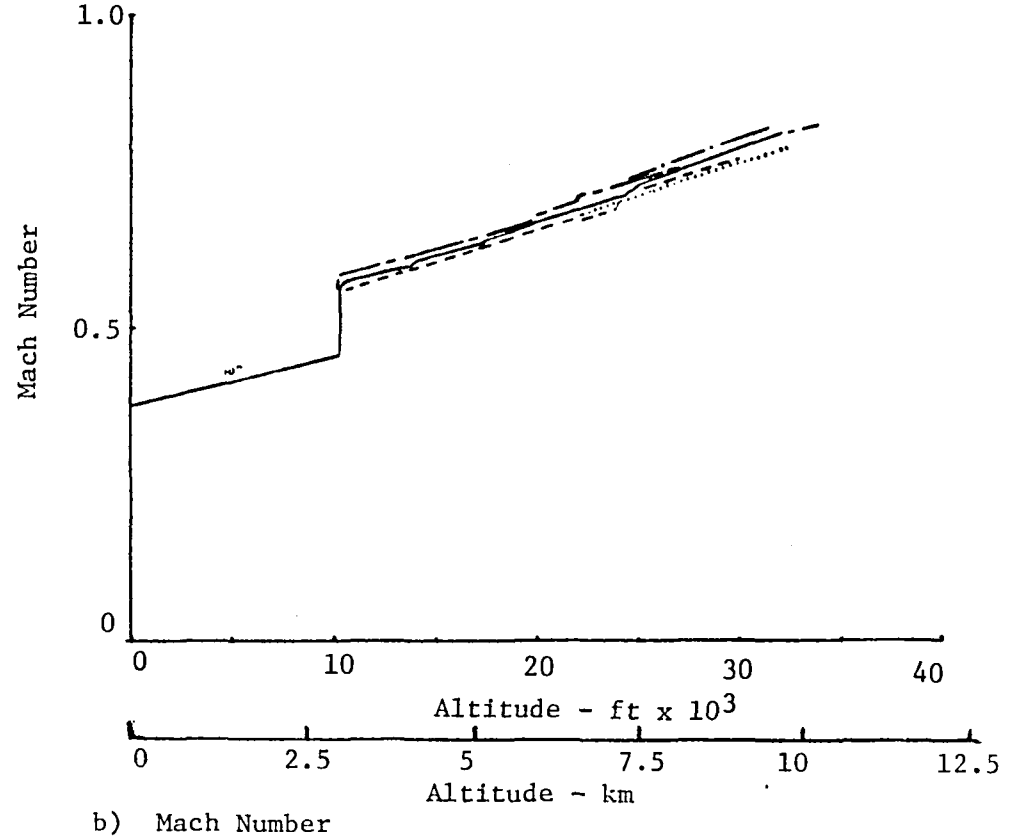

b) Mach Number

Figure 13. Effect of Wind Variations on Optimum Climb Flight Path Angle and Mach Number

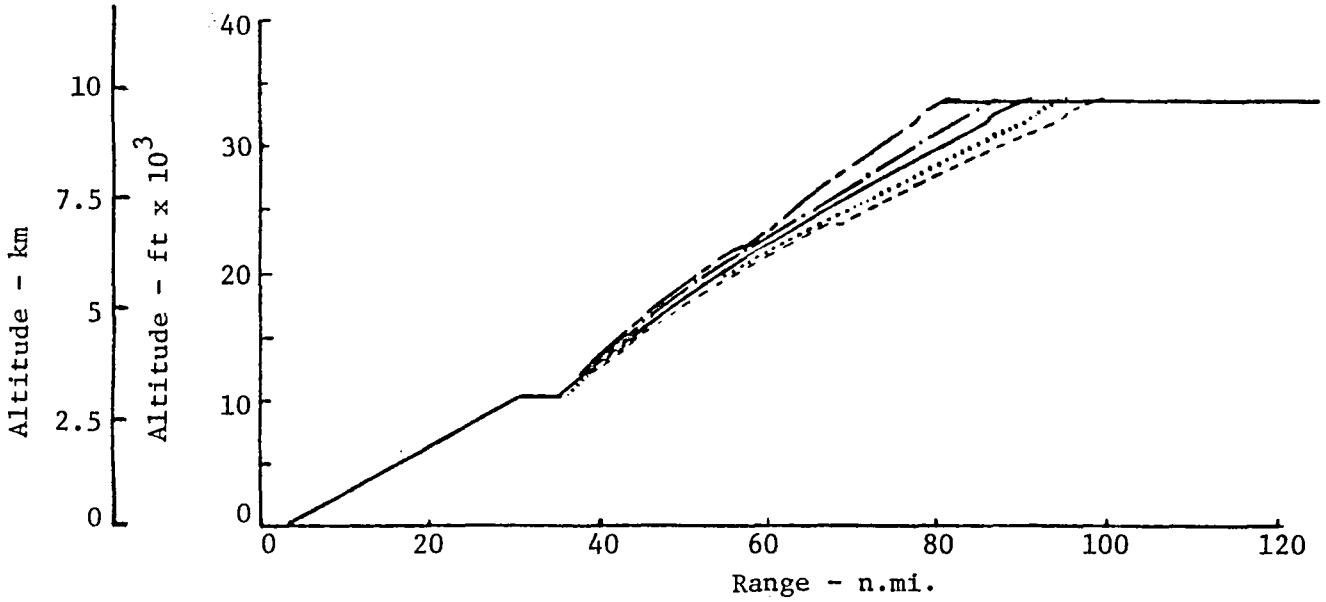

a) Altitude

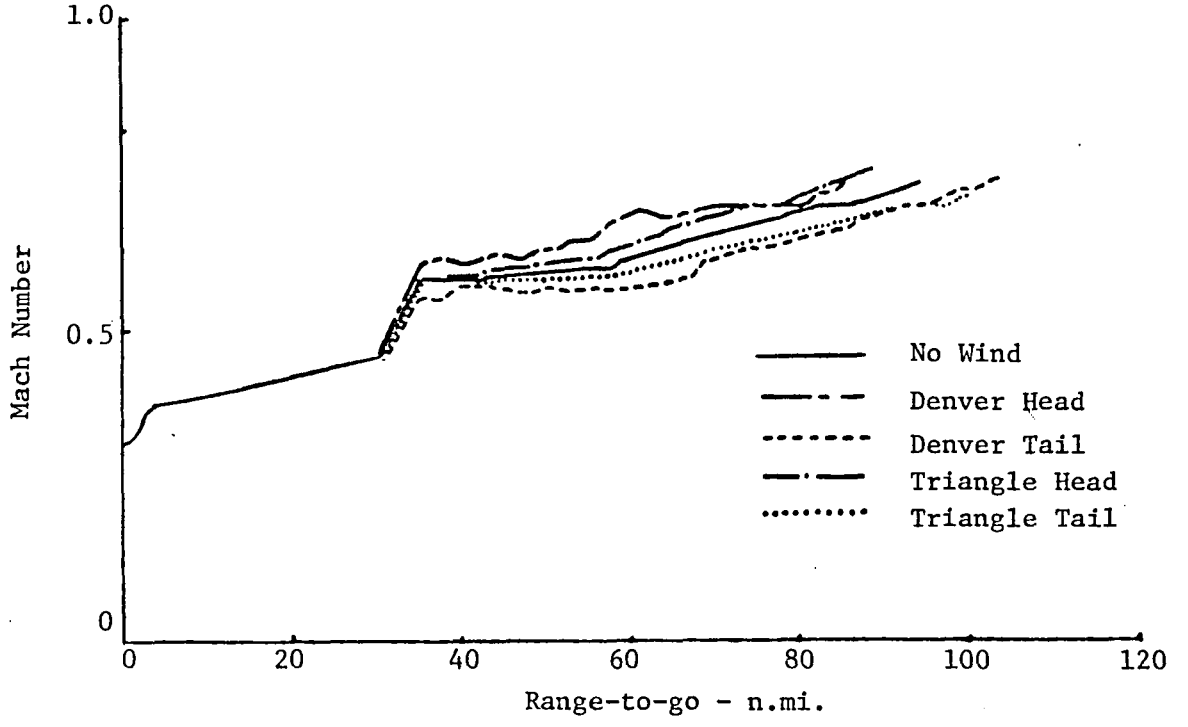

b) Mach Number

Figure 14. Effect of Wind Variations on Optimum Descent Altitude and Mach Number as Functions of Range-to-go.

The results seen in Figs. 10-14 are limited in scope, in that all possible variations are not addressed. For example, the effects of variations in cruise weight and cruise altitude for the descent trajectories should be explored. However, the one thing that can be concluded is that variations of total range, initial weight, and wind profiles have predictable effects that can be easily used to modify the characterization of the nominal optimum trajectory. Thus, the process of computing the optimum climb-descent profiles does not have to take place on-board the aircraft. Instead, a nominal profile plus modifications to account for off-nominal parameter changes can be pre-computed and stored in the aircraft flight management system. This provides a very simple on-board method of computing the optimum profile.

The second aspect of the sensitivity analysis was to study the effect of flying a non-optimal profile. This effort involved using TRAGEN to simulate following a given incorrect optimum profile when a different profile should have been used. Two error conditions were investigated:

a) Following an optimum profile specified for the incorrect initial weight.

b) Following an optimum profile specified for the incorrect wind profile.

Only the climb phase was investigated.

For initial weight errors, four runs were made as shown in Table 6. As can be expected, the increase in assumed initial weight causes a decrease in the optimum cruise altitude. Thus, if the aircraft is lighter than the assumed amount, it will climb faster to the lower altitude. This results in both time and fuel reduction from what was predicted. Cases 1a and 1d in Table 6 were of this nature, and they show a 13-14% reduction in fuel and a 14-16% reduction in climb time for an initial error of -6804 kg (-15000 lb) in initial weight.

Table 6. Initial Weight Error Cases Considered - Climb Profile

Run	Initial Weight - kg (lb)	Assumed Optimum Profile Weight - kg (lb)	Change in Climb Fuel kg (lb)-(%)	Change in Climb Time Sec - (%)
1a	61236 (135000)	68040 (150000)	-774 (-604) (-131%)	-159 (-14.4%)
b	61236 (135000)	54432 (120000)	+329 (+726) (+18.7%)	223 (+22.9%)
c	68040 (150000)	61236 (135000)	371 (+817) (+19.2%)	247 (+23.3%)
d	54432 (120000)	61236 (135000)	269 (-592) (-13.9%)	-167 (-15.8%)

On the other hand, if the initial weight is assumed too small, the heavier aircraft will attempt to climb to a higher than nominal altitude. Cases 1b and 1c of Table 6 show this condition for an initial weight error of +6804 kg (+15000 lb). The result was a 19% increase in required climb fuel and a 23% increase in required climb time. It was also seen that the aircraft did not achieve the required cruise airspeeds when the incorrect optimum input altitude was reached.

Based on the results of Table 6, it is seen that the initial weight is an important parameter to be entered into the computations. It is better to assume too large an initial weight than vice versa.

For the climb wind profile errors, four more cases were studied where optimum climb profiles based on the triangle wind profile of Fig. 12 were used. The results are shown in Table 7. As can be seen, if the tail wind is greater than assumed (Cases 2a and 2d), more time and possibly more fuel is required to achieve cruise conditions. Likewise, if the head wind is greater than assumed (Cases 2b and 2c), less time and possibly less fuel is required, although the results are mixed. It is seen that neglecting the wind profile can vary fuel cost up to $\pm$ 1.5%. However, this effect is not nearly as significant as assuming the incorrect value of aircraft weight.

Table 7. Wind Profile Error Cases Considered - Climb Profile

Run	Actual Wind Profile	Assumed Profile for Computing Optimum	Change in Climb Fuel kg (lb) - (%)	Change in Climb Time Sec - (%)
2a	No Wind	Head	-1 (-2) (-.05%)	+7 (+0.7%)
b	No Wind	Tail	+11 (+24) (+0.6%)	-3 (-0.3%)
c	Head	No Wind	-27 (-60) (-1.4%)	-15 (-1.4%)
d	Tail	No Wind	+29 (+64) (+1.5%)	+18 (+1.7%)

These type of sensitivity studies are important because they produce information necessary for the implementation process. Computing the optimum profile with the wrong aircraft or environment models can cause a large percentage of the expected gain to be obtained from the flight management system to not be realized.

Many more sensitivity cases than those described above need to be obtained for determining the sensor and measurement processing requirements associated with implementation of an optimum vertical flight management system. However, with the availability of the OPTIM and TRAGEN programs, the user is in a position to obtain these results.

V

MECHANIZATION OPTIONS

This chapter briefly describes two methods by which the optimum vertical profiles can be generated and used for automatic longitudinal steering on-board the aircraft. These are:

1) Computing the nominal optimum profile off-line and storing it on-board the aircraft. Empirical equations are used to adjust this nominal profile to account for perceived changes in initial weight, range, wind profile, etc.

2) Continually recomputing the nominal optimum profile on-board the aircraft. Here, changes in wind profile and range are continually being estimated, and their effects are directly entered into the nominal trajectory computation.

Each method is now discussed.

Off-line Optimum Profile Generation

This method would be based on sensitivity analysis results such as those presented in the previous chapter. A nominal optimum profile is computed off-line using the OPTIM program described earlier. Also, several other profiles are computed, where variations are made (one at a time) in the various key parameters that govern the shape of the profile. Parameters that would be varied include initial weight, wind profile, temperature profile, and range-to-destination.

A means would be derived for describing the nominal profile as a function of a suitable independent variable. For example, it is convenient to specify airspeed (or Mach number) and flight path angle as functions of altitude for climb and altitude and airspeed as functions of range-to-go for descent. Also, empirical functions would be derived for computing perturbations to the nominal profile for measured changes to nominal values of the key parameters.

The function describing the nominal trajectory and its perturbations are stored in the on-board flight management system's computer. Then, as the chosen independent variables change with the position along the flight path, the sum of the nominal and perturbation functions are used to compute and command the desired flight profile.

An example of this mechanization for the climb profile is depicted in the block diagram of Fig. 15. Here, the independent variable is altitude h. Its measurement is used to compute the nominal values of airspeed $V_{cn}(h)$ and flight path angle $\gamma_{cn}(h)$. The Nominal Trajectory computations are also used to compute the nominal wind profile $V_w(h)$ and the assumed aircraft weight $W_n(h)$. Other measurements are used to estimate or measure the prevailing values of wind $\hat{V}_w$ and weight $\hat{W}$. If range-to-destination r_d is changed, this is also entered. These variables are compared to the nominal values in the Empirical Perturbation Functions computations. These computations produce perturbations $\delta V_c(h)$ and $\delta\gamma_c(h)$ to the nominal commands. The perturbations and nominal values are added to obtain the total commands $V_c(h)$ and $\gamma_c(h)$.

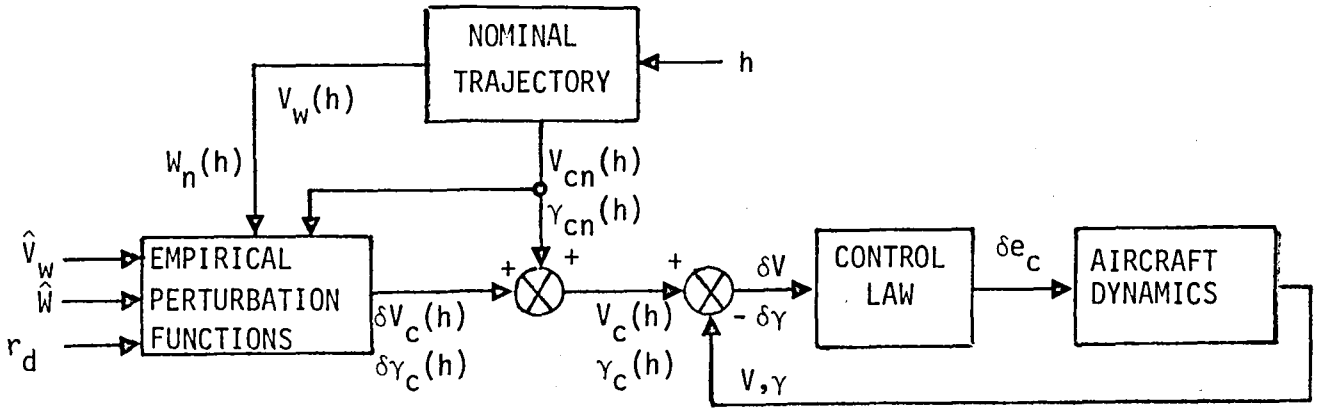

Figure 15. Block Diagram Depicting On-Board Climb Steering Based on Computing the Nominal Optimum Profile Off-line.

The total commands are compared with measured or estimated values of airspeed and flight path angle (V, γ). The differences ($\delta V, \delta\gamma$) are used to implement a linear control law based on perturbation analysis. This control law produces either a commanded angle-of-attack, pitch angle, or elevator deflection to produce the desired longitudinal response characteristics. The gains in the control law could be functions of altitude if desirable. Maximum thrust would be set during climb.

A similar mechanization would be used for the descent portion of flight but with the independent variable changed to range-to-go. For descent, the thrust would be set at idle value.

For cruise, the thrust is set to balance the drag at the best cruise airspeed. This airspeed is chosen to minimize the cost per unit of distance traveled. If a constant cruise altitude is required because of ATC constraints, then the elevator is trimmed so that lift balances the aircraft weight.

On-Board Optimum Profile Generation

This method would be based on the algorithms used to generate the optimum profile, as in the OPTIM program. The algorithms would be exercised every few minutes as background equations in the on-board flight management computer. The sequence of background computations would be similar to the seven steps described in Chapter III. As new estimates of the wind profile, aircraft weight, or other key variable were obtained, a new optimum profile would be generated based on the latest information. There would be no need for perturbation functions. This method would require a much larger computational capability then the first method described above. Information required by the system would include:

1) minimization algorithm;
2) functions or tables describing:
   a) standard atmosphere,

b) aircraft lift characteristics,

c) aircraft drag characteristics,

d) engine thrust characteristics (maximum and idle),

e) fuel burn characteristics;

3) function interpolation schemes; and

4) empirical equations for estimating cruise weight and landing weight.

An example of this mechanization for the climb portion of flight is shown in Fig. 16. Note that a new nominal trajectory is computed at regular intervals. After the commanded values of airspeed and flight path angle ($V_c(h)$, $\gamma_c(h)$) are computed, the mechanization is identical to that shown in Fig. 15.

This type of mechanization has been developed for a DC-10 and exercised in a cockpit simulator, as reported in Ref. 25. For short range flights (200 n.mi.), this mechanization was reported to save over 13% of the fuel requirements.

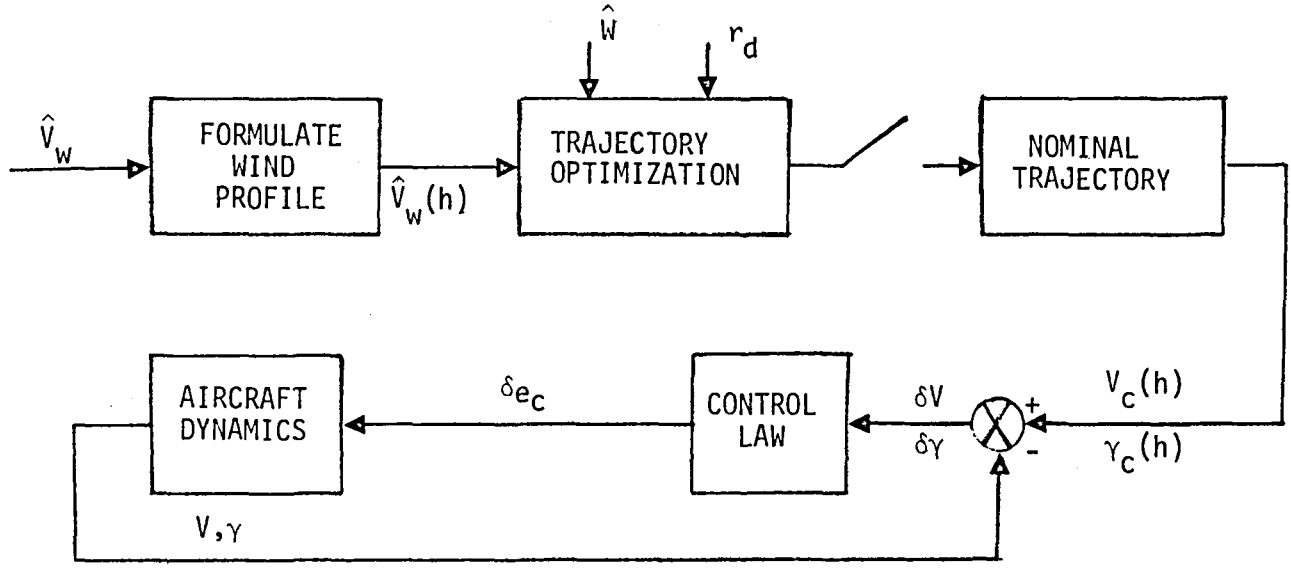

Figure 16. Block Diagram Depicting On-Board Climb Steering Based on Computing the Nominal Optimum Profile in the Background.

Instrumentation required to support these two flight management systems includes:

a) Vertical accelerometer,
b) Airspeed measurement system (Mach and/or true airspeed),
c) Baro-altimeter,
d) DME (or INS) so distance-to-go and wind speed can be obtained,
e) Free stream temperature measurement, and
f) Vertical gyro to measure pitch angle.

A complementary filter can be used to blend vertical accelerometer and baro-altitude measurements to obtain altitude rate. INS and airspeed measurements can be combined to obtain wind estimates. Altitude rate and airspeed can be combined to compute flight path angle. Pitch angle and flight path angle can be differenced to obtain angle-of-attack. Angle-of-attack can be used with temperature, airspeed, and altitude to compute lift and aircraft weight.

Also, this system must be coupled to measurement of the throttle and elevator deflections.

Method Comparison

The two methods described above cannot be directly compared without actual mechanization on the same type of computer and then tested under realistic operating conditions. However, some qualitative comparisons can be made before that point. Advantages to each method are:

Off-line Method

1. Simpler computations on-board. Does not require table interpolations, iterative optimization procedures, or foreground/background time sharing.

2. Smaller memory requirements. Few subroutines are necessary. Tabular data minimized.

3. Easy to incorporate simplifications.

4. Less expensive.

5. No concern over converging to correct answer.

On-board Method

1. More accurate optimum profile generated.

2. Need for flight engineer to enter information before flight is minimized.

3. More adaptable to changing flight conditions (i.e. re-routing due to weather constraints).

4. Not restricted to variations in a limited number of key parameters.

Thus, it is seen that both methods have advantages. It is recommended that both of these methods be investigated further by mechanizing them on an airborne system and then testing them in flight (or in a cockpit simulator using a realistic operating environment) so that further evaluation may be made.

VI

SUMMARY, CONCLUSIONS, AND RECOMMENDATIONS

Summary and Conclusions

All evidence indicates that we are rapidly consuming our supply of hydrocarbon fuels. This makes it mandatory that systems be developed that allow conservation of the remaining supplies until alternate fuels can be developed. This is especially true of aircraft flight which currently has no alternatives. This report addressed the development of on-board algorithms for vertical steering of the aircraft to minimize fuel consumption and cost.

Chapter II presents a summary of the research work conducted in the past twenty years to develop algorithms for fuel minimization and related topics. The trend has been to use the energy state approximation for obtaining a simple mathematical model of longitudinal aircraft dynamics. This simplification has facilitated development of algorithms that are relatively easy to solve so that they can be mechanized on-board the aircraft for in-flight solution. Furthermore, based on several researchers' results, fuel savings of from 5% to over 25% can be obtained by using these algorithms. (See Refs. 3, 4, 25, and 26).

Chapter III derives an algorithm for computing the optimum vertical profile using range as the independent variable. Both fuel and time are penalized, and the longitudinal wind effects are taken into account. The Hamiltonian is constant for this mechanization, and is equal to the minimum cruise cost per unit distance traveled. To obtain optimum climb and descent profiles involves minimizing a single function at discrete points along the trajectory by proper choice of thrust and airspeed. This algorithm proved to be a dual to the one derived by Erzberger where energy was used as the independent variable. A computer program (called OPTIM, described in Appendix A) was used to obtain optimum vertical profiles for typical 727 aircraft flights based on these algorithms.

In Chapter IV, the accuracy of the vertical profiles obtained from OPTIM were examined by using a more complete longitudinal model of the aircraft. This model was incorporated into a computer program called TRAGEN (described in Appendix B) which steers the aircraft to follow the input reference trajectory. Results showed that the OPTIM reference trajectories were both flyable and accurate in terms of the fuel burned and time expended.

Chapter IV presented the changes in characteristics of optimum 727 reference trajectories due to changes in range, initial weight, and wind profile. It was concluded that these changes were simple modifications to the nominal reference profiles; they could be used to compute perturbations to a nominal profile on-board without recomputing the entire reference profile.

Chapter IV also examined the effects of errors in the estimated values of initial weight and the wind profile on the performance obtained during climb. A 9% increase in initial weight (6804 kg (15000 lb)) can cause a 23% increase in time and a 19% increase in fuel required to achieve the desired cruise conditions. Wind errors have a smaller effect. These sensitivity studies are useful for specifying how accurately various parameters which affect the flight performance need to be measured.

Chapter V presented two alternate ways that optimum vertical profiles could be computed and mechanized in flight. One method is based on computing the reference profile and perturbation adjustments off-line, so that minimum computations are required on-board. The other method is based on continually computing the optimum reference profile on-board the aircraft so that measured changes to the nominal conditions can be directly taken into account. Both methods have qualitative advantages, and a choice between the two would have to be based on further mechanization studies.

Recommendations

Based on the experience obtained by review of previous work, the use of the OPTIM program, the development and use of the TRAGEN program, and conversations held with many government and industry personnel associated with research and design in the air transportation field, the following recommendations are made concerning future work.

OPTIM and TRAGEN extensions. The following extensions to these programs would provide the capability to obtain more realistic reference trajectories, correct known minor errors, and add capabilities which would be useful for obtaining improved solutions for other phases of flight:

a) Optimum climb to a fixed altitude. Currently, the aircraft is simulated to climb to the optimum altitude without considering ATC constraints. Also, OPTIM computes cruise costs based on the assumption that the aircraft will climb during cruise as fuel is burned. This added option would constrain the profile to climb to a fixed altitude and then hold it during cruise.

b) Flight path angle smoothing. Currently, because OPTIM computes climbs and descents at discrete changes in specific energy, jumps occur in the flight path angle producing a rough reference trajectory. Airspeed change constraints and post-run smoothing should be tested to remove or minimize the effect of this problem.

c) Optimum profile with multiple cruise minimums. If there is a high head wind shear condition, there will exist more than one best cruise altitude depending on range. Currently, OPTIM will only consider the lower altitude. Thus, for longer ranges, with certain wind profiles, better flight conditions than what OPTIM will produce will exist. The change would add logic to consider all altitude minimums in deciding the cruise condition.

d) Minimum fuel with fixed time of flight (4D requirement). OPTIM produces a profile which minimizes the cost function

$$J = \int_{o}^{t_f} (C_f \dot{w} + C_t) dt$$

where C_f and C_t are input costs of fuel ($/lb) and time ($/hr). OPTIM can be set up to iterate on C_t (with C_f held fixed) so that the desired flight time would be produced for 4D guidance.

e) Optimum cruise - step change in altitude. Currently, OPTIM is based on optimum cruise climbs. This added option would be an extension to (a) above where cruise altitudes are fixed by ATC constraints. This option would determine where to change altitudes in a step fashion as fuel is burned off during cruise.

f) Optimum cruise change in altitude due to range dependent wind profile change. For certain aircraft on certain routes in the future, the ATC requirement for fixed altitude during cruise will be removed. However, for long flights, the wind profile encountered during cruise is continually changing, and it will be desirable to adjust cruise conditions continually to minimize costs. This problem may require transient engine thrust and fuel flow models as a function of variable throttle. Also required are typical models of the changing enroute wind profile. OPTIM could be used to generate optimum cruise tables for variable wind and cruise weight. How to climb and descend as a function of range would be determined.

g) Follow arbitrary profiles. Currently, TRAGEN is designed so that the aircraft tracks a sequence of input points which come from OPTIM. Equations could be added so the aircraft could also track constant indicated airspeed, constant Mach number, profile descents, and other possibilities of interest. The result would be the ability to measure the cost (in time and fuel) to fly to follow these alternate reference profiles.

h) Maintain airspeed during descent. Currently, TRAGEN is programmed so that angle-of-attack is changed to track inertial flight path angle (i.e., altitude as a function of range) during descent. Thrust is set to idle value. Below 3048 m (10000 ft), the airspeed drops below 250 kts causing excess time and fuel burn. An option is to add throttle control to maintain appropriate airspeed. Another option is to add airspeed error to the control law as is done for climb control.

i) Conversion of OPTIM and TRAGEN to model the Boeing 737. Currently OPTIM and TRAGEN are based on mathematical models of the 727 aircraft. Because future research will be focused on the NASA Langley 737 TCV aircraft, it is appropriate to develop an alternate version of these programs based on 737 models. The subroutines and data tables associated with aerodynamic and propulsion characteristics would have to be changed. Also, empirical equations which exist within OPTIM associated with estimating initial cruise weight and final landing weight would have to be changed. This task would also include a written explanation of the steps involved in making the conversion.

Develop and test optimum vertical guidance methods. The purpose of this task would be to derive the specific requirements to design and test an airborne system for implementing optimum vertical guidance techniques on either a 737 cockpit simulator or the TCV aircraft. Both methods described in Chapter V should be considered. Subtasks include:

a) Generate perturbation guidance functions (Method 1) This task would parameterize the optimum profiles for the 737 (offline, as determined by converted OPTIM) to account for measured or input changes in range-to-destination, takeoff weight, wind profile, or temperature profile. This would involve describing the climb and descent profiles as functions or polynomials of altitude, range, etc. These parameterized profiles would be used to

generate the total (nominal plus perturbation) reference trajectories for climb and descent steering. Control gains would be scheduled as necessary to give appropriate steering response.

b) Test perturbation guidance on TRAGEN. This would involve testing the perturbation steering commands in the presence of wind, weight, temperature, range, and other variations on TRAGEN. The results, in terms of time and fuel expenditures, should match the results predicted by OPTIM. If not, the parameters in the profile equations would be adjusted. The result should be a set of near-optimum steering equations for the 737 that are simple to implement yet complex enough to account for most perceived perturbations.

c) Generate on-board optimum profile guidance computations (Method 2). This task would specify and code the tables, logic, and equations required for direct on-board computation of the optimum vertical profile. Essentially, this would duplicate the OPTIM calculations on-board the 737. This code would be validated by using the TRAGEN program.

d) Determine airborne computer mechanization requirements. The computer where the optimum guidance algorithms would reside would be chosen. The interface between the computer and the sensors and autopilot (or flight director) would be defined. Also, the interface between the vertical profile steering algorithms and other avionics functions would be defined. Block diagrams and flow charts would be developed of the required equations and logic in sufficient detail so that coding could take place.

e) Compare performance and mechanization requirements. Based on the results of subtasks (a) - (d) above, the performance and requirements for mechanizing the perturbation guidance algorithm (Method 1) would be compared with the performance and mechanization requirements of the optimum profile guidance algorithm (Method 2). The

comparison would include computation speed and memory requirements. Based on these results, a decision could be made concerning further mechanization on the TCV aircraft or 737 cockpit simulator.

f) Mechanize and test the preferred algorithm. Based on subtask (e), the chosen algorithm should be mechanized. A test plan should be developed, an extensive test should be made, and the results should be publicized. In this way, all avionics firms, airlines, and personnel associated with air transportation would have access to a near-optimum method for saving fuel and reducing flight costs.

APPENDIX A

TRAJECTORY OPTIMIZATION USING THE ENERGY STATE METHOD

The purpose of this Appendix is to summarize briefly the theoretical background used for optimization of trajectories. These principles form the basis of the numerical process used for computing the optimum vertical profile of a jet aircraft. More details are given in Refs. 5, 24, and 30. Reference 5 derives the principles upon which trajectory optimization is based. In Refs. 24 and 30, Erzberger and Lee apply these principles using the energy state approximation to obtain a practical, efficient means of generating the optimum vertical profile.

OPTIM is an extension of the original computer code developed by Erzberger and Lee that encompasses these principles and is based on their methods. The latter part of this appendix describes how OPTIM is organized.

In the following sections, the theory of trajectory optimization is first presented. Then, the application of this theory to minimizing the direct operating cost (DOC) of an aircraft traveling over a fixed range is outlined. This is followed by a discussion of the details of going from theoretical expressions to a practical computer code. The theoretical points are presented without proof, for conciseness. The reader wanting more detail should review the references.

Theoretical Principles

In Ref. 5., a description is given of the requirements for solving an optimization problem involving a continuous dynamic system with no terminal constraints but with fixed terminal time. This description is repeated here because it presents the basic principles which extend to the aircraft profile optimization problem.

A system (the aircraft) is governed by the nonlinear differential equations

$$\dot{x} = f(x,u,t) \quad ; \qquad x(t_o) \text{ given}; \qquad t_o \leq t \leq t_f \; ; \tag{A.1}$$

where x is the n-dimensional state vector and u is the m-dimensional control vector. The cost function which is to be minimized is of the form

$$J = \phi(x(t_f),t_f) + \int_{t_o}^{t_f} L(x,u,t)\, dt. \tag{A.2}$$

Here, ϕ is the terminal cost function, and L is the cost per unit time along the trajectory. The problem is to find the sequence of controls u(t) that minimize J.

First, the system equations are adjoined to J with the multiplier vector $\lambda(t)$:

$$J = \phi(x(t_f),t_f) + \int_{t_o}^{t_f} \{L(x,u,t)+\lambda^T(t)\{f(x,u,t)-\dot{x}\}\}\, dt. \tag{A.3}$$

Then the Hamiltonian function is defined as

$$H(x,u,t) = L(x,u,t) + \lambda^T(t) f(x,u,t). \tag{A.4}$$

Equation (A.3) is integrated by parts to yield

$$J = \phi(x(t_f),t_f) - \lambda^T(t_f)\, x(t_f) + \lambda^T(t_o)\, x(t_o) \tag{A.5}$$

$$+ \int_{t_o}^{t_f} \{H(x,u,t) + \dot{\lambda}^T(t)\, x(t)\}\, dt.$$

Next, the change in J due to variations in u(t) and x(t) is considered for fixed t_o and t_f:

$$\delta J = \left\{ \left(\frac{\partial \phi}{\partial x} - \lambda^T \right) \delta x \right\}_{t=t_f} + (\lambda^T \delta x)_{t=t_o} \tag{A.6}$$

$$+ \int_{t_o}^{t_f} \left\{ \left(\frac{\partial H}{\partial x} + \dot{\lambda}^T \right) \delta x + \frac{\partial H}{\partial u} \delta u \right\} dt.$$

The elements of $\lambda(t)$ are chosen to cause the coefficients of δx in Eq. (A.6) to vanish under the integral and at t_f:

$$\dot{\lambda}^T = - \frac{\partial H}{\partial x} = - \frac{\partial L}{\partial x} - \lambda^T \frac{\partial f}{\partial x} ; \qquad \lambda^T(t_f) = \frac{\partial \phi}{\partial x} . \tag{A.7}$$

Equations (A.7) are called the co-state equations. Then, Eq. (A.6) becomes

$$\delta J = \lambda^T \delta x(t_o) + \int_{t_o}^{t_f} \frac{\partial H}{\partial u} \delta u \, dt. \tag{A.8}$$

For J to be minimum, δJ must be zero for arbitrary u(t); this implies that for no bounds on u,

$$\frac{\partial H}{\partial u} = 0 \qquad , \quad t_o \leq t \leq t_f \tag{A.9}$$

on the optimum path. If the control variables are constrained as

$$C(u,t) \leq 0, \tag{A.10}$$

then for u(t) to be minimizing, we must have $\delta J \geq 0$ for all admissible u(t). This implies, from Eq. (A.8) that

$$\frac{\partial H}{\partial u} \delta u \triangleq \delta H \geq 0, \tag{A.11}$$

for all t and all admissible $\delta u(t)$. In other words, H must be minimized over the set of all possible u; this is known as the minimum principle [6].

In summary, to solve for u(t) that minimizes J, the differential equations (A.1) and (A.7) must be solved simultaneously, where u(t) is determined from Eqs. (A.9) or (A.11). The boundary conditions on the state x at t_o and λ at t_f are specified, resulting in a two-point boundary-value problem.

If L and f are not explicit functions of t, then

$$\dot{H} = \frac{\partial H}{\partial t} + \frac{\partial H}{\partial x}\dot{x} + \frac{\partial H}{\partial u}\dot{u} + \dot{\lambda}^T f, \tag{A.12}$$

$$= \frac{\partial H}{\partial t} + \frac{\partial H}{\partial u}\dot{u} + \left(\frac{\partial H}{\partial x} + \dot{\lambda}^T\right) f.$$

Each element of Eq. (A.12) is zero on the optimum trajectory, from which we can conclude that H is constant on the optimum trajectory. This latter point is used in the analysis presented in Chapter III.

Application to Aircraft Profile Optimization Using the Energy State Approximation

Here we are concerned with applying the above theory to the problem of choosing the thrust and airspeed values to control the aircraft vertical profile in going from one point to another. The cost function J is the direct operating cost (DOC) which is the sum of fuel and time costs. This is, in integral form,

$$J = \int_0^{t_f} (C_f \dot{w} + C_t)dt \triangleq \int_0^{t_f} C_d \, dt, \tag{A.13}$$

where C_f is the cost of fuel ($/lb), $\dot{w}$ is fuel flow rate (lb/hr), C_t is the cost of time ($/hr), C_d is the direct operating cost, and t_f is the time to fly the specified distance traveled d_f. It is also assumed that the typical vertical profile is as shown in Fig. A.1 - that is, it contains climb, cruise, and descent portions which have the constraint that

$$d_{up} + d_{dn} \leq d_f \tag{A.14}$$

where

d_{up} = $x(t_{ci})$ = the distance traveled from the start point to where the cruise segment begins (at time $t = t_{ci}$).

d_{dn} = $d_f - x(t_{cf})$ = the distance traveled from the end of cruise (at time $t = t_{cf}$) to where the descent segment ends.

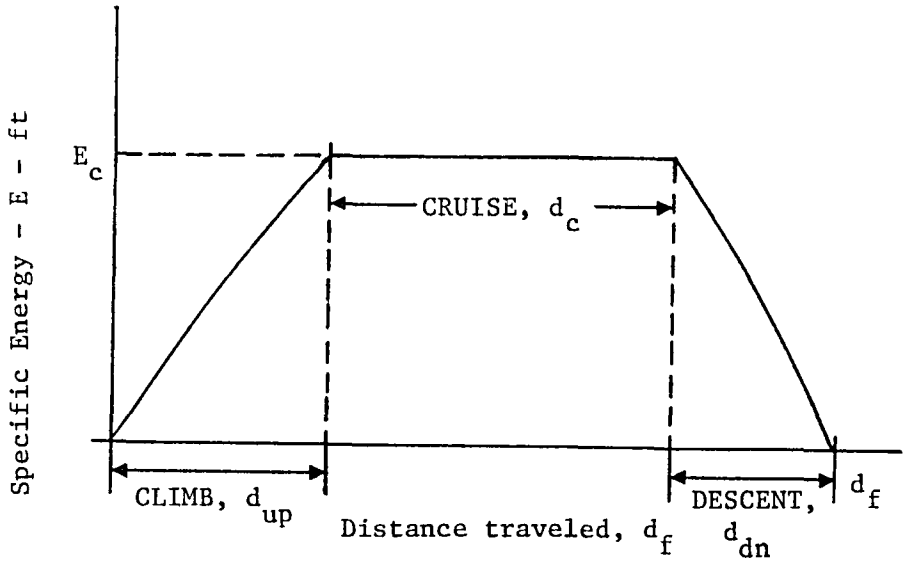

Figure A.1. Assumed Structure of Optimum Trajectories

Thus, the cost function (Eq. (A.13)) can be rewritten as

$$J = \int_0^{t_{ci}} C_d dt + (d_f - d_{up} - d_{dn})\psi + \int_{t_{cf}}^{t_f} C_d dt, \qquad (A.15)$$

$$= \int_0^{t_{ci}} C_d dt + (d_f - x(t_{ci}) - [d_f - x(t_{cf})])\psi + \int_{t_{cf}}^{t_f} C_d dt.$$

where ψ is the cost per unit distance while in cruise.

Simplified point-mass equations of longitudinal motion of the aircraft are

$$\begin{aligned} \dot{V} &= (T-D)/m - g \sin \gamma , \qquad (A.16) \\ \dot{h} &= V \sin \gamma , \\ \dot{x} &= V \cos \gamma + V_w , \end{aligned}$$

where the flight path angle (γ) dynamics and weight loss due to fuel burn are neglected. Here,

V = airspeed,

h = altitude,

V_w = longitudinal component of wind speed,

m = aircraft mass,

T = thrust,

D = drag.

Also, it is assumed that lift $L = mg \cos \gamma$. The effect of weight loss is accounted for by continuously updating weight without adding another state variable.

Specific energy E is defined as

$$E = h + V^2/2g, \tag{A.17}$$

which is the sum of potential and kinetic energy per unit mass. Its time derivative is found to be

$$\dot{E} = V(T-D)/mg. \tag{A.18}$$

The energy state approximation is based on the assumption that potential and kinetic energy can be interchanged instantaneously. In this approximation, the energy state variable replaces altitude and airspeed state variables [12]. Thus, Eq. (A.17) can be used in place of $\dot{V}$ and $\dot{h}$ in Eq. (A.16).

It is assumed that the aircraft specific energy increases monotonically during climb and decreases monotonically during descent. This assumption is used in the development to change the independent variable in Eq. (A.15) from time to energy. This uses the transformation

$$dt = \frac{dE}{\dot{E}} . \tag{A.19}$$

It is mathematically convenient to evaluate the last integral in Eq. (A.15) backwards in time so that the energy state is monotonically increasing during its evaluation. This means that the running distance (range) variable during the descent can be measured backwards from the end point. Thus we can think of range measured in two ways as shown in Fig. A.2.

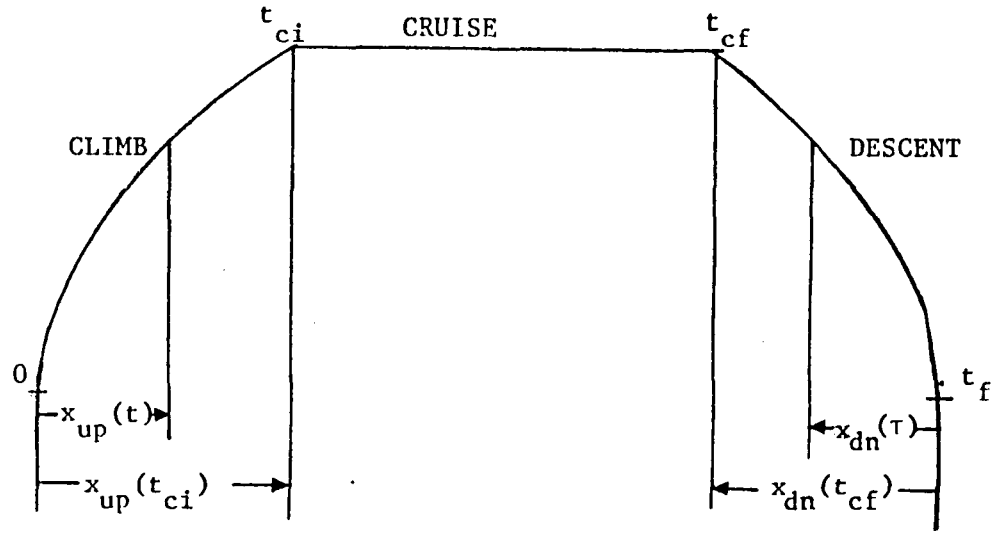

Figure A.2. Measurement of Range from the Origin or to the Destination.

In this sketch,

$x_{up}(t)$ = range measured on the way up in forward time t,

$x_{up}(t_{ci})$= value of x_{up} when initial cruise is reached,

$x_{dn}(\tau)$ = range measured on the way up in backward time τ,

$x_{dn}(\tau_{cf})$= value of x_{dn} when final cruise is reached ($\tau_{cf}=|t_{cf}-t_f|$).

Also, we define the variable x to be range traveled during climb and descent. The distance traveled during cruise is then contrained to be $(d_f - x)$. We can then see that an incremental change dx in the range variable x is equivalent to incremental changes in both x_{up} and x_{dn}. That is

$$dx = d(x_{up} + x_{dn}) . \tag{A.20}$$

From this discussion, the second of Eqs. (A.15) can be written as

$$J = \int_{0_i}^{t_{ci}} C_d dt + (d_f - x_{up}(t_{ci}) - x_{dn}(\tau_{cf})) + \int_{0_f}^{\tau_{cf}} |C_d| d\tau . \tag{A.21}$$

We use Eq. (A.19) and the transformation

$$d\tau = \frac{dE}{|\dot{E}|} \tag{A.22}$$

to rewrite Eq. (A.15) as

$$J = \int_{E_i}^{E_{ci}} \left(\frac{C_d}{\dot{E}} \, dE \right)_{\dot{E}>0} + (d_f - (x_{up}(E_{ci}) + x_{dn}(E_{cf}))) + \int_{E_f}^{E_{cf}} \left(\frac{dE}{|\dot{E}|} \, dE \right)_{\dot{E}<0} \tag{A.23}$$

Here, E_i, E_{ci}, E_{cf}, and E_f are the values of specific energy evaluated at time t equal to 0 and t_{ci} and time τ evaluated at t_{cf} and t_f respectively.

Note from Eq. (A.23) that the range variable x only appreas as the sum of climb and descent distances ($x_{up} + x_{dn}$). Thus, the state equation for this system of equations can be written as

$$\frac{dx}{dE} = \frac{d(x_{up} + x_{dn})}{dE} = \left(\frac{(V_{up} + V_{wup})}{\dot{E}} \right)_{\dot{E}>0} + \left(\frac{(V_{dn} + V_{wdn})}{|\dot{E}|} \right)_{\dot{E}<0} \tag{A.24}$$

Here, V_{wup} and V_{wdn} are the longitudinal components of the wind speed for climb and descent. Then, analogous to Eq. (A.4), the Hamiltonian is

$$H = \left[\left(\frac{C_d}{\dot{E}} \right)_{\dot{E}>0} + \left(\frac{C_d}{|\dot{E}|} \right)_{\dot{E}<0} + \lambda \left\{ \left(\frac{(V_{up}+V_{wup})}{\dot{E}} \right)_{\dot{E}>0} + \left(\frac{(V_{dn}+V_{wdn})}{|\dot{E}|} \right)_{\dot{E}<0} \right\} \right] \tag{A.25}$$

This can be divided as

$$H = \left[\frac{C_d + \lambda \, (V_{up}+V_{wup})}{\dot{E}} \right]_{\dot{E}>0} + \left[\frac{C_d + \lambda \, (V_{dn}+V_{wdn})}{|\dot{E}|} \right]_{\dot{E}<0} \tag{A.26}$$

Now, analogous to Eq. (A.7), the costate equation for λ can be written as

$$\frac{\partial \lambda}{\partial E} = -\frac{\partial H}{\partial x} = -\frac{\partial H}{d(x_{up}+x_{dn})} = 0 \tag{A.27}$$

and from Eqs. (A.7) and (A.23), this costate has the final value

$$\lambda(E_{ci}) = \lambda(E_{cf}) = \frac{\partial \phi}{\partial(x_{up}+x_{dn})} = \frac{\partial([d_f - x_{up} - x_{dn}]\psi)}{\partial(x_{up}+x_{dn})} = -\psi \tag{A.28}$$

where ψ is the cruise cost per unit distance.

Note, this problem could be placed in a slightly more conventional form by dividing it into two problems - one for climb and one-half of the cruise distance and the other for decent and the other half of the cruise distance. Then Eqs. (A.27) and (A.28) would be replaced by

$$\frac{\partial \lambda}{\partial E} = -\frac{\partial H}{\partial x_{up}} = 0 \tag{A.29}$$

$$\lambda(E_{ci}) = \frac{\partial([d_f/2 - x_{up}]\,\psi(E_{ci}))}{\partial x_{up}} = -\psi\,(E_{ci}),$$

for climb. For descend,

$$\frac{\partial \lambda}{\partial E} = -\frac{\partial H}{\partial x_{dn}} = 0 \tag{A.30}$$

$$\lambda(E_{cf}) = \frac{\partial([d_f/2 - x_{dn}]\,\psi(E_{cf}))}{\partial x_{dn}} = -\psi\,(E_{cf})$$

This allows splitting the Hamiltonian defined in Eq. (A.26) and allows for $\psi(E_{ci}) \neq \psi(E_{cf})$. In fact, in the actual implementation $E_{ci} \neq E_{cf}$ because optimum cruise energy changes as fuel is burned off. The principal results are unchanged, however.

Thus, from Eq. (A.11), (A.29) and (A.30) the trajectory optimization problem becomes

$$H_{up} = \min_{\substack{V_{up} \\ \pi_{up}}} \left[\frac{C_d}{\dot{E}} - \psi(E_{ci}) \left(\frac{V_{up} + V_{wup}}{\dot{E}} \right) \right]_{\dot{E}>0} , \tag{A.31}$$

$$H_{dn} = \min_{\substack{V_{dn} \\ \pi_{dn}}} \left[\frac{C_d}{|\dot{E}|} - \psi(E_{cf}) \left(\frac{V_{dn} + V_{wdn}}{|\dot{E}|} \right) \right]_{\dot{E}<0} .$$

Thus, the optimization problem reduces to solving pointwise minimum values of the algebraic functions defined by Eq. (A.31) during the climb and descent portions of the trajectory.

Equations (A.29) and (A.30) are the transversality condition for the free final state problem ($d_{up} + d_{dn} < d_f$) with terminal cost. Thus, the constant value of λ for climb and descent is found to be the negative of the cost per unit distance for cruise.

The cruise cost ψ ($= -\lambda$) is found by assuming that the aircraft is in static equilibrium during cruise ($T = D$), and that

$$\psi(E_c) = \min_{V_c} \frac{C_d}{(V_c + V_w)} . \tag{A.32}$$

In other words, for any cruise altitude, there is an optimum thrust and airspeed such that the cost per unit distance $\psi(E_c)$ is minimized. The optimum cruise cost as a function of cruise energy is typically of the shape shown in Fig. A.3. Thus, there is also an optimum cruise energy E_{copt} where cruise cost $\psi(E_{copt})$ is minimized. If the range is long enough so that there is sufficient range to reach optimum cruise energy E_{copt}, it should be done, and the cruise conditions should be set so that $\psi(E_c) = \psi(E_{copt})$.

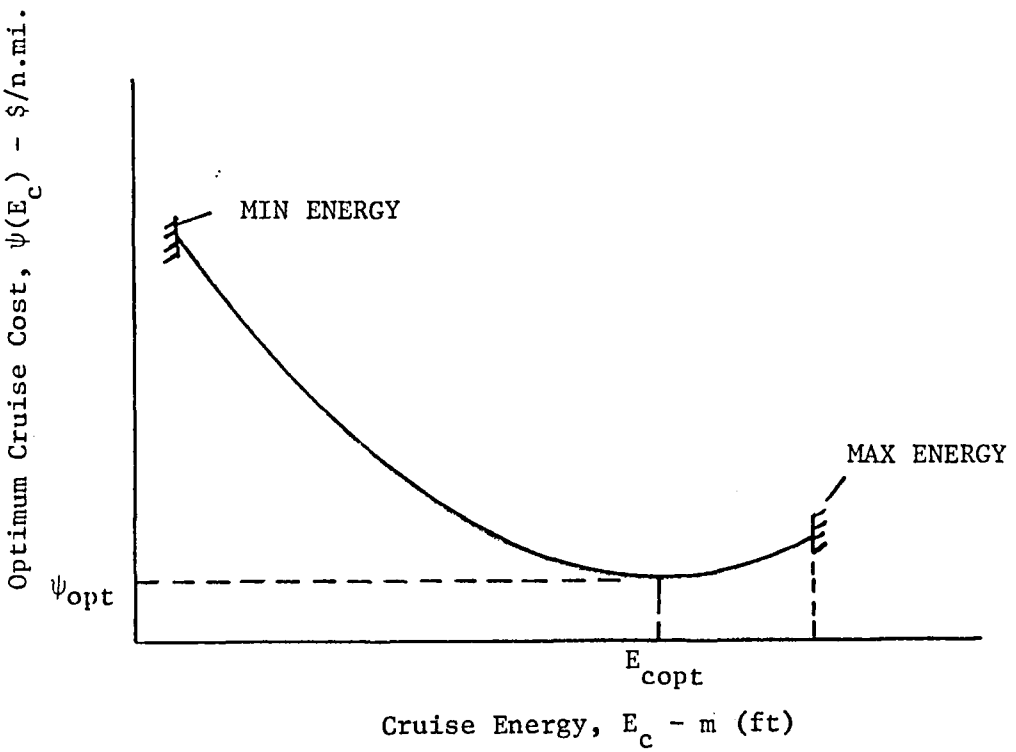

Figure A.3. Optimum Cruise Cost as a Function of Cruise Energy

For the case where there is no cruise segment ($d_f = d_{up} + d_{dn}$), the cost function contains only integral terms. Then, the transversality condition yields $\lambda = -\psi(t_c)$. That is, λ would be the negative of $\psi(t_c)$, where $\psi(t_c)$ is the optimum cost for cruising at the highest point reached on the climb trajectory.

The optimum cruise energy E_{copt} is only specifically reached when there is range enough to climb to and descend from the optimum altitude/airspeed values, where $\psi(E_c)$ is minimum. For ranges less than this value, the maximum value of E_c that is reached is a free variable less than the optimum value. Its choice is made to optimize the cost function of Eq. (A.23).

From Eqs. (A.23) and (A.25), one can write

$$\frac{\partial J}{\partial E} = H + \left[\frac{\partial [(d_f - d_{up} - d_{dn})\ \psi(E_c)]}{\partial E} \right] = 0, \qquad \text{(A.33)}$$

at $E = E_c$. This is

$$H_c + d_c \frac{\partial \psi}{\partial E_c} = 0 \quad , \tag{A.34}$$

where d_c is the cruise distance, and H_c is the total value of H ($H_{up} + H_{dn}$) at the cruise point. Thus, Eq. (A.34) can be used, along with other characteristics of ψ and H, to determine the relationship between ψ, E_c, and d_c. The Hamiltonian evaluated at $E = E_c$ is the cost penalty to achieve a unit increase in cruise energy. For $H_c > 0$, Eq. (A.34) can be written as

$$d_c = -H_c/(\partial\psi/\partial E)_{E = E_c} \tag{A.35}$$

Figure A.4 shows the family of trajectories which have this characteristic. These occur at values of E_c below E_{copt} where $\partial\psi/\partial E < 0$ (see Fig. A.3). That is, non-zero cruise segments occur at short ranges with cruise energies less than the optimum energy value for long range.

For the case where $H_c = 0$, d_c is zero for $\partial\psi/\partial E < 0$. The distance d_c can be non-zero only at optimum cruise energy where $\partial\psi/\partial E = 0$. This family of trajectories is shown in Fig. A.5.

Thus, we have a situation where positive values of H_c dictate one type of trajectory and zero values dictate another. In Ref. 24, it is shown that if the aircraft engine specific fuel consumption S_{FC} is independent of the thrust T (so that $\dot{w} = S_{FC}T$), then the structure of the trajectories will be like Fig. A.5 with no cruise segment occuring except at E_{copt}. (This implies that the Hamiltonian H_c is zero at the maximum energy point). For this case, the optimum thrust setting for climb is T_{max}, and the optimum setting for descent is T_{idle}.

If the engine specific fuel consumption is dependent on thrust, and the thrust values are not constrained during climb or descent, it is shown in Ref. 2, that the Hamiltonian H_c is again zero at the cruise energy, and again the trajectory structure is like those of Fig. A.5.

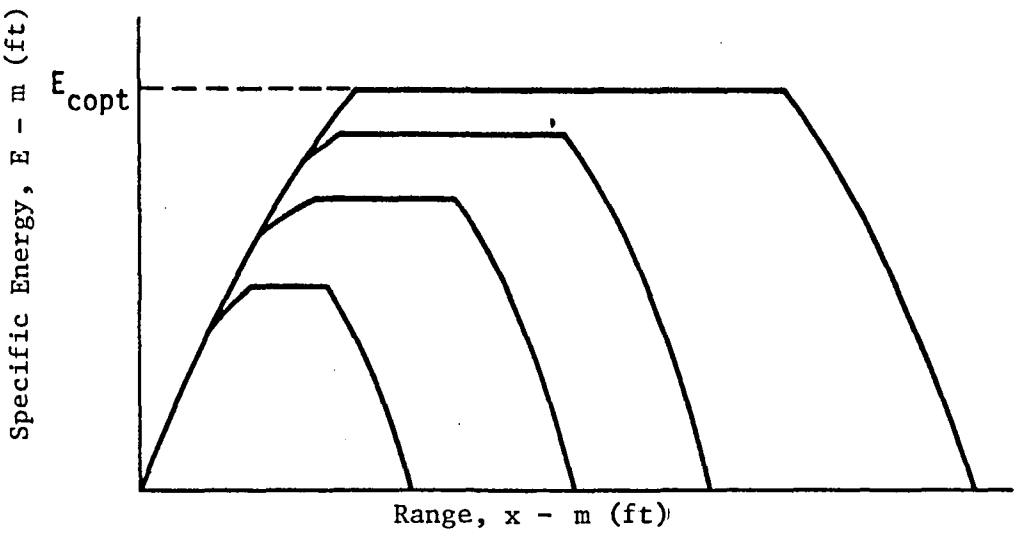

Figure A.4. Optimum Profile Energy vs Range for $H_c > 0$ at Cruise.

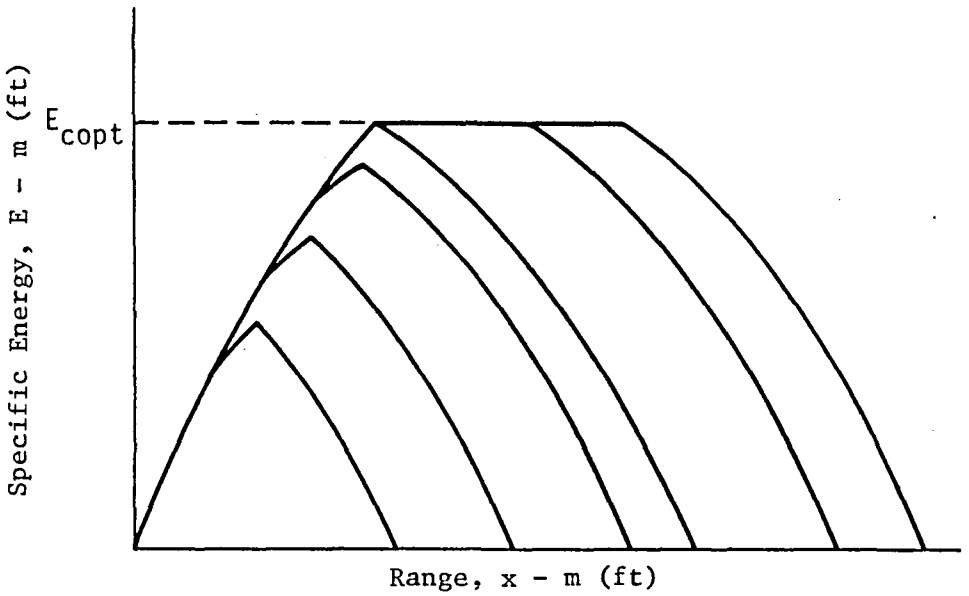

Figure A.5. Optimum Profile Energy vs Range for $H_c = 0$ at Cruise.

If the S_{FC} is dependent on thrust, and constrained to the maximum value for climb and to the minimum idle value for descent, then the Hamiltonian is positive at cruise. This causes positive cruise segments according to Eq. (A.35) at cruise energies below the optimum. For this case, the optimum trajectories will have shapes similar to Fig. A.4. These trajectories are slightly less efficient than those of Fig. A.5. because one less control is available for optimization.

Some Mechanization Details of the Computer Program

The remaining sections of this Appendix describe how the previous theoretical material has been utilized to construct an offline computer program for generating optimum vertical profiles for a model of the Boeing 727-100 aircraft provided by the NASA Ames Research Center. This material is presented in an alternate way in Ref. 30, and the program is referred to here as OPTIM.

By examining the specific fuel consumption data of the JT8D engine, it is determined that S_{FC} is dependent on thrust. Thus, for the 727, two types of short range profiles must be considered - those represented by Fig. A.4 (Type 1 profile) when thrust is constrained and airspeed is the single control - and those represented by Fig. A.5 (Type 2 profile) when both thrust and airspeed are used as controls.

The solution to optimum climb and descent profiles is found by minimizing the Hamiltonian expressed in Eqs. (A.31). The independent variable (energy) is stepped along in fixed increments (e.g., 150 m (500 ft)), and the Hamiltonian is minimized at each energy setting. Minimization occurs by finding the best values of air speed (V_{up}, V_{dn}) and possibly thrust (π_{up}, π_{dn}) so that the climb function and the descent function are individually minimized.

To solve Eqs. (A.31) requires knowing two more quantities:

$\psi(E_c)$ - the cruise cost per unit distance. This comes from evaluating Eq. (A.32) at the desired cruise altitude.

E_c - the cruise energy. This is a function of the cruise altitude and the associated cruise airspeed obtained in Eq. (A.32).

Note that for the Type 2 profile at short ranges, there is no cruise segment. In this case, the maximum energy achieved at maximum altitude is referred to as the cruise energy E_c. At that altitude, there still is defined a minimum cruise cost according to Eq. (A.32).

For the Type 1 trajectory of short range, there exists a non-zero cruise segment which is determined by use of Eq. (A.35). To solve Eq. (A.35) requires that the Hamiltonian defined by Eqs. (A.31) be solved at the point of transition from climb-to-cruise. It also requires knowing the slope $\partial\psi/\partial E$ of the cruise cost for a change in cruise energy at that point.

Cruise Optimization

The first step that must be taken to compute optimum trajectories is to derive the optimum cruise cost ψ and its derivative $\partial\psi/\partial E$. This is done by computing what is referred to as the "cruise table". The parameters that affect this table are the assumed cruise weight, the wind profile, and the lift L, drag D, thrust T, and fuel flow rate $\dot{w}$ characteristics of the aircraft. The optimization process searches over the acceptable ranges of altitude and airspeed for a given weight. The results are collected in tabular form for a series of different assumed cruise weights.

Again, the minimum cost of flight during cruise per unit distance for a fixed cruise weight W_c is found by

$$\psi(W_c) = \min_V \left[\frac{C_f \dot{w} + C_t}{V + V_w} \right] . \qquad \text{(A.36)}$$

This assumes that the aircraft is in static equilibrium during cruise, i.e.,

$$T \cos \alpha = D, \qquad L + T \sin \alpha = W, \tag{A.37}$$

where the angle-of-attack α is found by solving these equations simultaneously. The altitude is stepped in 305m (1000 ft) increments from sea level to ceiling altitude (where maximum thrust just balances drag). At altitudes below ceiling altitude, the airspeed - dependent drag curve crosses the maximum thrust curve at two points (V_1 and V_2) as illustrated in Fig. A.6. Thus, for each altitude level, the values of V_1 and V_2 are determined, and then $\psi(W_c,E_c)$ is minimized with respect to airspeed V between these two limits. Restrictions are that V_1 be greater than 0.1 Mach and that V_2 be less than 0.89 Mach for structural reasons.

After the cruise cost is minimized at each discrete altitude level, these numbers are stored in a table with altitude as the independent variable. Typical results are plotted in Fig. A.7. Presented here are also the optimum cruise Mach number M_{opt} and the optimum thrust setting EPR_{opt}. After results are obtained in steps of 305 m (1000 ft), the minimum cost point is found as a function of altitude. In the OPTIM program, the cruise table optimization results are obtained by using a Fibonacci search with 8 Fibonacci numbers.

The cruise table results are obtained for cruise weights varying as dicated by the program input. Usually, the cruise weight is incremented in steps of 2268 kg (5000 lb). Up to 10 values of cruise weight can be used. For each cruise weight, the optimal cruise altitude, cost, speed, power setting, fuel flow rate, and specific energy are computed. An example of optimum cruise cost as a function of cruise weight is shown in Fig. A.8.

Climb Optimization

After the cruise tables are generated, the program procedes with obtaining the optimum climb trajectory. This requires guessing what the cruise weight will be, based on the takeoff weight. The guess is used to obtain a trial value for ψ_c (or λ) in the Hamiltonian from the cruise tables. The procedure to obtain this guess is based on an empirical formula which iterates until convergence is made.

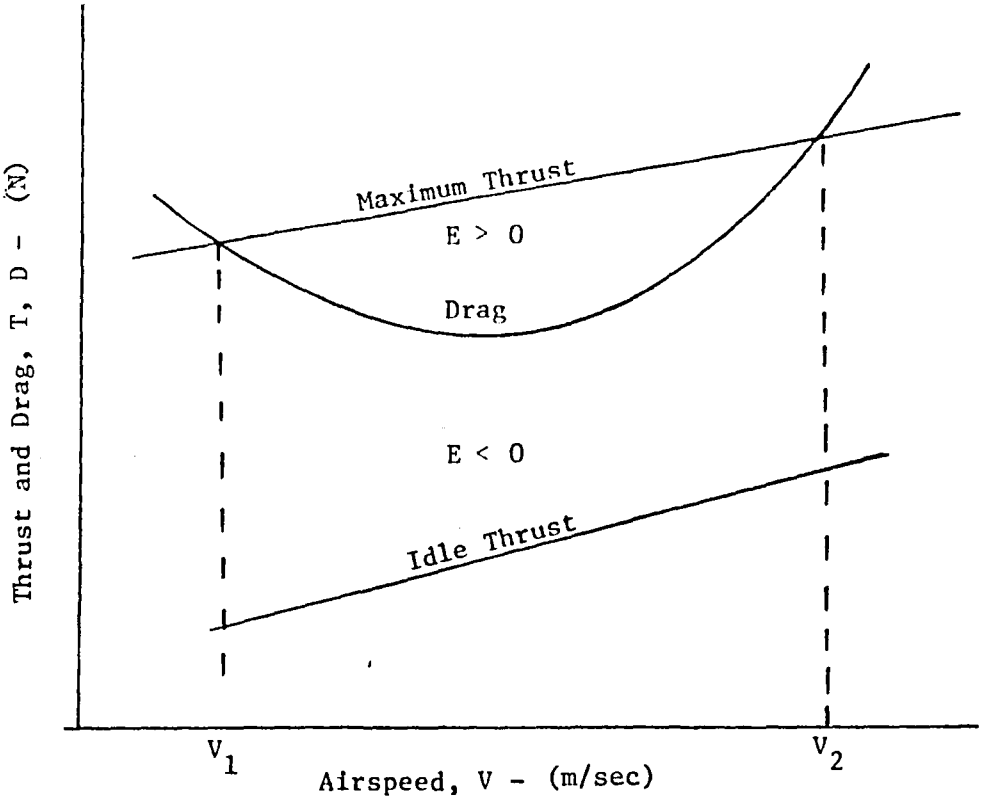

Figure A.6. Plot of Thrust and Drag vs Airspeed at a Particular Altitude

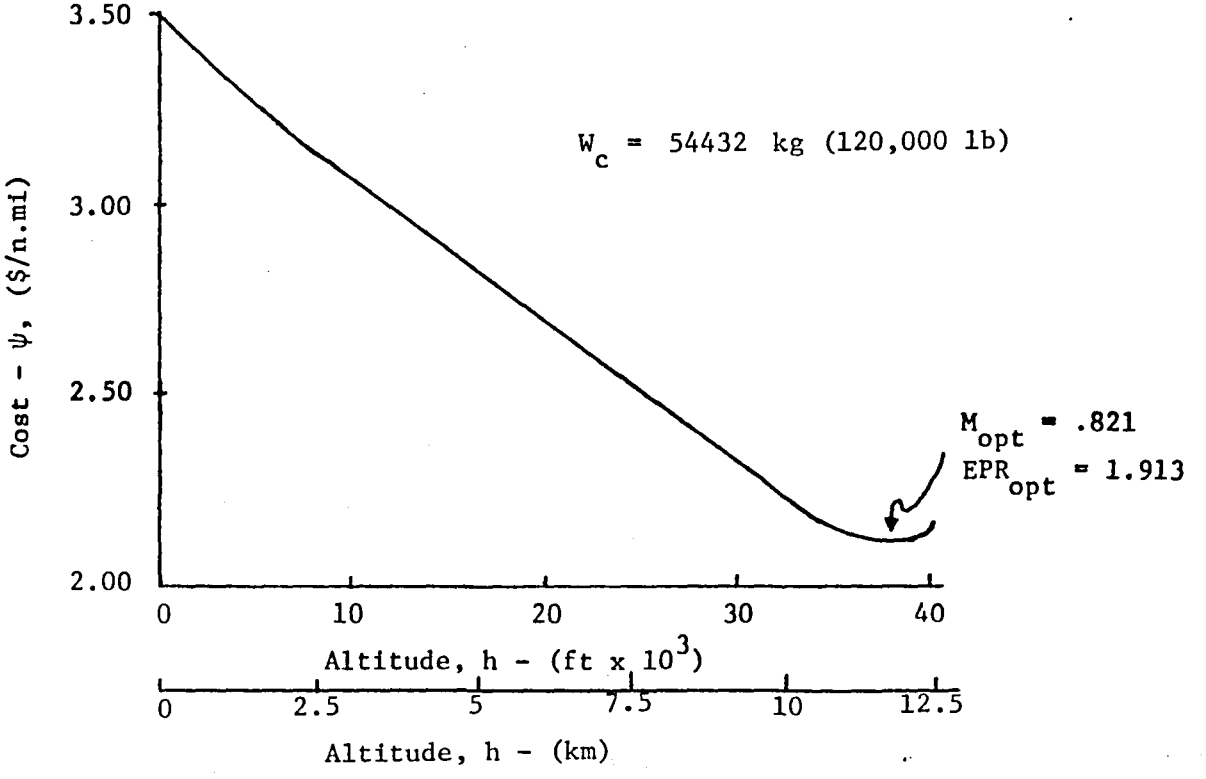

Figure A.7. Optimum cruise cost as a function of altitude for cruise weight of 54432 kg (120,000 lb).

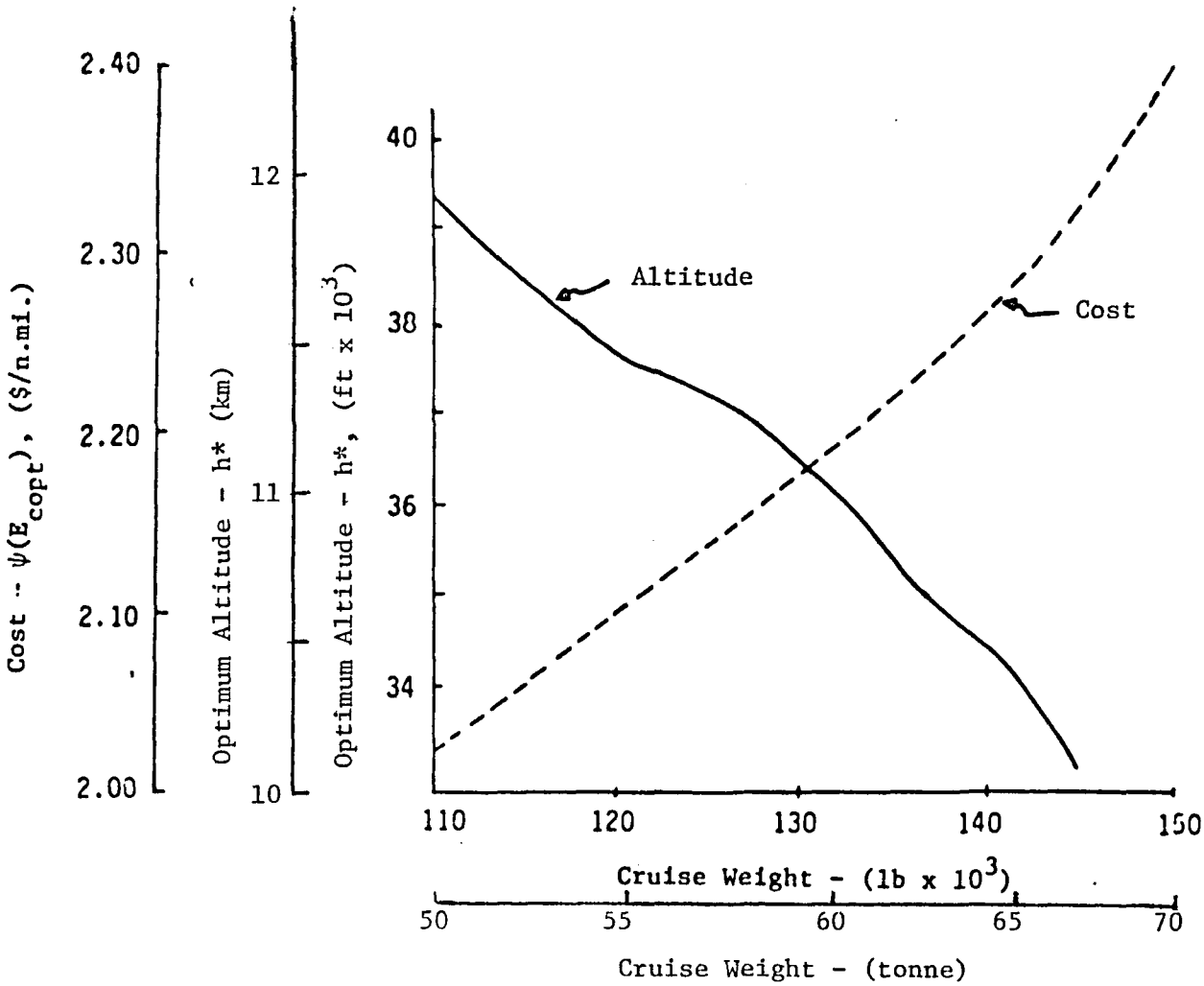

Figure A.8. Optimum Cruise Cost and Cruise Altitude as Functions of Cruise Weight for the 727 Flying into a Particular Head Wind.

The climb optimization process starts by assuming $\psi(E_c) = 1.5\,\psi(E_{copt})$, where $\psi(E_{copt})$ is first obtained by setting the initial cruise weight W_{ci} equal to the takeoff weight (an input). The appropriate cruise tables are used to interpolate to find the corresponding value of E_c associated with $1.5\,\psi$. Then, an empirical formula of the form

$$F_{up} = 0.11\ (E_{ci} - E_i)\ (1 + 4.7\ C_t/C_f)\ W_{ci}/W_{ref}\ , \qquad (A.38)$$

is used to obtain an approximation to the fuel burned to reach E_c. Here, E_i is the takeoff aircraft energy, W_{ref} is a reference weight (61690 kg (136000 lb) for the 727), and W_{ci} is the previous value of cruise weight.

Then, the cruise weight is updated at $W_{ci} = W_{ci} - F_{up}$. This process is repeated until the difference in consecutive estimates of F_{up} falls below 45 kg (100 lb).

When the cruise weight estimate is obtained, the corresponding values of E_c and $\psi(E_c)$ are obtained from the cruise tables. Then, the program is ready to generate points on the optimum climb trajectory. This is done by stepping along at discrete increments of specific energy and minimizing the Hamiltonian function

$$H_{up}(E) = \frac{C_f \dot{w} + C_t - \psi(E_c)\,(V + V_w)}{\dot{E}} \qquad (A.39)$$

at each point. (This is the first of Eqs. (A.31)). That is, the program starts with initial energy $E_o = h_o + V_o^2/2g$. It steps the energy a fixed amount ΔE (say 150 m (500 ft). At this point, it searches over airspeed V (and possibly thrust setting π) so that Eq. (A.39) is minimized. For the 727's JT8D engines, thrust is governed by EPR settings which vary between 1.1 (idle thrust) and some maximum value less than 2.4. The airspeed has an upper limit governed by

a). 0.89 Mach structural limits,
b). 250 kt (IAS) below 3048 m (10000 ft) for ATC restrictions,
c). $\sqrt{2g(E-h)}$ which insures that the aircraft climbs, and
d). V_2, the upper value shown in Fig. A.6 where max thrust equals drag.

The lower limit is governed by

a). V_1, the lower value shown in Fig. A.6 where max thrust equals drag,
b). 0.1 Mach
c). 5 ft/sec less than the previous value of V to limit large jumps in flight path angle.

The Fibonacci search technique is again used to determine V and π which minimize Eq. (A.39) for the fixed value of energy E. The value chosen for airspeed is accurate to within .0056 Mach, and EPR is accurate

to within .009. Associated with these values of V and π are values of energy rate $\dot{E}$ (Eq. (A.16)) and altitude h:

$$h = E - V^2/2g \ . \tag{A.40}$$

From these, approximate values of time, range, flight path angle, and fuel burned are obtained from

$$\begin{aligned} \Delta t &= \Delta E/\dot{E}, \\ \sin\gamma &= (\Delta h/\Delta t)/V, \\ x &= \Sigma\Delta x \ ; \quad \Delta x = (V\cos\gamma + V_w(h))\ \Delta t \\ F &= \Sigma\Delta F \ ; \quad \Delta F = \dot{w}\ \Delta t. \end{aligned} \tag{A.41}$$

The above process is repeated by stepping along energy in increments of ΔE until E_c is reached. The last value of Eq. (A.39) is stored for possible use in evaluating the cruise distance.

The above climb optimization procedure is repeated with $\psi = 1.5\psi_c$, $1.01\psi_c$, and perhaps other values until the total range of flight converges to the appropriate value. This is discussed in further detail later.

Descent Optimization

The descent optimization is very similar to the climb optimization with regard to the equations which are evaluated. The optimization process requires estimated values of E_c and W_c at the beginning of descent, and an estimate of weight W_f at the end of descent. The method used to obtain these estimates is discussed in the next section.

If there is a cruise portion of flight, fuel will be burned off during cruise. Thus, the value of E_{cf}, ψ, and W_{cf} at the beginning of descent will be different than at the beginning of cruise. If there is no cruise portion, then these values will be identical.

The descent profile is obtained by starting at the final energy state and then going backwards in time. The energy rate is constrained to be negative with respect to forward time.

Similar descent profile constraints exist on airspeed as for those of the climb profile. The thrust level is on or near the idle value during descent.

Cruise Fuel Burn

To estimate the final weight during cruise (W_{cf}) and landing (W_f), the following steps are taken:

1). Determine ψ_c, the initial cruise cost based on the initial cruise weight W_{ci} obtained from the climb optimization.

2) Use the initial cruise weight and ψ_c to compute the fuel flow rate $\dot{w}(\psi_c)$.

3). Estimate the cruise range d_c by the empirical equations,

$$P = \psi_c/\psi_{copt} = 1.5 \ , \tag{A.42}$$

$$d_c = b_1P^4 + b_2P^3 + b_3P^2 + b_4P + b_5 \ .$$

4). Compute the cruise fuel as

$$F_c = \dot{w}(\psi_c)\ d_c/(V_c + V_w(h_c)) \ . \tag{A.43}$$

5). Estimate the average cruise weight as

$$\overline{W}_c = W_c - 0.5F_c \tag{A.44}$$

6). Use the cruise table to obtain the corresponding cruise cost $\overline{\psi}_c$, altitude $\overline{h}_c$, fuel flow rate $\dot{\overline{w}}(\overline{\psi}_c)$, airspeed $\overline{V}_c$, and wind speed $\overline{V}_w(\overline{h})$.

7). Recompute Eq. (A.43) and then find the final cruise weight,

$$W_{cf} = W_{ci} - F_c. \tag{A.45}$$

8). Use the value W_{cf} in the cruise tables to obtain $\psi(W_{cf})$. As with the climb, set $\psi = 1.5\ \psi(W_{cf})$.

9). Use this value of ψ to obtain h_{cf} and E_{cf} from the cruise tables. These are the end conditions for the descent trajectory obtained backwards in time.

10). Estimate the landing weight from the empirical formula

$$P = 1.5, \tag{A.46}$$
$$W_f = W_{cf} - (c_1 P^2 + c_2 P + c_3).$$

The values of ψ, E_{cf} and W_f obtained by the above procedure are used for obtaining the optimum descent trajectory. The descent portion of the Hamiltonian is of the form

$$H_{dn}(E) = \frac{C_f \dot{w} + C_t - \psi(E_{cf})\ (V + V_w)}{|\dot{E}|}; \tag{A.47}$$

this function is also minimized at each of the given values of energy.

After the first descent profile is completed, a new estimate of cruise distance is obtained by using Eq. (A.35), or

$$d_c = -(H_{up} + H_{dn})/(\partial\psi/\partial E) \quad . \tag{A.48}$$

Then, step (4) above is repeated to obtain an improved cruise fuel burn. Then, the improved landing weight estimate is

$$W_f = W_i - (F_{up} + F_c + F_{dn}) \ . \tag{A.49}$$

The landing trajectory is reoptimized with this new value of landing weight. Then, improved values of total range traveled, time required, and fuel burned during climb, cruise, and descent are made.

For short range flight, the above steps assumed that a Type 1 trajectory is generated because thrust is constrained to maximum value during climb and idle value during descent. If thrust is free, then a Type 2 trajectory will result, with no cruise portion. For this case, the steps required to estimate cruise distance d_c and final cruise cost, weight, and energy can be eliminated.

Cruise Cost Estimation

The first climb and descent profiles are generated with $\psi_c = 1.5\psi(E_{copt})$. The next set is generated with $\psi_c = 1.01\psi(E_{copt})$. Each of these values of cruise cost have an associated range on the curve shown in Fig. A.9. If the total range desired is greater than R_{max}, the value obtained using $1.01\psi(E_{copt})$, then it is assumed that the optimum cruise altitude and energy are reached. Then a third set of climb and descent profiles is generated using $\psi(E_{copt})$. In this case, the cruise distance is computed so that the desired overall range is exactly achieved.

If the desired range is between R_{min} and R_{max} in Fig. A.9, then an iterative process is used to obtain $\psi(E_c)$ and the associated desired range. Iterations are stopped when the total range traveled is within some ε of the desired range. (In OPTIM, ε is set at 5 n. mi.)

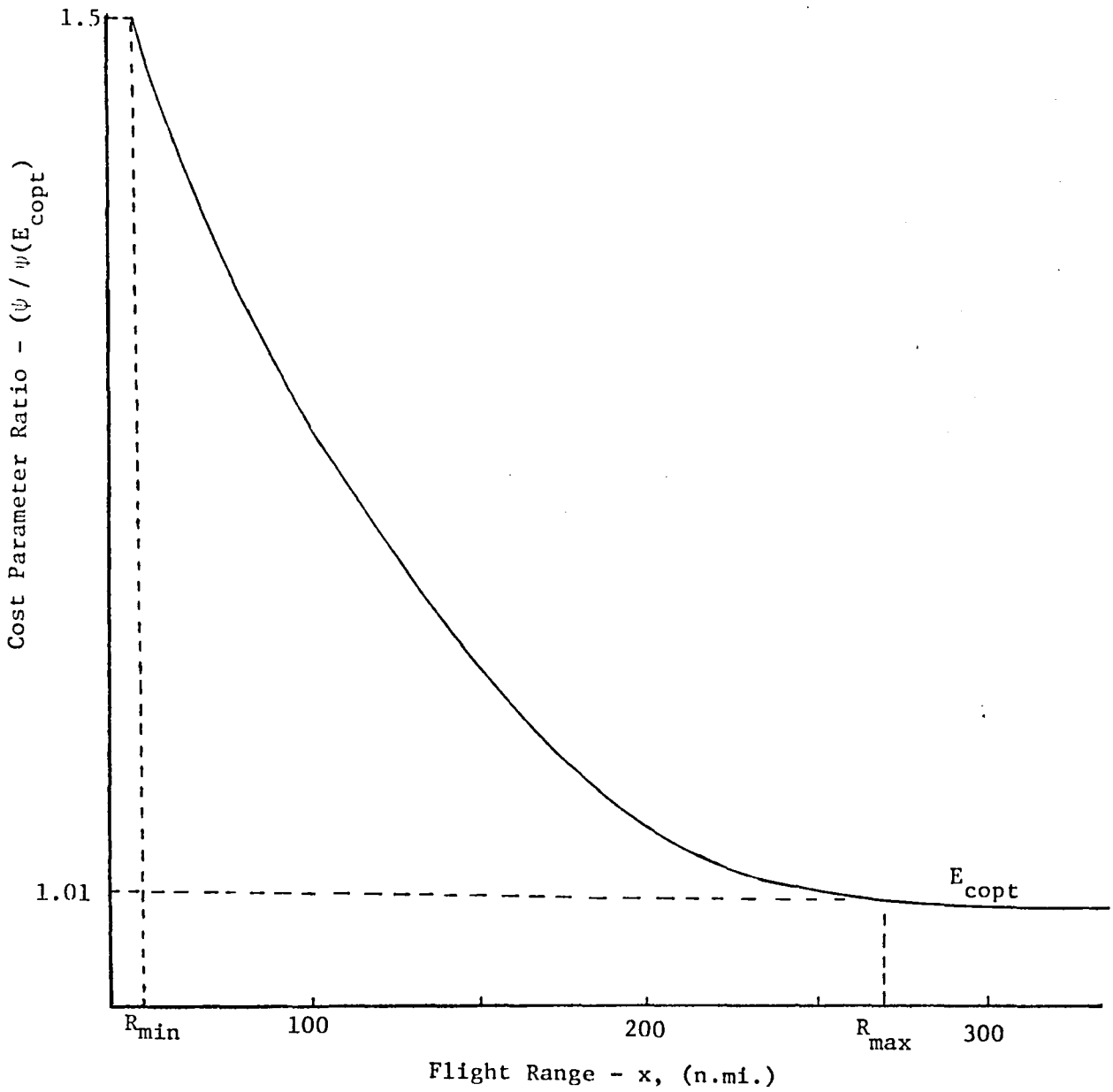

Figure A.9. Relationship between the Cruise Cost Parameter ψ and the Associated Range of Flight

APPENDIX B

AIRCRAFT EQUATIONS OF MOTION AND AUTOPILOT MODELS

The objective of the TRAGEN program is to simulate a 727 aircraft being steered to fly along an input reference trajectory. This trajectory may either be a climb or descent profile. The simulation must be accurate enough such that the performance of the aircraft (in terms of fuel burned and time required to reach the destination point) is adequately determined, as measured from the output. Adequate accuracy is obtained with a five-state variable longitudinal aircraft model.

The purpose of this appendix is to present the analytical expressions upon which the simulation was developed; this is done in two parts. The first section below defines the overall system and presents the differential equations of motion and fuel burn. The second section describes different methods for generating typical guidance commands and autopilot equations.

Equations of Motion and Fuel Burn

To examine the vertical profile of the aircraft (i.e., altitude and airspeed vs range), the longitudinal equations of motion are of primary importance. The short period equations of motion and the throttle dynamics are ignored. Thus, the control variables in this longitudinal plane are the angle-of-attack α and the magnitude of the thrust vector T. These quantities are shown with respect to aircraft airspeed V_a, lift L, drag D, weight W, and flight path angle γ in Fig. B.1.

The kinematic equations of motion of the aircraft in the longitudinal plane are

$$\begin{aligned} \dot{x} &= V_a \cos\gamma + V_w \,, \\ \dot{h} &= V_a \sin\gamma \,, \end{aligned} \tag{B.1}$$

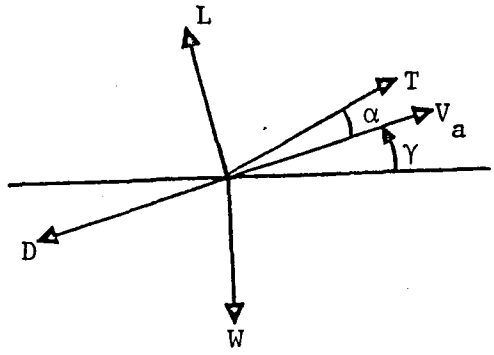

Figure B.1 Vector Diagram of Longitudinal Forces

where

x - distance, or range, measured on the ground,

h - altitude,

V_w - wind speed.

The inertial speed along the airspeed vector V_a is

$$V_I = V_a + V_w \cos\gamma \tag{B.2}$$

From Fig. B.1, the time rate of change of this vector for constant γ is

$$\dot{V}_I = \dot{V}_a + \dot{V}_w \cos\gamma = \frac{1}{m}(T\cos\alpha - D - W\sin\gamma). \tag{B.3}$$

The time rate of change of the wind speed is

$$\dot{V}_w = \frac{\partial V_w}{\partial h}\dot{h},$$

$$= \frac{\partial V_w}{\partial h} V_a \sin\gamma \quad . \tag{B.4}$$

Substituting Eq. (B.4) into Eq. (B.3) and solving for $\dot{V}_a$ leaves

$$\dot{V}_a = \frac{1}{m}(T\cos\alpha - D - W\sin\gamma) - \frac{\partial V_w}{\partial h} V_a \sin\gamma\cos\gamma \tag{B.5}$$

Also, from Fig. B.1, one can write

$$\ddot{h} = \frac{1}{m} (L \cos \gamma - W + T \sin (\gamma + \alpha) - D \sin \gamma), \qquad (B.6)$$

Equations (B.5) and (B.6) represent the kinetic equations of motion of the aircraft.

The remaining term that must be accounted for is the time-varying weight of the aircraft. Specifying the thrust also specifies the fuel burn rate $\dot{w}$. Thus, the weight changes at the rate

$$\dot{W} = -\dot{w} . \qquad (B.7)$$

Equations (B.1), (B.5), (B.6), and (B.7) are the five basic equations used to represent the longitudinal dynamics of the aircraft. Lift and drag (L and D) are computed as functions of V_a, h, and α . Fuel flow rate $\dot{w}$ is a function of V_a, h, and thrust T.

Further refinement could be added to these equations to include the effects of the following:

1). throttle dynamics (including transient fuel flow rates);

2). relationship between throttle position, EPR setting, and thrust;

3). short period dynamics relating time rate of change of angle-of-attack, pitch rate, and pitch angle to elevator deflection;

4). required turning (lateral) motion for flying over fixed waypoints; and

5). lateral wind and gust effects.

However, these effects are considered to be of second order, and not required for the intent of this simulation. For a more exact autopilot simulation, they would be required.

The flight path angle is defined as

$$\gamma = \sin^{-1} (\dot{h}/V_a) \tag{B.8}$$

By differentating this expression and using Eqs. (B.5) and (B.6), one obtains

$$\dot{\gamma} = \frac{1}{mV_a} (T \sin \alpha - W \cos \gamma + L + m \frac{\partial V_w}{\partial h} V_a \sin^2 \gamma). \tag{B.9}$$

Equation (B.9) can be used in place of Eq. (B.6).

Steering Procedures

The reference trajectories which are given to be followed consist of a sequence of points containing values of time, range, altitude, airspeed, flight path angle, specific energy, weight, and other variables. Any of these quantities which is measurable and monotonically changing can serve as the independent variable. To minimize airborne computer memory requirements, it is important to make the stored data representing the reference trajectory as compact as possible.

In this study, a set of steering equations is used to take points from the reference trajectory, convert these points to reference trajectory commands, and then use these commands to set values of the control variables. This steering process represents a rudimentary form of an autopilot.

The steering process consists of commanding the thrust T and angle-of-attack α values so that the aircraft follows the reference as closely as possible. The system that includes this process is depicted by the block diagram in Fig. B.2. Note that flying along a reference trajectory consists of steering to connect a series of reference points. When a reference point is reached, new steering commands must be issued so that the aircraft will then be guided to the next reference point.

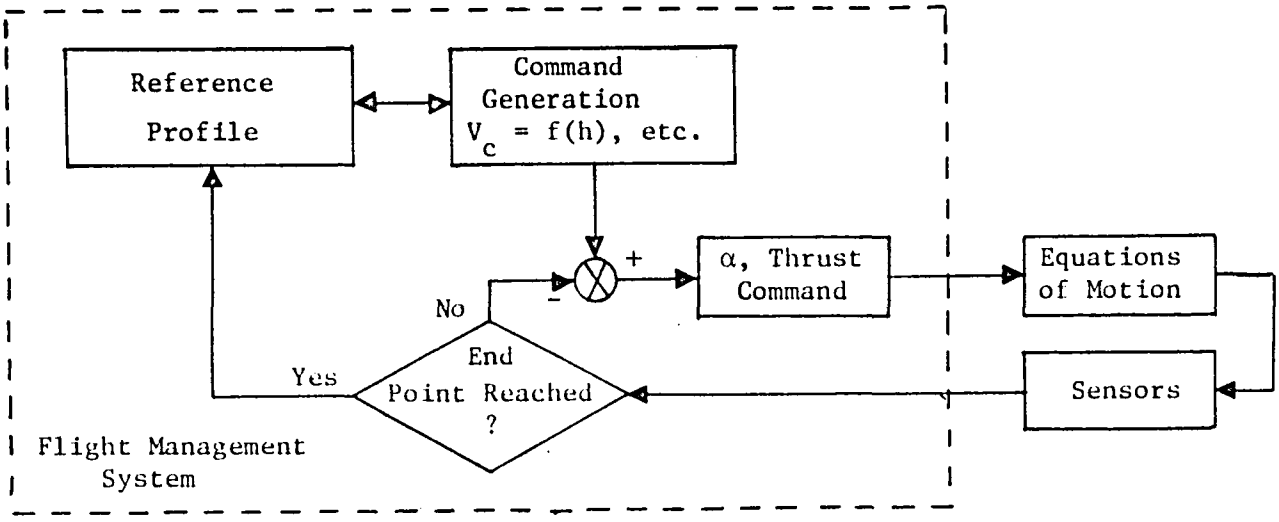

Figure B.2. Elements of the Longitudinal Aircraft Model

To fly along the reference path, an independent variable is first chosen. For this study, two different independent variables were chosen - altitude for climb and range for descent. Then, the remaining variables - primarily airspeed, flight path angle, and altitude (for range as the independent variable) - are stored as tabular functions of the chosen independent variable.

Also, it is possible to fly along a nominal path using two approaches:

1). An open-loop approach where the thrust vector is directed in such a way over the next period that by the end of that period the next reference point is reached.

2). A closed-loop approach where the aircraft is continually steered to a continuously commanded trajectory which connects the reference points.

Both of these approaches were examined for simulation of flying the climb profile. However, good results were only obtained with the closed-loop approach.

A problem with open-loop steering is that it assumes that constant or linearly varying controls will cause the end points of a reference profile to be connected. This assumption does not account for perturbations due to wind, etc. along the way. Although the open-loop methods produce paths which have roughly correct values of airspeed and altitude at given range values, there were large excursions from the reference flight path angle for the climb profiles.

Another problem with the open-loop approaches was that both α and T were varied to achieve fixed values of V_a and h for given range points. For optimum climb, thrust is usually set at the maximum value. Thus, usually only α remains as a valid control variable.

Another consideration for implementing the climb profile is that there is no reason why a particular cruise condition (altitude, airspeed) has to be achieved when a certain range x is reached. Thus, a more logical independent variable is altitude, with range allowed to be a free variable.

For these reasons, a closed-loop steering approach was devised where reference values of flight path angle (with respect to the air mass) and airspeed are obtained as functions of altitude. (This assumes that altitude is monotonically increasing during climb.) A perturbation control law was set up so that variations in α from a reference value α_o were proportional to variations in γ and V_a from their respective command values.

Because γ and V_a tend to change linearly with time, they can be considered as ramp functions. Thus, the closed-loop controller should be considered to be at least a Type 1 system. From Eqs. (B.5) and (B.9), with no wind, the system perturbation equations are

$$m\delta\dot{V}_a = -T \sin\alpha\,\delta\alpha - \frac{\partial D}{\delta\alpha}\,\delta\alpha - \frac{\partial D}{\delta V_a}\,\delta V_a - W\cos\gamma\delta\gamma, \qquad \text{(B.10)}$$

$$m V_a\delta\dot{\gamma} = T\cos\alpha\,\delta\alpha + \frac{\partial L}{\partial\alpha}\,\delta\alpha + \frac{\partial L}{\partial V_a}\,\delta V_a + W\sin\gamma\delta\gamma.$$

The resulting transfer functions between γ, V_a, and α are of the form

$$\frac{\delta\gamma}{\delta\alpha} = \frac{G_B\ (\tau_B\ s + 1)}{(s/\omega)^2 + 2\zeta\ (s/\omega) + 1}\ , \tag{B.11}$$

$$\frac{\partial V_a}{\delta\alpha} = \frac{G_c\ (\tau_c\ s + 1)}{(s/\omega)^2 + 2\zeta(s/\omega) + 1}\ ,$$

where the time constants and other parameters are functions of the parameters in Eq. (B.10).

The control problem can now be interpreted as shown in Fig. B.3. To obtain the Type 1 system, the control law has to be of the form

$$\delta\alpha = (K_1 + \frac{K_2}{s})\ \ (V_{a_c} - V_a) + (K_3 + \frac{K_4}{s})\ \ (\gamma_c - \gamma), \tag{B.12}$$

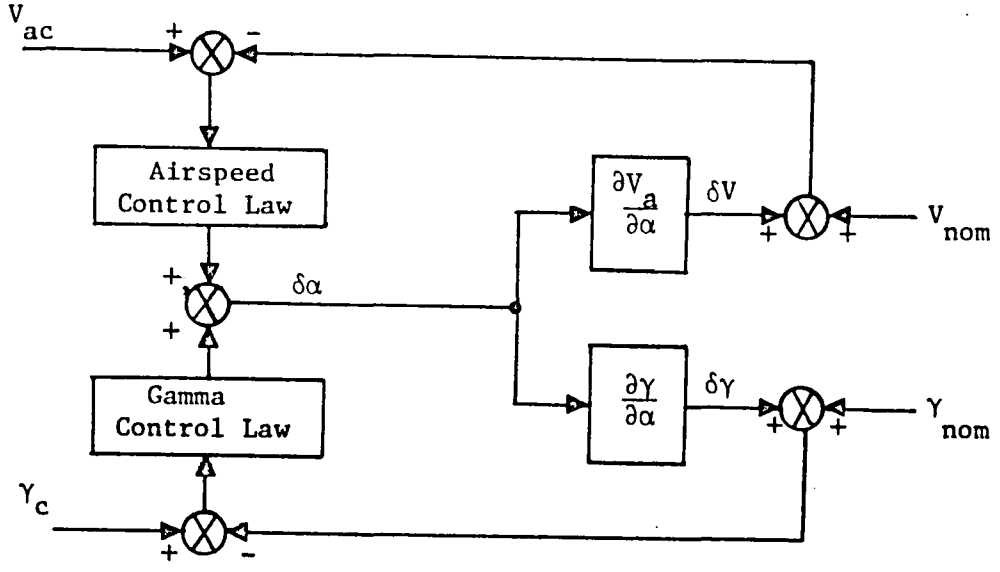

Figure B.3 Control Loops for Perturbation Control of Airspeed and Flight Path Angle.

where V_{a_c} and γ_c are the commanded values of V_a and γ. This is the classical proportional-plus-integral controller. Gains are chosen to produce the desired response for removal of profile errors.

To generate the continuous commands V_{a_c} and γ_c during climb, the computations made at each reference point are

$$\frac{\partial \gamma}{\partial h} = \frac{\gamma_{n+1} - \gamma_n}{h_{n+1} - h_n} , \tag{B.13}$$

$$\frac{\partial V_a}{\partial h} = \frac{V_{a\ n+1} - V_{a_n}}{h_{n+1} - h_n} .$$

Then

$$\gamma_c = \gamma_n + (h - h_n) \frac{\partial \gamma}{\partial h} , \tag{B.14}$$

$$V_{a_c} = V_{a_n} + (h - h_n) \frac{\partial V_a}{\partial h} .$$

When the flight path angle is very small (during the initial period of flight and when the aircraft levels off at 3048m (10000 ft) to gain speed before resuming climb), Eqs. (B.14) do not work well. For these cases, it is more appropriate to set

$$\gamma_c = 0., \tag{B.15}$$

$$V_{a_c} = V_{a\ n+1} ,$$

and use the control law

$$\delta\alpha = (K_3 + \frac{K_4}{s}) (\gamma_c - \gamma). \tag{B.16}$$

The above method worked quite well in causing the simulated profile to closely follow the reference path. Only one set of gain values was sufficient for the entire trajectory.

For decending flight, the thrust again is usually constrained (idle) for optimum performance. Also, for this case, the main concern is to reach a fixed altitude when range-to-go to the destination point is a certain value. Thus, above 10000 ft, the airspeed can be allowed to be a free variable. For this case, only inertial flight path γ_{Ic} is required to be controlled.

To generate a continuous command γ_{Ic}, the computation made at each reference point is

$$\gamma_{Ic} = \tan^{-1} \left[(h_{n+1} - h_n) / (x_{n+1} - x_n) \right] . \qquad (B.17)$$

Then, the control law is similar to Eq. (B.16), i.e.

$$\delta\alpha = (K_3 + \frac{K_4}{s}) (\gamma_{Ic} - \gamma_I) , \qquad (B.18)$$

where inertial values of flight path angle are used rather than those with respect to the air mass. Equations (B.17) and (B.18) form the basis for closed-loop control of descending flight. Again, one set of gains in sufficient for the entire descent profile.

REFERENCES

1. Covey, R.R., Mascetti, G.J., and Roessler, W.U., "Examination of Commercial Aviation Energy Conservation Strategies," Report No. ATR-79(7761)-1, Aerospace Corp., El Segundo, CA. October 1978.

2. Hanks, G.H., "Overview of Technology Advancements for Energy Efficient Transports," AIAA Atmospheric Flight Mechanics Conference, Paper No. 79-1651, Boulder, CO. August 1979.

3. Stengel, R.F., and Marcus, F.J., "Energy Management Techniques for Fuel Conservation in Military Transport Aircraft," AFFDL-TR-75-156, Analytic Sciences Corp., Reading, MA, February 1976.

4. Aggarwal, R., et al., "An Analysis of Fuel Conserving Operational Procedures and Design Modifications for Bomber/Transport Aircraft," AFFDL-TR-78-96, Vol. II, Dynamics Research Corp, Wilmington, MA, July 1978.

5. Bryson, A.E., and Ho, Y.C., "Applied Optimal Control," Blaisdell, Waltham, MA, 1969.

6. Pontryagin, L.S. et al., The Mathematical Theory of Optimal Processes, Interscience, New York, NY, 1962.

7. Dreyfus, S.E., Dynamic Programming and the Calculus of Variations, Academic Press, New York, NY, 1965.

8. Reinkens, L., "Lockheed Jet Plan," presented at Stanford University Flight Mechanics and Control Seminar, Stanford, CA, January 1979.

9. Stein, L.H., Matthews, M.L., and French, J.W., "STOP-A Computer Program for Supersonic Transport Trajectory Optimization," NASA CR-793, May 1967.

10. Bryson, A.E., and Denham, W.F., "A Steepest-Ascent Method of Solving Optimum Programming Problems," J. of Applied Mechanics, Vol. 29, June 1962.

11. Rutowski, E.S., "Energy Approach to the General Aircraft Performance Problem," J. of Aeronautical Sciences, Vol. 21 No. 3, March 1954, pp. 187-195.

12. Bryson, A.E., Desai, M.N., and Hoffman, W.C., "Energy-State Approximation of Supersonic Aircraft," J. of Aircraft, Vol. 6, No. 6, Nov-Dec 1969, pp. 481-488.

13. Zagalsky, N.R., Irons, R.P., and Schultz, R.L., "Energy State Approximation and Minimum-Fuel Fixed-Range Trajectories," J. of Aircraft, Vol. 8, No. 6, June 1971, pp. 488-490.

14. Schultz, R.L., and Zagalsky, N.R., "Aircraft Performance Optimization," J. of Aircraft, Vol. 9, No. 2, January 1972, pp. 108-114.

15. Zagalsky, N.R., "Aircraft Energy Management," AIAA 11th Aerospace Science Meeting, Washington, D.C., January 1973.

16. Schultz, R.L., "Fuel Optimality of Cruise," J. of Aircraft, Vol. 11, No. 3, September 1974, pp. 586-587.

17. Speyer, J.L., "Nonoptimality of the Steady-State Cruise for Aircraft," AIAA Journal, Vol. 14, No. 11, November 1976, pp. 1604-1610.

18. Kelley, H.J. "Aircraft Maneuver Optimization by Reduced-Order Approximation," Control and Dynamic Systems, Vol.10, C.T. Leondes, ed., Academic Press, New York, NY, 1973.

19. Calise, A.E., "Extended Energy Management Methods for Flight Performance Optimization," AIAA 13th Aerospace Sciences Meeting, Pasadena, CA, January 1975.

20. Ardema, M.E., "Solution of the Minimum Time-to-Climb Problem by Matched Asymptotic Expansions," AIAA Journal, Vol. 14, No. 7, July 1976, pp. 843-850.

21 Erzberger, H., McLean, J.D., and Barman, J.F., "Fixed-Range Optimum Trajectories for Short Haul Aircraft," NASA TN D-8115, December 1975.

22. Barman, J.E., and Erzberger, H., "Fixed-Range Optimum Trajectories for Short-Haul Aircraft," J. of Aircraft, Vol. 13, No. 10, October 1976, pp. 748-754.

23. Shoaee, H., and Bryson, A.E., "Airplane Minimum Fuel Flight Paths for Fixed Range," SUDAAR No. 499, Stanford University, Stanford CA, March 1976.

24. Erzberger, H., and Lee, H.O., "Characteristics of Constrained Optimum Trajectories with Specified Range," NASA TM 78519, September 1978.

25. Bochem, J.H., and Mossman, D.C., "Simulator Evaluation of Optimal Thrust Management/Fuel Conservation Strategies for Airbus Aircraft on Short Haul Routes," NAS2-9174, Sperry Rand Corp., Phoenix, AZ, June 1978.

26. Anon, "Integrated Energy Management Study," NAS1-14742, Boeing Commercial Airplane Co., Renton, WA, August 1978.

27. Knox, C.E., and Cannon, D.G., "Development and Flight Test Results of a Flight Management Algorithm for Fuel Conservative Descents in a Timed Based Metering Traffic Environment," IEEE Decision and Control Conference, Ft. Lauderdale, FL, December 1979.

28. Kyser, A.C., "The Aerial Relay System - An Energy Efficient Solution to the Airport Congestion Problem," AIAA Aircraft Systems and Technology Meeting, New York, NY, August 1979.

29. Erzberger, H., and McLean, J.D., "Fuel-Conservative Guidance System for Powered-Lift Aircraft," AIAA Guidance and Control Conference, Paper No. 79-1709, Boulder, CO, August 1979.

30. Lee, H.Q., and Erzberger, H., " Algorithm for Fixed Range Optimal Trajectories," NASA Technical Paper 1565, 1979.

31. Kidder, M.K., and Sorensen, J.A., "OPTIM - Computer Program to Generate a Vertical Profile which Minimizes the Aircraft Direct Operating Costs," NAS1-15497, Analytical Mechanics Assoc., Inc., Mountain View, CA, June 1979.

32. Kidder, M.K., and Sorensen, J.A., "TRAGEN - Computer Program to Simulate an Aircraft Steered to Follow a Specified Vertical Profile," NAS1-15497, Analytical Mechanics Assoc., Inc., Mountain View, CA, June 1979 .